Factors Affecting Selective Hydrogenation of Acrolein over Supported Silver and Silver Alloy Catalysts

BY

Payoli Aich

B.Tech, West Bengal University of Technology, 2011

THESIS

Submitted as partial fulfillment of the requirements

for the degree of Doctor of Philosophy in Chemical Engineering

in the Graduate College of the

University of Illinois at Chicago, 2016

Chicago, Illinois

Defense Committee:

Randall Meyer, Chair and Advisor

Brian Chaplin

Robert Klie, Physics

Jeffrey Miller, Argonne National Laboratory

Christopher Marshall, Argonne National Laboratory

Acknowledgement

Last four and a half years of journey was memorable for me. It was not only about doing research but also adapting as an international student in a foreign country, learning new techniques, running overnight experiments and excitement of showcasing work in conferences. In all, it was a life-learning experience for me.

This was not plausible without guidance and mentoring of few individuals. Firstly, I would like to thank my advisor Dr. Randall Meyer, who is extremely helpful and inspiring and gave me a lot of opportunities to learn different nuances of heterogeneous catalysis. His constant advising and mentoring really helped me to grow as a researcher.

I also thank Dr. Jeff Miller. His knowledge in the field of heterogeneous catalysis and thoughtful ideas motivated me during my research. I am also grateful to Dr. Chris Marshall for providing guidance and the resources of his lab. His availability all the time whenever we faced problems while troubleshooting reactor was priceless.

Prof. Robert Klie, Dr. Alan Nicholls and Dr. Tad Daniel also helped us by allowing to use high resolution microscopes (JEM-ARM200CF and JEOL JEM-3010) to do TEM study on our catalysts.

Dr. Hongbo Zhang, Dr. Robert McCoy, Dr Richard Pauls and Dr. Jeremy Kopf, also helped with their amazing technical expertise. I am also grateful to Dr. Jeffrey Bunquin, Dr. Andrew Getsoian, Dr. Guanghui Zhang and Dr. James Gallagher for sharing their knowledge with me and giving me ideas for the project. I also want to thank all my group members, especially Ruzica Todorovic, Haojuan Wei for their support on this project. I also thank my other committee member Prof. Brian Chaplin for being in my committtee.

Last but not the least, I want to thank my wonderful parents Deb and Mahua, and friends who constantly supported me through thick and thin during my PhD. It was not possible to come this far without their thorough motivation and unconditional love.

Contribution of Authors

Chapter 1 is a literature review that places my thesis question in the perspective of the larger field and points the significance of my research question. Chapter 2 represents a published manuscript for which I was the primary author along with Dr. Haojuan Wei (second author) who performed initial experiments. Dr. Haojuan Wei, the second author conducted the experiment shown in Figure 9. Dr. Jeff Miller, Dr. Chris Marshall, Dr. Jeremy Kropf and Dr. Neil Schweitzer also contributed with their suggestions and ideas for this research project. Bridget Basan helped with DFT calculations for figure 14. My research advisor, Dr. Randall Meyer contributed substantially to the writing of the manuscript and with the ideas on the project. Chapter 3 and 4 represents unpublished work for which I was the primary author. For chapter 3, initial studies were done by Dr. Haojuan Wei. My research mentor, Dr. Randall Meyer contributed to the writing of the chapters. Chapter 5 represents overall conclusions of my research and future goals.

Table of Contents

List of Figures

List of Tables

List of Abbreviations

Acac	**Acetylacetonate**
APS	**Advanced photon source**
BEP	**Brønsted−Evans−Polanyi**
CN	**Coordination number**
cNEB	**climbing nudged elastic band**
DFT	**Density functional theory**
DI	**Deionized**
DP	**Deposition precipitation**
EDX	**Energy-dispersive X-ray spectroscopy**
EXAFS	**Extended X-ray absorption fine structure**
FID	**Flame ionization detector**
GC	**Gas chromatography**
GC-MS	**Gas chromatography-Mass spectrometry**
GGA	**Generalizedgradientapproximation**
HAADF	**High angle annular dark field**
HREELS	**High resolution electron energy loss spectroscopy**
HRTEM	**High resolution transmission electron microscopy**
HTR	**High temperature reduction**
I	**Impregnation**
ICP	**Inductively coupled plasma**
IRA	**Infrared absorption**
IWI	**Incipient wetness impregnation**

LTR	**Low temperature reduction**
mIWI	**modified incipient wetness impregnation**
ML	**Monolayer**
MPV	**Meerwein-Ponndorf-Verley**
MRCAT	**Materials research collaborative access team**
NEXAFS	**Near edge X-ray absorption fine structure**
PAW	**Projector-augmented wave**
PW	**PerdewWang**
RAIRS	**Reflection absorption infrared spectroscopy**
RRC	**Research resources Center**
SAA	**Single atom alloy**
SEA	**Strong electrostatic adsorption**
SG	**Sol gel**
SMSI	**Strong metal support interaction**
SSHC	**Single site heterogeneous catalyst**
STEM	**Scanning transmission electron microscope**
TCD	**Thermal conductivity detector**
TEM	**Transmission electron microscopy**
TOF	**Turnover frequency**
TOR	**Turnover rate**
TPD	**Temperature programmed desorption**
TPR	**Temperature programmed reaction**
TS	**Transition state**

UHV	**Ultra high vacuum**
VASP	**Vienna ab initio simulation package**
WGS	**Water gas shift**
XANES	**X-ray absorption near edge structure**
XAS X	**X-ray absorption spectroscopy**
XPS	**X-ray photoelectron spectroscopy**
XRD	**X-ray diffraction**

Summary

This work investigates critical factors of catalysts, which play an important role in modifying activity and selectivity of heterogeneous catalysis. One such example is the selective hydrogenation of α,β-unsaturated aldehyde to α,β- unsaturated alcohol (using acrolein as a model reactant), which was used here as a probe reaction. Selective hydrogenation of acrolein to allyl alcohol is particularly challenging as it is difficult to obtain substantial selectivity towards C=O bond hydrogenation both thermodynamically and kinetically. The hydrogenation of C=C bond is about 35 kJ/mole easier than that of C=O bond. This is because acrolein molecule lacks substituents at C=C bond, which makes it especially vulnerable to hydrogenation towards saturated alcohol. Previous research has made great progress in understanding some of the factors (choice of metal, process condition, particle size1) that may improve selectivity. But there is no reported catalyst that provides high activity and selectivity at the same time. Thus we studied this reaction systematically from two aspects: 1) alloying effect by doping silver with a very dilute amount of hydrogen active metal; 2) support effects.

Pd−Ag alloy catalysts with very dilute amounts of Pd were synthesized. Extended X-ray absorption fine structure spectroscopy (EXAFS) results demonstrated that when the concentration of Pd was as low as 0.01 wt %, Pd was completely dispersed as isolated single atoms in Ag nanoparticles. The activity for the hydrogenation of acrolein was improved by the presence of these isolated Pd atoms due to the creation of sites with lower activation energy for H_2 dissociation. For the support effect study, a series of supported Ag catalysts using standard supports were prepared (SiO_2, Al_2O_3, TiO_2, CeO_2, ZrO_2, and La_2O_3) of different particle sizes to study the support effect on selectivity of acrolein hydrogenation towards allyl alcohol. On each support, a similar

particle size effect on selectivity (larger particle size, better selectivity) was observed. We found support reducibility plays an important role in modifying the selectivity towards the unsaturated alcohol as the selectivity towards allyl alcohol was higher for TiO_2, CeO_2, La_2O_3 supported catalysts than over SiO_2 and Al_2O_3 supported catalysts at the same particle size and at same conversion. A detailed pathway analysis and kinetics study is done on Ag/TiO_2 in an effort to understand the role of the support on catalyst performance. It is observed that the selectivity is as high as 88% at 1% conversion and then decreases to a stable 52% at 10% conversion. The selectivity to allyl alcohol was better than Ag/SiO_2 of same size at the same conversion. The reaction orders of both reactants were noticeably different for Ag/TiO_2 compared to Ag/SiO_2. Formation of Ti^{3+} sites is believed to favor the adsorption of acrolein through carbonyl bond which is also confirmed by DFT calculations. To conclude, we were able to demonstrate that both alloying and support effects play an important role in modifying both selectivity and activity, of Ag catalysts for selective hydrogenation of acrolein towards allyl alcohol. Another aspect studied, was structure sensitivity for this reaction where we observed Ag(100) is the most favorable surface for adsorption of acrolein (among Ag(221), Ag(111), Ag(100) surfaces) through carbonyl bond and thus shifting the reaction towards unsaturated alchol (desired product).

1.0 Introduction

1.1 Motivation and Background

Heterogeneous catalysts are known for their stability and robustness but tuning their selectivity at an atomic specific level remains a grand challenge for the catalysis community. In contrast, homogeneous catalysts are far more tunable than their heterogeneous counterparts but frequently suffer from poor activity and are not amenable to high throughput processes. The main disadvantage which flows from using heterogeneous catalysts is the availability of multiple active sites which possess their own activity, selectivity as well as energetics. For example, when examining the surface of a metal nanoparticle, a myriad of sites are available as shown in Figure 1, 2.[1]

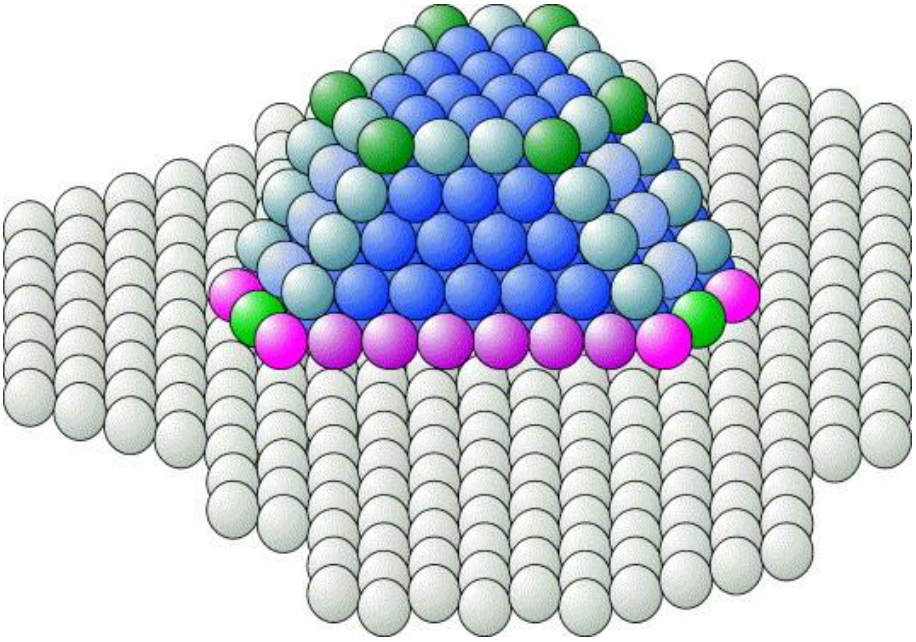

Figure 1 : Graphic representation of a cubo octahedral metal cluster on an insulating substrate.[1]

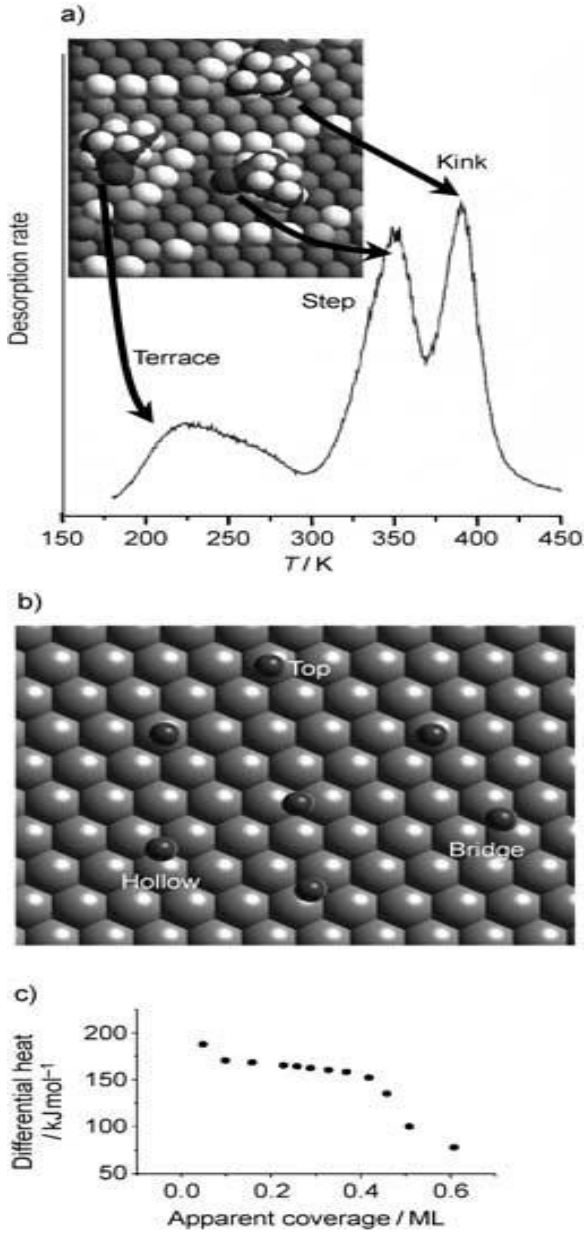

Figure 2 : a) A temperature-programmed spectrum showing three peaks corresponding to progressively stronger bound states of an adsorbate molecule (methylcyclohexanone) at terrace, step, and kink sites of a roughened copper surface.[2] b) Even on a flat surface, such as the (111) face of platinum, there are distinct sites for a molecule such as CO to be adsorbed. c) The decline in the heat of adsorption with increasing coverage of a flat single-crystal surface arises because of the heterogeneity of sites and mutual repulsion of species adsorbed at neighboring sites (ML=monolayer).[3]

It is seen the atoms located at the steps or kinks are stereo chemically completely different than the atoms located at the terrace sites and flat exterior surface. Even on terraces, sites of metal nanoparticles, adsorbate can interact with the surface in different bonding modes. For example, CO may adsorb on a Pt(111) surface in three different types of sites: atop, bridge and hollow. As a result, the adsorption enthalpy varies with site type and surface coverage resulting in the presence of different adsorbed species each exhibiting different energetic situations.[3]

Recently many groups have tried to heterogenize the homogenous catalysts as an approach to catalyst design whereby one can reap the benefits of both homogeneous (site specificity) and heterogeneous (high volume throughput) catalysts.[4-8] Most of these approaches rely on the use of organometallic precursors to generate highly disperse "single sites" on an oxide support. However, the metal atoms are typically in high oxidation states and lack metallic character and often deactivate quickly. This limits the type of reactions that may occur at these sites since many metal catalyzed reactions would no longer be accessible at temperatures and pressures that are typically employed. Therefore an alternative strategy has[9] recently been advanced by the Sykes group built on the creation of metallic single sites called Single Atom Alloys (SAA). The main characteristics of a SAA are: (1) the more active metal is present on the surface at very low concentration, (2) the atoms of this metal are thermodynamically quite stable when surrounded by the inert host metals such that dimers or trimers of the active metal are not formed. SAAs allow for the minimization of the use of the active expensive noble metals in typical heterogeneous catalysts while preserving their electronic character with minimal modification. The Sykes group showed how single Pd atoms could be adsorbed on Cu (111) surface which in turn act as active sites for selective

hydrogenation of acetylene to ethylene and the selective hydrogenation of styrene to ethyl benzene.[10] The authors used DFT calculations to show that the presence of single atom sites allows for the facile dissociation of hydrogen but the change in site geometry also results in weakly bound hydrogen atoms on the metal surface which then are very active for further reaction. In addition, the lack of contiguous Pd atoms prevents strong interactions between the hydrocarbon adsorbate and the metal surface so the hydrocarbons adsorb molecularly to the surface with low adsorption energies. In contrast, on a pure Pd substrate, hydrocarbon decomposition may occur and hydrogenation products such as ethylene are too strongly bound to desorb leading to unwanted over-hydrogenation. Recently in another study from the same group, they reported synthesis of Pd-Cu nanoparticle catalysts by incipient wetness impregnation of copper nitrate trihydrate using aluminum oxide (γ-Al_2O_3) as support.[11] Galvanic replacement, via the reaction of Cu with Pd^{2+} (in the form of Pd $(NO_3)_2$) to create Pd and Cu^{2+} was used to synthesize Pd/Cu SAA catalysts. $Pd_{0.18}Cu_{15}/Al_2O_3$ catalysts (numbers refer to mole percent) were observed to have more than an order of magnitude higher activity for phenyl acetylene hydrogenation when compared to their monometallic Cu- counterpart while sustaining high selectivity towards styrene for several hours at high conversion.[11] In this way, these SAA catalysts perform with the high selectivity of a low activity metal, but with a minimal decrease in the activity. In this study we will utilize this concept to exploit one of the factors (alloying) affecting selective hydrogenation of acrolein, an α, β–unsaturated aldehyde using conventional synthesis methods to demonstrate the viability of these materials for commercial processes.

Acrolein is the most challenging among the, *β*–unsaturated aldehydes to selectively hydrogenate to the unsaturated alcohol as it lacks any substituents on the C=C bond. Bulky

substituents sterically hinder the interaction between the olefinic bond and surface of the catalyst which deactivates the C=C bond and induces selectivity towards unsaturated alcohol. In this work, we are using the selective hydrogenation of acrolein as a probe reaction to study the reaction kinetics and mechanism of the chemo selective hydrogenation of α, β–unsaturated aldehydes. Reaction pathway is shown below in figure 3

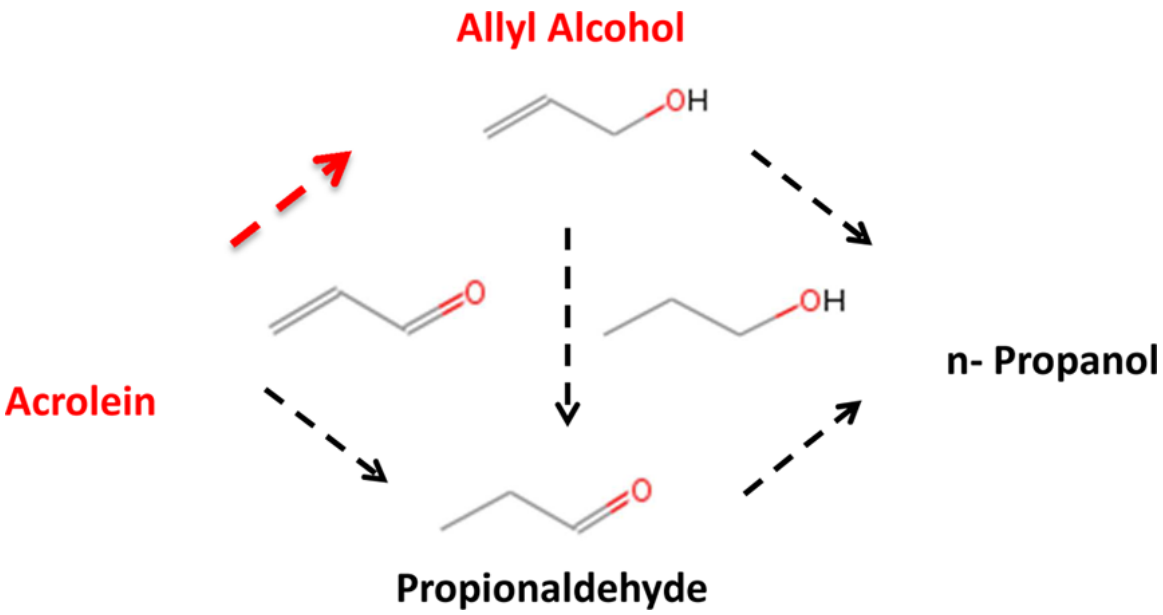

Figure 3: Schematic representation of Acrolein hydrogenation

Typical hydrogenation catalysts like Pd, Pt, Ru, and Ni exhibit poor selectivity to hydrogenate acrolein to allyl alcohol and produce either the saturated aldehyde or decomposition products instead. However, Claus and co-workers have reported that Ag catalysts exhibit up to 50% selectivity towards allyl alcohol, but they are not particularly active.[12] In previous work from our group, Wei *et al.* [7]showed how the particle size also affects the activity and selectivity to allyl

alcohol, showing the larger the particle size, the higher the activity and selectivity which can be attributed to favorable adsorption of acrolein through the carbonyl bond on terrace sites.[8, 13] Density functional theory calculations from our group also showed the activation energy for H_2 dissociation on Ag (111) surface (1.4 eV) is the quite high and is the rate determining step for acrolein hydrogenation.

A second metal may be alloyed with the active metal (in our case Ag) or a support may be used to improve selectivity (and possibly activity as well). The characteristic complexity of the bimetallic systems offers us additional possibilities and parameters to modify the reactivity and selectivity of the catalysts. The presence of the alloy or a support can result in a modification of the electronic properties of the catalytically active surfaces/sites. The adsorption site preference of the adsorbents, the reaction ensemble, the thermodynamics of the elementary reaction, the reaction mechanism can be affected and thus the reaction activity and selectivity, can be accordingly tuned. Changes in reactivity due to alloy creation or creation of new active sites due to use of metal oxide supports can include both electronic and geometric effects. Electronic effects that arise from changes in the bonding resulting from replacement of one metal with another or use of support, include charge transfer between the metals and changes in bonding hybridization. In contrast, structural variation can lead to ensemble effects in catalysis whereby the adsorbate(s) will adsorb in a particular geometry due to the arrangement of the surface atoms. In many cases, deciphering which of these two effects (if not both) are controlling the kinetics is difficult (if not impossible).

Most of the alloys used for selective hydrogenation of α, β–unsaturated aldehydes have employed a hydrogen active metal (usually a platinum group metal) with a more electropositive

metal in an effort to improve selectivity.[14] The electropositive metal acts as an electron-donor to increase the electron density on host metal. The selectivity to α, β–unsaturated alcohol can be rationalized to the preference of the catalyst surface for the carbonyl group in α, β–unsaturated aldehyde over the competing olefinic group. The increase in electron density in the active metal is repulsive to the C=C bond and as a result, the binding energy of C=C bond is weakened thus improving the selectivity to α, β–unsaturated alcohol. The metals in the first transition row, such as Fe or Co, and *p*-electron metals like Ge or Sn are often chosen as promoters.[15]

Several groups have previously examined the use of alloy catalysts for selective hydrogenation of carbonyl bonds in α, β–unsaturated aldehydes. For example, Englisch *et al*. found incorporating Ni, Co and Fe in SiO_2 supported Pt catalysts increased both selectivity and activity towards the unsaturated alcohol during crotonaldehyde hydrogenation while addition of Ga, Sn, Ge to Pt/SiO_2 increased selectivity but decreased activity. [16]Margitfalvi *et al*. describe how silica supported Pt-Sn catalysts show improved selectivity towards crotyl-alcohol formation compared to their monometallic counterparts. They observed highest S_{CO} selectivity (around 70%) and it was obtained at atomic ratio of Sn/Pt =3.[17] Sokolskii *et al*. studied the addition of iron (III) oxide to group VIII metals for the hydrogenation of crotonaldehyde in water at 293 K. They observed that upon addition of iron (III) oxide the activity decreased for osmium, ruthenium and platinum but increased for palladium, rhodium and iridium. The selectivity towards the carbonyl group increased for all group VIII metals upon addition of iron (III) oxide, except palladium. The selectivity to hydrogenation of the carbonyl group over the group VIII metals followed the given order Os > Pt > Ir > Ru > Rh. Before addition of iron (III) oxide to platinum, the selectivity to the

hydrogenation of the carbon-carbon double bond was 91%, but after addition of iron(III) oxide the selectivity changes to 80 % towards hydrogenation of the carbonyl group.[18]

Galvagno and coworkers have worked broadly on the selective hydrogenation of α, β - unsaturated aldehydes in the liquid phase over platinum and ruthenium catalysts with and without promoters. Galvagno and coworkers observed the selective hydrogenation of acrolein and cinnamaldehyde by using platinum/nylon catalysts promoted with tin or germanium as a promoter. They obtained 65% allyl-alcohol and 75% cinnamyl alcohol in hydrogenation of acrolein and cinnamaldehyde respectively over nylon supported unpromoted platinum catalysts.[14] When germanium was used as promoting agent, 95% selectivity to cinnamyl alcohol was obtained.[19] Other promoting agents were also examined including sodium, aluminum, calcium, selenium and iron, but only iron promoted catalysts showed improved selectivity. Galvagno and coworkers proposed that addition of promoters has two principal effects. First, tin results in the deactivation of platinum sites for hydrogen addition to the unsaturated carbon-carbon bonds. The presence of the promoter blocks the active platinum sites or modifies the electronic interaction between the adsorbate and the platinum site to weaken the chemisorption bond between the molecule and the platinum site. In addition, the promoter may help activate the carbonyl group to facilitate selective hydrogenation of crotonaldehyde. The presence of an additive increases the charge of polarization on the carbonyl group which again increases its reactivity towards hydrogen.[20]

Marinelli and Ponec previously examined Sn for its ability to improve the selectivity of Pt catalysts for acrolein hydrogenation and found that selectivity to allyl alcohol jumped from 1% to 27% after addition of tin. The authors suggested that tin was, in fact, not present as an alloy (based on the fact that similar PtCu systems did not show enhanced selectivity) but rather as SnOx.[21]

However, Sautet and coworkers used density functional theory studies of the adsorption of crotonaldehyde and acrolein on PtSn surfaces to show that perhaps reactive ensembles could be important. The adsorption of the unsaturated aldehyde in the proper configuration for selective hydrogenation was favored on the Pt_3Sn and Pt_2Sn surfaces due to charge transfer from Sn to Pt, leading to a Sn+ site which allows for bonding with the aldehyde functionality.[22]

In the PtSn system, it is not clear if the improvement in selectivity is due to electronic or geometric effects since one could also note that the presence of Sn greatly weakened the adsorption energy of acrolein to the surface and therefore prevented deleterious C-C bond cleavage reactions from occurring. Bimetallic alloys can also adopt core-shell configurations whereby the surface is uniform but the presence of the alloying metal in the subsurface affects its reactivity. One unique version of a core-shell type alloy is a sandwich alloy by which a single layer of one metal is inserted into the second layer of a slab of the second host metal. Chen and co-workers have examined the effect of a Pt sandwich alloy with Ni present in the subsurface. Acrolein would not bond to Pt(111) and Ni/Pt(111) via the di-σ-C=O configuration, but does bond in this configuration to the Pt/Ni/Pt(111) surface. The authors speculate that the selectivity could be further improved with proper tuning of the electronic structure of the surface to shift the binding energy difference between different adsorption configurations of acrolein. [11, 23-25]

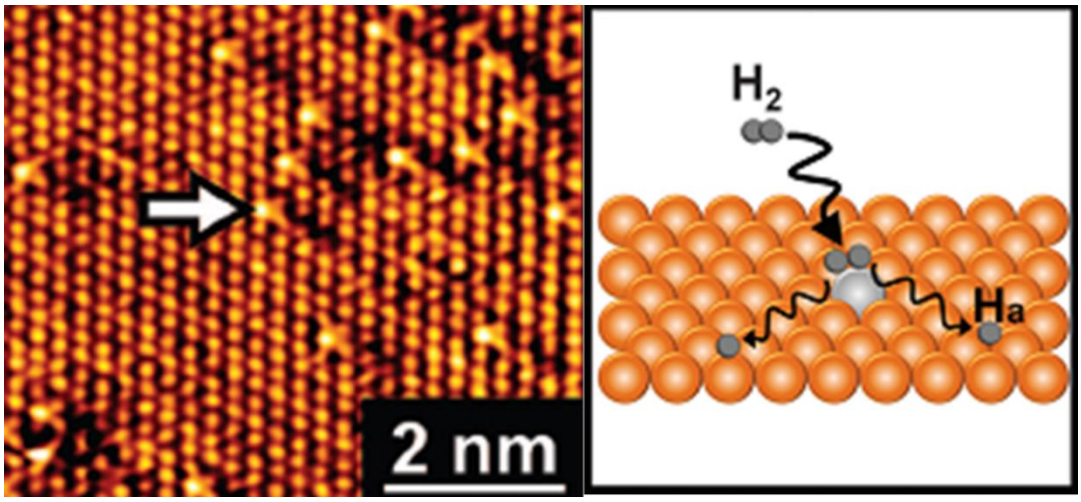

Figure 4: STM images showing atomically dispersed Pd atoms in a Cu(111) surface and hydrogen atoms that have dissociated and spilled over onto the Cu surface.[10]

As mentioned above, we will use a novel class of catalysts denoted by Sykes *et al*. as Single Atom Alloys (SAA).[10] Using this strategy of Single Atom Alloy catalysts by embedding a small amount of a H_2-active metal in an otherwise inert host metal allows for an active catalyst while maintaining high selectivity. Sykes *et al*. used a combined temperature programmed desorption and scanning tunneling microscopy study to show how individual Pd atoms are embedded on Cu (111) surface. 0.01 ML, and 0.1 ML of Pd were deposited on Cu surface and hydrogenation of styrene and acetylene were used to measure catalytic properties of this SAA. STM images confirm hydrogen atoms were able to dissociate on isolated Pd atoms which act as active sites and then spilled over to the Cu-surface depicted in figure 4.

DFT calculations with the experimental results showed reduction of the barrier for hydrogen dissociation from 0.40 eV (on bare Cu surface) to 0.02 eV (on Pd@Cu SAA), but enthalpy was not extensively affected (-0.35 eV on SAA but -0.20 eV on Cu(111)). Temperature Programmed

Reaction exhibited selectivity of acetylene to ethene as high as 95% on 0.01 ML Pd/Cu (111) while the selectivity to ethene on 1 ML Pd/Cu (111) was barely 33%. Selectivity of styrene hydrogenation to ethylene benzene was also improved using Pd@Cu SAA and showed much less hydrogenation of the aromatic ring. Also, the desorption temperature reduced interestingly from 310 K on Cu(111) to 220 K on 1 ML Pd/Cu(111) followed by further reduction to around 180 K on 1 ML Pd/Cu(111). These results motivated us to employ this new technique for our study.

In their study Sykes et al. [11]reported a new method of synthesis of Pd-Cu SAA catalysts which showed greater than 94% selectivity of phenyl acetylene hydrogenation to styrene which is a significant improvement compared to Pd- monometallics with same amount of Pd loading and at same conversion. X-ray photoelectron spectroscopy and UV-vis spectroscopy measurements confirmed uptake of Pd and alloying of Pd with Cu by galvanic replacement. In their temperature programmed study, they showed how a single desorption peak shifted to a lower temperature as Pd coverage increased. Hydrogen saturation is reached at a coverage of Pd greater than 2ML. At this point, a second layer of island of Pd is formed before first layer is completed. Boucher et al. also argued that detailed observation of the H coverage at low Pd coverages (< 1ML) showed H uptake is much higher than amount of Pd present on the surface. This clearly indicates spillover of H atoms onto Cu (111) surface due to the presence of Pd which facilitates H_2 activation on the otherwise inert surface.

In one of the earlier studies, Lucas and Claus reported that a 9Ag-0.75In/SiO_2 (9 wt% of Ag, 0.75wt% of In) catalyst showed 61% selectivity towards allyl alcohol at 97% conversion.[26, 27] X-ray diffraction studies were also done on these alloys which confirmed an Ag_3In alloy phase formation with reduction of catalyst at 603 K which again agrees with the calculations of Delbecq

and Sautet [21] that presence of a main group alloying metal favors hydrogenation of acrolein through carbonyl bond.

Another important factor which comes into play for heterogeneous catalysis is choice of support. We have chosen selective hydrogenation of an α, β–unsaturated aldehyde as a probe reaction to explain the changes in kinetics and mechanism of the reaction introduced by interaction of different supports with the active metal which often result in enhancing catalytic activity and selectivity of the metal catalyst. The selection of the best catalytic support [28-31] is not only important for proper dispersion of the active metal, but can also modify the observed reactivity by altering the electronic structure of the metal or by formation of interface sites. Hydrocarbon hydrogenation reactions generally do not exhibit strong support effects since the reaction occurs solely on the metal. However, CO hydrogenation has been observed to be among those reactions, most cited for support and promotional effects.

Vannice and coworkers studied the effects of the support on the intramolecular selectivity of crotonaldehyde hydrogenation over platinum. They discovered that certain supports such as TiO_2 can drastically increase the rate of carbon monoxide hydrogenation over Group VIII metals. However, this rate increase has not been observed for hydrogenation of carbon-carbon double bonds or aromatic rings. From this, they inferred that a metal-support interaction is responsible for activation of carbon monoxide and by analogy activated the carbonyl function of crotonaldehyde instead of the olefinic bond. They suggested new special sites are formed at metal-support interface. The site is proposed to be composed of at least one metal atom adjacent to a defect site on the support such as Ti^{3+} cation or an oxygen vacancy. The interaction is thought to occur between the oxygen atom of the carbonyl group and the support. Reducing the catalyst at high

temperature allows these TiO_x species to move to the surface forming more Pt-TiO_x sites to activate the carbonyl bond.[30, 31]

In another study, Bron et al. investigated support effects for acrolein hydrogenation using Ag catalysts on SiO_2, Al_2O_3 and ZnO, all synthesized by Incipient Wetness Impregnation and tested under same temperature and pressure. SiO_2, Al_2O_3 showed similar selectivities of around 39% and 42%, respectively, while Ag/ZnO exhibited a selectivity of 50%. However, the particle size of the catalysts varied as well (Ag/SiO_2 was only 2.5 nm; that of Ag/Al_2O_3 was 11 nm; Ag/ZnO had very broad size distribution and the particle size could not be estimated). So, the difference in selectivity could also be a result of a particle size effect rather than a support effect.[4]

In another study of selective acrolein hydrogenation showing a different type of geometric effect, Claus and co-workers studied Au catalysts that were coated with indium. High resolution TEM images showed that the indium coated the terraces of the Au nanoparticles leaving only the edges exposed. The gold particles covered with indium were still half as reactive as those not covered by indium with a much better selectivity to allyl alcohol (63% vs. 34%). This led the authors to conclude that the exposed corners and edges must be the reactive site for the selective hydrogenation of the C=O group.[32]

In our study, we will be using Ag alloys as well as supported Ag catalysts using various reducible oxide supports to see the alloying effect and support effects on acrolein hydrogenation (as opposed to platinum which is more suitable for larger α, β unsaturated aldehydes). Moreover we will also explore how surface structure of Ag plays an important role in modifying the selectivity of Ag catalysts

1.2 Theoretical studies

Theoretical studies of the Pt-Sn system by Van Santen [33] and Williams [34] led to the inference that the surface of bimetallic cluster will be strongly dominated by tin, with a depletion of tin in the layer directly below the surface. Bowman and Biloen[35] used XPS and Auger spectroscopy and Verbeek and Schatler used TPD to examine Pt-Sn alloys and found that the experimental results they obtained were in agreement with the predictions of Van Santen and Williams. Verbeek and Schatler [36] also used TPD to examine Pt-Sn alloys and found that as the proportion of tin in the alloys was increased, the desorption of carbon monoxide and deuterium became much easier. This activity can be a shift in the d-band center of Pt to lower energy due to charge transfer between Pt and Sn. The authors referred this as ligand effect.

Delbecq *et al.*[37] examined various adsorption modes for acrolein on the (111) surface of Pt [38] and $Pt_{80}Fe_{20}$ with spin-polarized density functional theory. Acrolein showed its main interaction with the surface with the C=C bond over a large range of coverages on the Pt(111) surface, combined with weak interaction with the oxygen atom. This could clearly result in a predominant hydrogenation of the C=C bond, as was seen experimentally. As for the $Pt_{80}Fe_{20}$ (111) surface, a strong segregation of platinum atoms towards the surface layer occurred when the surface was clean. However, the significantly greater aldehyde-surface interaction energy upon the formation of O–Fe bonds can alter the surface composition (the adsorption energy of acrolein on Pt(111) via a di-σ CO configuration was 0.25 eV but its counterpart on $Pt_{80}Fe_{20}$(111) was 0.68 eV) and increase the Fe content in the surface layer. Thus the presence of Fe allows the potential to influence the hydrogenation selectivity in favor of unsaturated alcohols.[37]

Silver is particularly interesting because of its exceptional selectivity for selective hydrogenation of acrolein. Rösch and co-workers studied the adsorption of acrolein on flat Ag(110) and stepped Ag(221) surfaces.[39] C=O bond was expected to be activated according to experimental results. However, the calculations showed acrolein to interact only weakly with all adsorption sites under study (by at most 35 kJ·mol-1, obtained on Ag(211) step through a η4(C,C,C,O) configuration), resulting restricted C=O bond activation. Though Rosch and coworkers found weaker adsorption on denser Ag(111) surface (~10 KJ/mol^{-1}) with molecular plane parallel to the surface, the energetics switched such that the selectivity favors allyl alcohol when O was present in the subsurface.[40]

However, Ferullo *et al.*[13] explained that there is a coverage dependence of the structure of adsorbed acrolein on Ag(111) surface. They calculated the adsorption modes of acrolein at various coverages by changing the sizes of Ag(111) supercells. *p*(4×4) and *p*(2×2) were used in the case of "head to tail" adsorption, representing low and high coverages while supercells *p*(5×3) and *p*(4×2) were employed to examine the "head-to -head" adsorption mode. In the case, where acrolein molecules were arranged in head-to-tail manner, change of coverage did not modify the mode of adsorption. Acrolein remained parallel to the Ag(111) surface at both low and high coverages. For the *p*(5×3) supercell, the adsorbates form almost isolated dimers and adsorbed parallel to the surface. However, for the *p*(4×2) structure, an entirely different scenario of adsorption evolved as the molecular network revealed chains of adsorbed acrolein in a zigzag pattern,. Each molecule in this case, interacted with two closest neighbors through O···H contacts (figure 5). It is evident that in one row of the zigzag structure, the molecules were almost perpendicular to the surface. Thus oxygen atoms from the carboxyl group were much closer to the

surface, so that reaction with adsorbed atomic hydrogen should be more facile. This result provides a potential explanation for the observation [41]that increasing reaction pressure improves the selectivity to allyl alcohol. This work also implies that improvements in selectivity as the particle size increases (due to increasing fraction of (111) facets) should be expected.

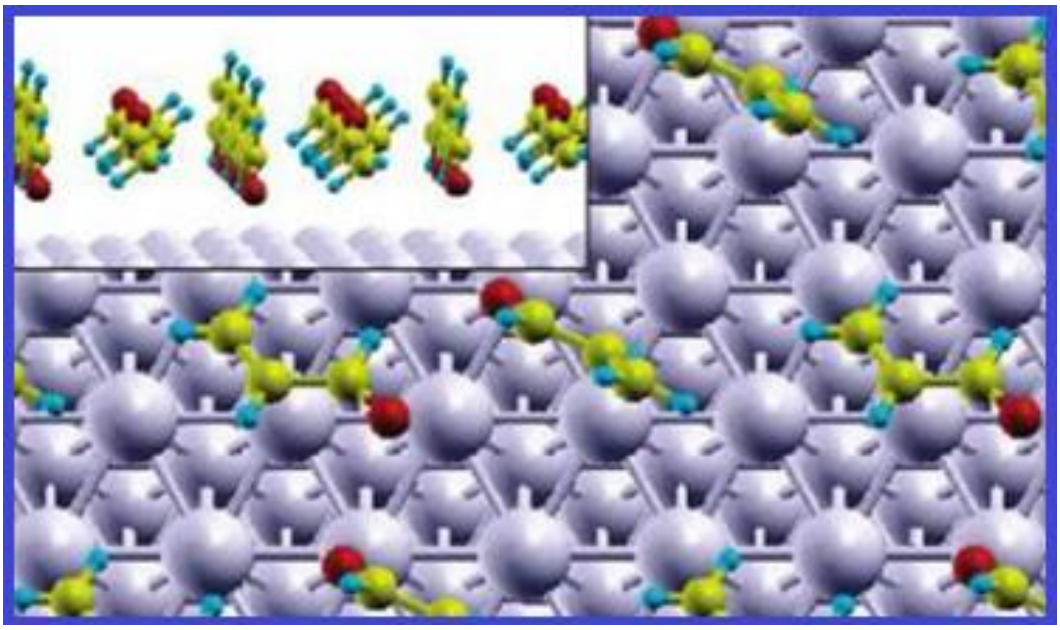

Figure 5: Optimized geometry of the network of adsorbed acrolein on Ag(111) corresponding to the *p*(4×2) supercell.[13]

1.3 Experimental

1.3.1 Experimental methodology: kinetics study and pathway analysis

Detailed kinetic studies, including determination of rate laws, reaction orders and rate constants help us develop understanding of the reaction mechanism. This in turn leads us to design a better catalyst to increase the process selectivity/reactivity and achieve optimum reaction conditions.

1.3.1.1Kinetics study

One of the major problems of kinetics study is the accurate determination of reaction rate avoiding mass transfer limitation. The reaction rate should be measured in kinetically controlled regime. When the catalyst grain size is reduced, the Thiele modulus decreases as the reactant molecule decreases as the reactant molecule can easily travel in or out of pores. The first thing to ensure is that catalysts testing is done in the limit of differential conversion. The reaction rate should be derived at low conversion, where concentration is almost constant. A linear relationship between conversion and 1/F (F= flow rate) should exist if it is in the limit of differential conversion. Also reproducibility can be checked by repeating the tests several times. However, when using porous materials as supports, it is possible that the diffusion of the reactant molecules into the support pores is the rate limiting step, which then interferes with the intrinsic reaction kinetics. A possible way to estimate the effect of mass transfer is through the use of a dimensionless variable, $\Phi=\sqrt{kR^2/D}$, known as the Thiele modulus (where k is the intrinsic rate constant, R is the characteristic diffusion length (i.e. the catalyst pellet radius) and D is the diffusion coefficient). If Thiele modulus has a high value (generally $\Phi >> 1$), we are in the mass transfer limited regime. However, if we have a low Thiele modulus ($\Phi << 1$), we are under kinetic control. To prove the rate measurement is within the kinetics-control regime, this catalyst is ground to larger mesh size (60 to 325 mesh; R changes from 250 to 44 μm) and was retested. If the rate is the found to be the same, the rate is observed is the true intrinsic rate. However, if the rate increases, this implies that the rate at the smaller mesh (larger grain size) is actually mass transfer limited.

Once we have successfully proved that we can estimate intrinsic kinetics with high reproducibility (within 4%), we can continue to evaluate the kinetic parameters. We begin with a simple rate law[7]**:**

$$\mathbf{r= k[Acrolein]^m[H2]^n}$$

where k is the intrinsic rate constant. By changing the concentration of each reactant, m and n can be calculated. A linear relationship between ln(r) and ln[Acrolein] will develop by taking the natural logarithm of the rate equation as following equation:

$$\mathbf{ln[r] = ln[k] + mln[Acrolein] +nln[H_2]}$$

Since k is a constant at a certain temperature, the slope of plotting ln(r) against ln[acrolein] is m when keeping the concentration of H_2 constant. n can be achieved in the same manner. At the same time we can also calculate the reaction constant k. As a result the pre-exponential factor A in Arrhenius Equation is found.

According to Arrhenius Equation: $\mathbf{k = A\ exp[-E_a/(RT)]}$, taking the natural logarithm of it yields:

$$\mathbf{ln[k] = [-E_a/(RT)] + ln[A].}$$ [7]

Plotting ln(k) against 1/T generates a straight line, the slope of it is –Ea/R. Thus the activation energy can be calculated.

1.0.1.1 Pathway analysis

In a complex reaction network, explanation of the reaction pathway is not easy. A pathway analysis has also been done for 8Ag/TiO2_IWI_R325. This method was developed by Bhore et al. [42] for discernment of the rank (i.e., primary, secondary, etc.) of a reaction product. We begin by examining a first rank plot whereby the selectivity to various products as a function of conversion.[7]

The first-rank delplot method, permits one to separate the primary product from non-primary products. The conversion vs. selectivity plot is developed and extrapolated to zero conversion. If the intercept for a particular product is nonzero, the product is primary. If the intercept is zero, the product is non-primary. Higher rank products can be determined by a higher rank delplot. For example, secondary products can be separated by plotting (component selectivity)/ (conversion) against conversion. At zero conversion, primary products have infinite intercepts, secondary products have finite intercepts and higher-order ones have zero intercepts.

The advantage of doing the first-rank plotting is not only to distinguish the primary products from the higher rank products, but also to develop a relationship between selectivity and conversion so that the selectivity for a specific conversion can be estimated. The selectivity at 10% conversion and that at 90% are frequently quite different depending upon the nature of the reaction network. Once the relationship between selectivity and conversion is determined (holding temperature constant and varying conversion via changes in space velocity), the conversion can be calculated for all the catalysts and also selectivities at a given conversion. [7]

1.3.1.2 Characterization techniques

Extended X-Ray Absorption Fine Structure Spectroscopy*:* Ag K edge EXAFS was employed to estimate the particle sizes since the loading of palladium was very low and therefore the particle size can be estimated directly from the Ag coordination number.[7, 43] Pd K edge EXAFS was used to investigate the environment of palladium. EXAFS spectra were taken at the beamline of the Materials Research Collaborative Access Team (MRCAT, 10-ID) at the Advanced Photon Source (APS), Argonne National Laboratory. However, for the Pd K edge of the SAA materials, we perform the experiment in the fluorescence mode, which enhances the sensitivity by orders of

magnitude over transmission EXAFS.[44] Fluorescence EXAFS measurements were made using a log-spiral-bent silicon Laue analyzer with scintillation detectors as described by Kropf et al.[45] All the samples were ground and packed into a sample holder. They were then reduced in 3.5% H_2/He at 200°C for one hour, cooled in H_2/He and scanned at room temperature in H_2/He in an environmental cell. Samples were scanned in transmission mode at Ag edge and in fluorescence mode at Pd edge. Metal foils were scanned at the same time for energy calibration. The WINXAS 3.1 program was used to fit the data to calculate the coordination number and bond distance between neighboring Ag atoms, using a k^2-weighted Fourier transform. The least squares fit in k-space of the k^2weighted Fourier transform is done using data from 2.6 to 12.1 $Å^{-1}$.The Ag-Ag phase and amplitude functions were acquired from the first coordination shell of Ag foil (N_{Ag-Ag} = 12 at 2.889 Å). An empirical relationship between the coordination number and particle size previously obtained from a series of platinum samples was used since both silver and platinum are fcc (face centered cubic) metals.[43] However, since there is no specific rule to choose the Debye–Waller factor (DWF), some error is introduced in our size estimation. This error in the fits was determined by fixing the difference in the DWF between the reference and the samples at 0.001 $Å^2$. The error in the absolute particle diameter we estimate to be ±10% and in R was ±0.02 Å[46], within the normal range of fitting errors of EXAFS. Fits were performed by changing the coordination number (CN), bond distance (R), σ^2, and energy shift (E0). The σ^2 value was fixed through all sample fits, and CN and R were allowed to change in turn to determine the correct fit.

Transmission Electron Microscopy (TEM): High Resolution TEM images were obtained at UIC's Research Resources Center facility using the JEM-3010 (a 300kV transmission electron microscope with a LaB_6 electron source). The JEM-3010 is an ultrahigh resolution analytical

electron microscope with a point resolution of 0.17 nm. Sample was dispersed in deionized water or isopropanol and sonicated for 20 min. Imaging was performed in a bright field mode with an objective aperture selected to permit lattice imaging. A minimum of 100 particles were counted to get an accurate representation of the particle size distribution for each catalyst using Digital Micrograph software.

1.3.2 Preview of experiments

1.3.2.1 Effect of Alloying on Selective Hydrogenation of Acrolein: Single Atom Alloy

Pd-Ag alloy catalysts with very dilute amounts of Pd were synthesized. EXAFS results demonstrated that when the concentration of Pd was as low as 0.01 wt%, Pd was completely dispersed into isolated single atoms in Ag nanoparticles. Activity for the hydrogenation of acrolein was improved by the presence of these isolated Pd atoms due to the creation of sites with lower activation energy for H_2 dissociation. In addition, for the same particle size, the 0.01%Pd/8%Ag alloy nanoparticles exhibited higher selectivity than their monometallic counterparts, suggesting that the Pd atom may act as a site for the favorable bonding of the acrolein molecule for facile hydrogenation of the aldehyde functionality.[25]

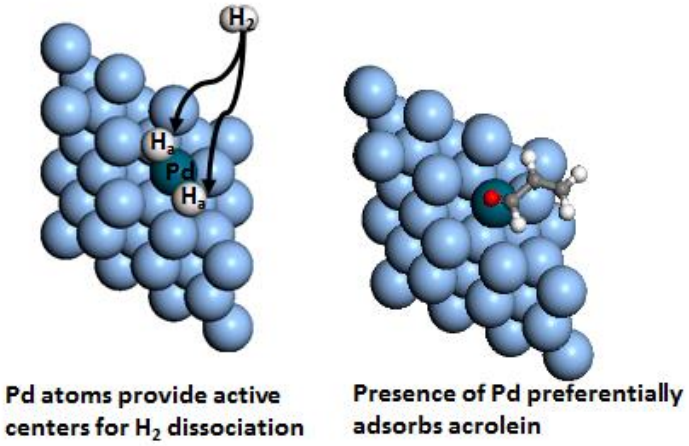

Figure 6: Hydrogen dissociation on adsorbed Pd atoms on Ag(111)[25]

1.3.2.2 Effect of Supports on Selective Hydrogenation of Acrolein using Silver Catalysts

A series of supported catalysts using standard supports are prepared (SiO_2, Al_2O_3, and TiO_2, CeO_2, ZrO_2, La_2O_3) of different particle size to study the support effect on selectivity of acrolein hydrogenation towards allyl alcohol. On each support, a similar particle size effect on selectivity (bigger particle size, better selectivity) was observed. We found partially reducible supports play an important role in modifying the selectivity towards the unsaturated alcohol as the selectivity towards allyl alcohol was better on TiO_2, CeO_2, La_2O_3 as well as on ZrO_2 (not a partially reducible support) than over SiO_2 and Al_2O_3 at the same particle size and at same conversion. A detailed pathway analysis and kinetics study is done on Ag/TiO_2 in an effort to understand the role of the support on catalyst performance. It is observed that the selectivity is as high as 88% at 1% conversion and then decreases to a stable 52% at 10% conversion. For both higher and lower conversions, the selectivity to allyl alcohol was better than Ag/SiO_2 of same size. The order of the

reaction with respect to both reactants noticeably changed on TiO_2 compared to SiO_2 (with H_2, it changed from 0.65(on SiO_2) to 0.74 (on TiO_2) and for acrolein changed from 0.77 to 0.18). In addition the pathway was significantly different compared to SiO_2 (on SiO_2, allyl alcohol and propanal both were primary products while on TiO_2, only allyl alcohol is observed to be the primary product). Formation of Ti^{3+} sites are believed to favor the adsorption of acrolein through carbonyl bond which is also confirmed by DFT calculations (Acrolein adsorbs more favorably (-0.99 eV) through carbonyl bond than olefinic bond (-0.45 eV)).

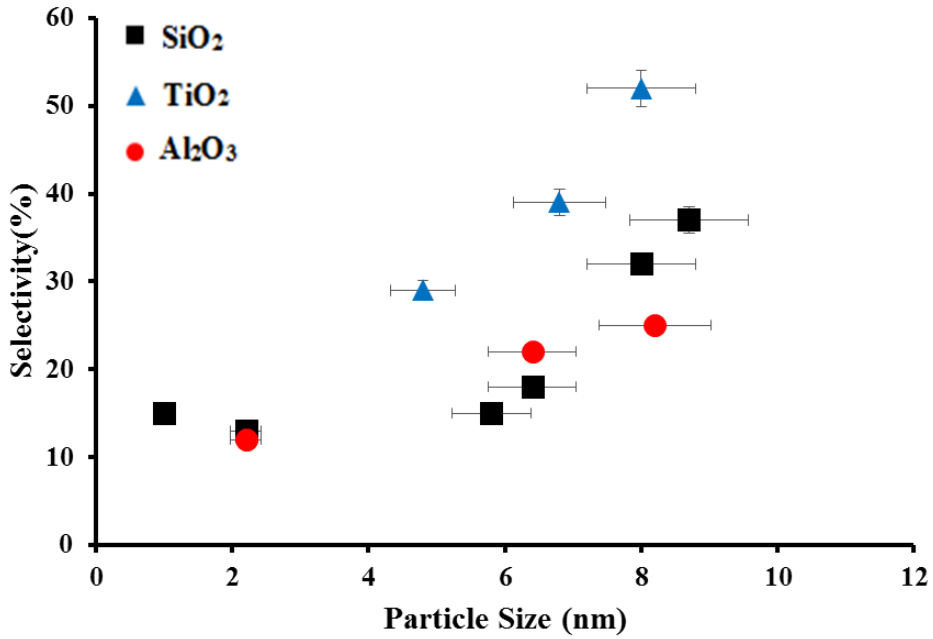

Figure 7: Change in Selectivity due to support effects

1.3.2.3 Effect of Surface Structure on Selective Hydrogenation of Acrolein using Silver Catalysts

Structure sensitivity plays an important role on adsorption of acrolein on the surface of Silver. Previously, different scientists have explored various types of surfaces (stepped and flat) to understand role of surface geometry on adsorption of acrolein. For example, Rösch and co-workers investigated the adsorption of acrolein on flat Ag(110) and stepped Ag(221) surfaces[39, 40]. C=O bond was predicted to be activated according to experimental results. However, the calculations showed acrolein to interact only weakly with all adsorption sites studied, (by at most 35 kJ·mol-1, obtained on Ag(211) step through a η4(C,C,C,O) configuration), causing very limited C=O bond activation. They also mentioned that weaker adsorption was observed on denser Ag(111) surface (~ 10 kJ·mol-1) with the molecular plane parallel to the surface. Rösch and co-workers went on to examine hydrogenation of acrolein over Ag(110) and Ag(111) with O in the subsurface[40]. The authors found presence of O on the surface brought a significant change in energetics switching the pathway to favor selectivity towards allyl alcohol.

However, opposing the results of Rosch, Ferullo *et al.* [13]showed that there was a coverage dependence of the structure of adsorbed acrolein on Ag(111) surface. They calculated the adsorption modes of acrolein at different coverages by changing the sizes of Ag(111) supercells and found a dependence of mode of adsorption of acrolein on the surface coverages. In our study, we chose three different surfaces Ag(100), Ag(111) and Ag(221). We have found using DFT calculations that acrolein bonds through the carbonyl bond more favorably on the Ag(100) surface. This is in stark contrast to other surfaces where acrolein prefers to bond through the C=C bond. It seems logical that strong improvements to the selectivity to allyl alcohol might be realized if

nanoparticles with only (100) surfaces could be utilized in this reaction as the C=O will be easier to hydrogenate on this surface. In this project, we are investigating different transition states for this reaction to understand the actual pathway for this reaction on different surfaces.

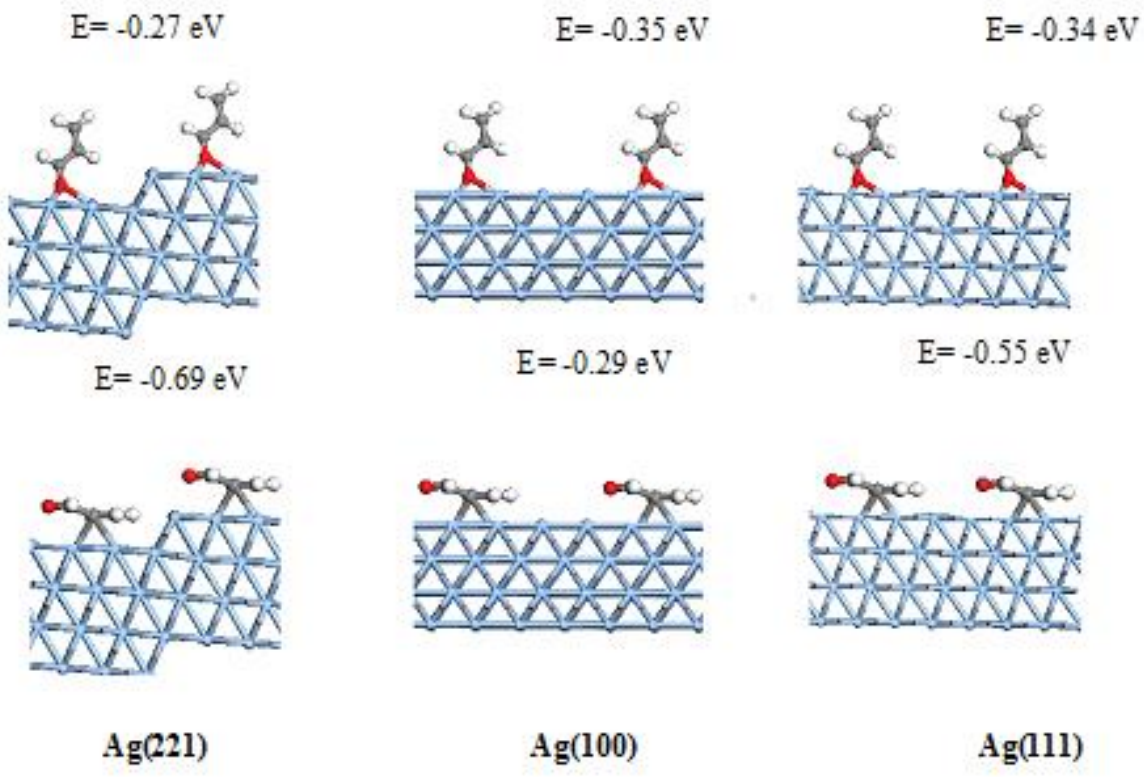

Figure 8: Acrolein favorably adsorbed through C=O bond on Ag(100) surface

2.0 Single Atom Alloy Pd-Ag Catalyst for Selective Hydrogenation of acrolein

This work is previously published in Journal of physical chemistry as Aich, P., Wei, H., Basan, B., Kropf, A. J., Schweitzer, N. M., Marshall, C. L., Miller, J. T., and Meyer, R. (2015) Single-Atom Alloy Pd–Ag Catalyst for Selective Hydrogenation of Acrolein, The Journal of Physical Chemistry C 119, 18140-18148.

2.1 Introduction

The creation of atomically uniform sites in heterogeneous catalysis remains a long standing goal of the catalysis community. To this end, several groups have recently attempted to heterogenize homogenous catalysts either through tethering to the support [47-51] or by exchanging ligands with active center-support bonds that tune the electronic structure of the active site.[52-60] Another strategy for atomically uniform sites comes from the example of Sykes et al., who showed that single Pd atoms could be embedded in a Cu(111) surface and act as active sites for the selective hydrogenation of acetylene to ethylene and the hydrogenation of styrene to ethylbenzene.[10] The creation of single atom alloys is based upon the creation of a metal nanoparticle (of a relatively inert metal) with an active metal embedded in the particle. Here we exploit this idea to show an enhancement in another selective hydrogenation reaction: the hydrogenation of acrolein.

Acrolein is an α, β–unsaturated aldehyde which is particularly difficult to selectively hydrogenate to produce α, β–unsaturated alcohol compared to all the other higher homologues due to a lack of substituents on C=C bond (a reaction scheme is shown in figure 3). Typical hydrogenation catalysts using platinum, palladium, or ruthenium are very active but not selective

to allyl alcohol (the desired product). Instead the primary metal of choice is Ag, [4, 6, 7] which has been shown to exhibit higher selectivity, but low activity. This low activity is not surprising since silver is known to exhibit poor hydrogen activation. Therefore one factor for increasing the reaction is to facilitate the dissociation of H_2. However, there is a trade-off between high selectivity and high activity in that high selectivity to allyl alcohol is a result of the weak binding of acrolein (which is favored over Ag) whereas the efficient dissociation of H_2 takes place over metals such as Pd and Pt which are too reactive for molecular adsorption of acrolein and selectivity shifts towards undesired products.[61-64]

Alloys have been employed previously for the selective hydrogenation of *α, β*–unsaturated aldehydes. For example, Rh-Cu/SiO_2 alloy catalysts showed both higher selectivity and activity to crotyl alcohol in the selective hydrogenation of crotonaldehyde.[65] While the selectivity to crotyl alcohol was 55% and 18% on pure Cu and pure Rh catalyst, respectively, the selectivity to crotyl alcohol increased to 74% over a Rh-Cu alloy (having 33% atomic ratio of Rh) catalyst. Similarly, the Turn over Frequency (TOF) was increased from 7.6×10^{-3} s^{-1} over pure Rh/SiO_2 to 11.7×10^{-3} s^{-1} over 0.33Rh-Cu/SiO_2. It was claimed that the improvement of catalyst performance was due to better Rh dispersion when Cu was present.

In another study of alloy effects in selective hydrogenation, Marinelli and Ponec examined Sn for its ability to improve the selectivity of Pt catalysts for acrolein hydrogenation and found that the selectivity to allyl alcohol jumped from 1% to 27% after addition of tin .[66] The authors suggested that tin was in fact not present as an alloy (based on the fact that PtCu systems did not show enhanced selectivity which forms an alloy) but rather as SnO_x. However, Sautet and coworkers used density functional theory studies of the adsorption of crotonaldehyde and acrolein

on PtSn surfaces to show that perhaps reactive ensembles involving Sn could be important. [21]The hydrogenation of acrolein, crotonaldehyde and prenal was studied over two Pt-Sn alloy surfaces, p(2×2) Pt_3Sn(111) and ($\sqrt{3}\times\sqrt{3}$) R30° Pt_2Sn(111). The adsorption energies on alloy surfaces were lower than on pure Pt for each of the unsaturated aldehydes studied in every configuration. However, the changes in the adsorption energies varied such that the adsorption of the unsaturated aldehyde in the proper configuration for selective hydrogenation was favored on the Pt_3Sn and Pt_2Sn surfaces due to charge transfer from Sn to Pt, leading to a Sn+ site which allows for bonding with the aldehyde functionality. The repulsive effect of the substituents on the C=C bond was also found to increase as the molecule size increased, so the selectivity enhancement was most prominent for prenal.[21, 67]

Subsequent experiments by Haubrich et al. on the adsorption and thermal decomposition of crotonaldehyde on the same Pt-Sn alloy surfaces,(i.e. Pt_3Sn/Pt(111) and Pt_2Sn/Pt(111), and Pt (111) surface as comparison ,[67] showed that the higher the surface composition of Sn, smaller the desorption peak of crotonaldehyde was observed in the TPD spectra, implying weaker interaction between crotonaldehyde and the surface with addition of Sn. Accompanying DFT calculations suggested that the saturation coverage of crotonaldehyde on Pt_3Sn and Pt_2Sn, involves the favorable η^1-top-OSn configuration which could explain better selectivity to unsaturated alcohol over Pt-Sn alloys.

Bimetallic alloys can also adopt core-shell configurations whereby the surface is uniform but the presence of the alloying metal in the subsurface affects its reactivity. One unique version of a core-shell type alloy is a sandwich alloy by which a single layer of one metal is inserted into the second layer of a slab of the second host metal. Chen and co-workers have examined the effect

of a Pt sandwich alloy with Ni present in the subsurface.[68, 69] Acrolein would not bond to Pt(111) and Ni/Pt(111) via the di-σ-C=O configuration, but does bond in this configuration to the Pt/Ni/Pt(111) surface. The authors speculate that the selectivity could be further improved with proper tuning of the electronic structure of the surface to shift the binding energy difference between different adsorption configurations of acrolein.

In another study of selective acrolein hydrogenation showing a different type of geometric effect, Claus and co-workers studied Au catalysts that were coated with indium.[70] High resolution TEM images showed that the indium coated the terraces of the Au nanoparticles leaving only the edges exposed. The gold particles covered with indium were still half as reactive as those not covered by indium with a much better selectivity to allyl alcohol (63% vs. 34%). This led the authors to conclude that the exposed corners and edges must be the reactive site for the selective hydrogenation of the C=O group.

Ag alloys have been previously considered for acrolein hydrogenation. In a prominent example of improved selectivity, Lucas and Claus reported that a 9Ag-0.75In/SiO_2 (9 wt% of Ag, 0.75wt% of In) catalyst had a selectivity of 61% to allyl alcohol even when acrolein was fully converted (conversion=97%).[26, 27] X-ray diffraction (XRD) measurements showed that an Ag_3In alloy phase was formed when the catalyst was reduced at 603 K, which might provide the active sites for the outstanding performance. In this case, the presence of In is speculated to serve as a binding site for the C=O bond of acrolein in a manner echoing the calculations of Delbecq and Sautet.[21] It is also observed with increase of particle size, there is an increase in activity and selectivity.[7] This activity increase is believed to be related to larger portion of (111) surfaces on larger particles, where acrolein adsorbs preferentially through the carbonyl bond.[7] The

computational efforts of Ferullo et al.[13] support the idea that the adsorption mode of acrolein is highly sensitive to coverage.

An extreme version of a geometric (ensemble) effects would be the creation of an isolated atom in a matrix of another element termed by Sykes et al. as a single atom alloy (SAA).[9-11] In their combined temperature programmed desorption/scanning tunneling microscopy study, Kyriakou et al. [10]deposited 0.01 ML, and 0.1 ML of Pd on Cu (111) surface to form structures where individual Pd atoms were alloyed into the Cu (111) surface. Hydrogenation of acetylene and styrene were employed as test reactions to investigate the catalytic properties of the Pd@Cu SSA. The presence of hydrogen atoms was clearly observed on 0.01 ML Pd/Cu(111) surface in STM images indicating that isolated Pd atoms were able to dissociate hydrogen molecules to H atoms which then spilled over to the Cu surface. DFT calculations predicted that the barrier for hydrogen dissociation was reduced from 0.40 eV to 0.02 eV but that the adsorption enthalpy (-0.35 eV on the alloy and -0.20 eV on Cu(111)) was not strongly affected. In agreement with this prediction, the desorption temperature (manifested as the barrier to association- the reverse of the dissociation process) dropped dramatically from 310 K on Cu(111) to about 220 K on 0.01 ML Pd/Cu(111) (and even lower to ~180 K on 0.1 ML Pd/Cu(111). Temperature programmed reaction (TPR) results showed the selectivity of acetylene hydrogenation to ethene (as opposed to overhydrogenation to ethane) was greatly improved on Pd@Cu SAA surface. The selectivity to ethene for acetylene hydrogenation was >95% on 0.01 ML Pd/Cu(111)while the selectivity to ethene was only 33% on 1 ML Pd/Cu(111). Similar results were obtained for the selective hydrogenation of styrene to ethylbenzene (i.e. minimal hydrogenation of the aromatic ring).

Recently Boucher et al. reported synthesis of Pd-Cu SAA nanoparticle catalysts via galvanic replacement of Cu with Pd.[11] $Pd_{0.18}Cu_{15}/Al_2O_3$ catalysts (numbers refer to mole percent) were observed to have more than an order of magnitude higher activity for phenyl acetylene hydrogenation when compared to their monometallic Cu counterpart while sustaining high selectivity (94%) towards styrene for several hours at high conversion. The presence of palladium in these systems greatly increases the activity, suggesting that hydrogen dissociation is a kinetically important step in the reaction. Previous work from Rosch et al has found that the activation barrier for dissociation of hydrogen over Ag is higher than any single step in the acrolein hydrogenation mechanism.[40, 71] Previous experiments from Zanella et al.[72]also provide support that hydrogen dissociation is rate limiting for crotonaldehyde hydrogenation over Au/TiO_2. This implies that increasing hydrogen activation could be beneficial to selective acrolein hydrogenation, provided that the presence of the palladium does not significantly decrease the selectivity.

Here we present results for the selective hydrogenation of acrolein over a Pd-Ag bimetallic system with dilute Pd in Ag as a host metal. The situation is similar to the Pd@Cu SAA described by Sykes and co-workers but extend to simple, scalable methods for making high surface area supported nanoparticles. The activity and selectivity (considering particle size effect) are both improved by addition of Pd compared to monometallic silver catalyst.

2.2 Experimental

2.2.1 Preparation of catalysts

Silver alloy catalysts were prepared using inorganic precursors via incipient wetness impregnation (IWI) and SiO_2 as the support (silica gel, Sigma-Aldrich, 250-500 μm, 285 m^2/g). Depending how

the precursors (eg. $AgNO_3$ and $Pd(NO_3)_2$) were added to make the alloy; we name the impregnations as Co-IWI or Sequential IWI. For sequential impregnation, metal salts were dissolved in water separately and impregnated successively. Palladium aqueous solution was impregnated first and the catalysts were dried at room temperature for an hour then at 125 °C overnight. Calcination was then performed at 250 °C for 2 hours in a furnace open to the atmosphere, but without flow. Silver solution was impregnated after calcination. The catalysts were dried again and reduced at 325 °C without being calcined. The reduction treatments were performed in a tube furnace with a 50 mL/min flow of 3.5% H_2 for 2 hours.

Two low Pd loading samples were made following the same procedure, 0.01%Pd+8%Ag/SiO2_Seq_IWI_R325 and 0.05%Pd+8%Ag/SiO_2_Seq_IWI_R325. For co-incipient wetness impregnation (co-IWI), palladium solution is mixed with the silver solution. After impregnation, the catalysts were dried at room temperature for an hour and at 125°C overnight. Finally, these materials are reduced at 325°C. The notation for naming the catalysts includes dilute metal loading, host metal loading, support, preparation method and treatment. For example, sample 0.01%Pd+8%Ag/SiO2_Co-IWI_R325 is a .01 wt% loading of Pd with 8 wt% of silver supported over silica by co- incipient wetness impregnation and reduced at 325°C. A 2 wt% palladium catalyst was prepared in the same way by incipient wetness impregnation, supported on silica and reduced at 300°C in a 1/2" OD plug flow reactor with a 50 mL/min flow of 3.5% H_2 for 2 hours and was used for comparison.

2.2.2 Characterization

EXAFS : Ag K edge EXAFS was employed to estimate the particle sizes since the loading of palladium was very low and therefore the particle size can be estimated directly from the Ag

coordination number [7, 43] Pd K edge EXAFS was used to investigate the environment of palladium. EXAFS spectra were taken at the beamline of the Materials Research Collaborative Access Team (MRCAT, 10-ID) at the Advanced Photon Source (APS), Argonne National Laboratory. However, for the Pd K edge of the SAA materials, we perform the experiment in the fluorescence mode, which enhances the sensitivity by orders of magnitude over transmission EXAFS.[44] Fluorescence EXAFS measurements were made using a log-spiral-bent silicon Laue analyzer with scintillation detectors as described by Kropf et al.[45] All the samples were ground and packed into a sample holder. They were then reduced in 3.5% H_2/He at 200°C for one hour, cooled in H_2/He and scanned at room temperature in H_2/He in an environmental cell. Samples were scanned in transmission mode at Ag edge and in fluorescence mode at Pd edge. Metal foils were scanned at the same time for energy calibration. The WINXAS 3.1 program was used to fit the data to calculate the coordination number and bond distance between neighboring Ag atoms, using a k^2-weighted Fourier transform. The least squares fit in k-space of the k^2weighted Fourier transform is done using data from 2.6 to 12.1 $Å^{-1}$.The Ag-Ag phase and amplitude functions were acquired from the first coordination shell of Ag foil (N_{Ag-Ag} = 12 at 2.889 Å). An empirical relationship between the coordination number and particle size previously obtained from a series of platinum samples was used since both silver and platinum are fcc (face centered cubic) metals.[43] However, since there is no specific rule to choose the Debye–Waller factor (DWF), some error is introduced in our size estimation. This error in the fits was determined by fixing the difference in the DWF between the reference and the samples at 0.001 $Å^2$. The error in the absolute particle diameter we estimate to be ±10% and in R was ±0.02 Å[46], within the normal range of fitting errors of EXAFS. Fits were performed by changing the coordination number (CN), bond distance (R), σ^2, and energy shift

(E0). The σ^2 value was fixed through all sample fits, and CN and R were allowed to change in turn to determine the correct fit.

2.2.3 Catalysis

Gas phase acrolein hydrogenation was performed in a 1/2 inch OD stainless steel fixed-bed continuous flow reactor. Control of the reaction feed gas (hydrogen and argon) flow was done using mass flow controllers (Brooks® Models 5964, 5850EM). Acrolein (Fluka ≥ 95%) was delivered by a liquid pump (VICI M6), evaporated at 70°C in a heat tape traced four way cross packed with quartz wool, and carried in to the system by reaction feed gas. The molar ratio of H_2 to acrolein is kept constant at 20:1 with pump's set flow rate of acrolein 3.2 µL/min. ~ 15-20 mg of catalyst was used for each test, depending on the activity of the catalyst. Before each run the concentration of acrolein was checked via a reactor bypass line that connects directly to the gas chromatograph (GC). Catalyst samples were reduced *in-situ* in 20% H_2/Ar flow at 200°C for an hour before testing to ensure the catalysts are in a fully reduced metallic state. The reaction temperature was also 200°C and pressure was 5 atm. The reactor effluent was analyzed by an on-line GC (Agilent 6890) equipped with a dual column formed by a RT-Msieve 5A and a RT-QPLOT (Restek) for lighter gaseous species and a EC-Wax (Alltech) for less volatile species such as alcohols. TCD (thermal conductive detector) and FID (flame ionization detector) were both utilized for detecting H_2 and other organic/flammable compounds, respectively. The whole system was built with high-pressure-tolerant stainless steel parts and heat-traced to avoid condensation of any product.

2.2.4 Density Functional Theory Calculations

The density functional theory (DFT) calculations are performed using the Vienna Ab Initio Simulation Package (VASP).[73, 74] A plane-wave basis set with a cut off energy of 500 eV and projector-augmented wave (PAW) based pseudopotentials [73, 75] are employed. The Perdew Wang (PW-91) form of the generalized gradient approximation (GGA) exchange and correlation functional is used in all calculations reported herein.[76] A five-layer slab model with 3 × 3 surface unit cell is adopted to model the Ag(111) surface. The Brillouin zone is sampled with a 3× 3 × 1 k-points grid.[77] The geometries of all structures were located with the conjugate gradient method and were considered to be converged with energy within 0.001 eV and forces of less than 0.025 eV/Å. The top three layers are allowed to relax. A vacuum space of 16 Å was applied to separate the slabs. The transition states (TS) are determined by the climbing nudged elastic band (NEB) method of Henkelman and Jónsson.[78]

2.3 Results and Discussion

Our initial study involves the creation of a series of PdAg alloy nanoparticle catalysts via sequential impregnation in varying Ag:Pd ratios (8:1, 160:1, 800:1) as well as their monometallic counterparts. The selectivities of the catalysts at 10% conversion and reaction rates of the four catalysts (the 8:1 Ag:Pd sample is excluded because its activity and selectivity are essentially identical to Pd) were analyzed and compared in Figure 9. As expected, Pd is extremely active, but not at all selective to allyl alcohol even under very mild reaction conditions. The reaction rate at 100°C and 5 atm pressure is 38.9×10^3 mmol/(h·g_{Pd}) and selectivity to allyl alcohol is zero . In contrast, the 8%Ag/SiO_2 catalyst has the highest selectivity for allyl alcohol. For this Ag catalyst, the selectivity can reach 37% at 200 °C and at 5 atm total pressure.

Surprisingly, the 0.05%Pd+8%Ag/SiO_2_Seq_IWI catalyst behaves more like Pd than Ag. Its activity approaches that of Pd alone (at T=100°C, the rate was 5.3×10^3 mmol/(h·g_{metal}) and its selectivity is only about 1% (Fig 9 (a)). Our result implies that even at this dilute ratio, the Pd is so much more active than Ag, that its presence completely dominates the observed reactivity. In contrast, the selectivity of 0.01%Pd+8%Ag/SiO_2 _SeqIWI to allyl alcohol is 31%, only slightly lower than 8%Ag/SiO_2. In addition, the activity was almost double that of 8%Ag/SiO_2 (303 vs. 158 mmol/(h·g_{metal}) (figure 9a)). Our result demonstrates that the Pd is having a strong effect on the catalytic results, although the amount of Pd present is very small. It is important to mention that the reaction temperature for the Pd catalyst is 100ºC while the less active Ag catalysts were tested at 200ºC. Since propionaldehyde is the thermodynamic product, we would expect that the selectivity to allyl alcohol should decrease as the temperature increases**.** Based upon an estimate of the rate at 200ºC using an activation energy of 45 kJ/mol (obviously the activation energies not the same for the Pd and Pd@Ag SAA catalysts), the results imply that the Pd catalyst is actually about 2000 times more active than Ag.

EXAFS experiments were performed in order to understand the increased activity but similar selectivity of the dilute alloy catalyst. By fitting EXAFS spectra, the coordination numbers and bond distances of the 0.01%Pd+8%Ag/SiO_2_SeqIWI catalyst at both the Pd K edge and the Ag K edge were obtained and listed in Table 1. The numbers for bulk metals were also given for comparison. The coordination numbers at the Ag K edge were used to estimate particle size. The particle sizes of 0.01%Pd+8%Ag/SiO_2_SeqIWI and 0.05%Pd+8%Ag/SiO_2_SeqIWI are 5.8 nm and 5.4 nm respectively. Although these two catalysts were treated in the same way that we used to prepare a pure silver catalyst (d = 8.7 nm) [18], the particle sizes of bimetallic samples are smaller

than the monometallic sample. The addition of palladium seems to help disperse the silver nanoparticles probably due to the creation of nucleation centers of Pd upon which Ag aggregates. As discussed below, the size of particle also has a critical effect on the reactivity (and selectivity).

9(a)

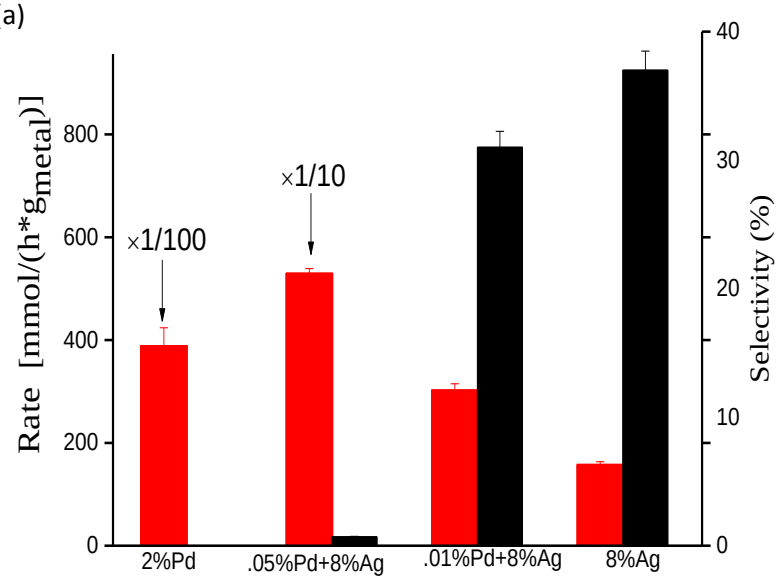

9(b)

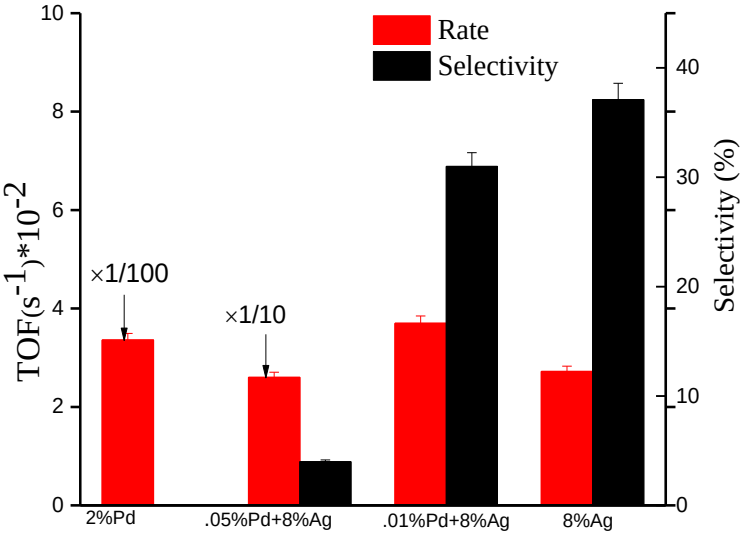

Figure 9: Activities (both per metal atom basis and TOF) and selectivities to allyl alcohol of Pd, Ag, and Pd-Ag catalysts synthesized via sequential IWI. All samples are supported on SiO_2. 2% Pd/SiO_2 and 0.05%Pd+8%Ag/SiO_2 were tested at 100 °C and 5 atm pressure; the reaction temperature of 0.01%Pd+8%Ag/SiO_2 , 0.03%Pd+8%Ag/SiO_2 and 8%Ag/SiO_2 was 200 °C and the reaction pressure of them was 5 atm.[25]

Pd K edge spectra (figure 10) give additional insight into the structure of the PdAg catalyst. For the 0.01%Pd+8%Ag/SiO_2_SeqIWI catalyst, the coordination number of Pd is 10.5 (Table 1) which is very close to the value of Ag (10.2), and shows that Pd atoms are uniformly distributed and present both in the surface and in the bulk. If Pd atoms had segregated completely to the surface, they should be under-coordinated relative to Ag and the coordination number should be smaller. In contrast, if all Pd atoms are in the bulk the coordination number will be closer to 12 since they would be completely coordinated in a fcc environment. From the EXAFS data we conclude that when the loading of Pd is very low (0.01 wt%) the Pd-Ag alloy forms in a way that silver serves as the host metal while isolated single Pd atoms are uniformly atomically dispersed. In addition, the bond distance of the palladium atoms to the nearest neighbors is 2.82 Å (Table 1). The Pd-M bond distance is intermediate between the M-M bond distance in bulk silver (2.89 Å) and bulk palladium (2.74 Å). This result implies that Pd is surrounded only by silver atoms, and that the Pd atoms are totally dispersed in Ag nanoparticles. Therefore our materials seem to be nanoparticle analogs to the single crystal models of SAA catalysts described by Kyriakou et al.[10] In effect, our work has validated the ideas of Kyriakou et al. for yet another example of selective hydrogenation. We suggest that the dilute alloy is actually a SAA catalyst possessing isolated Pd atoms in a Ag matrix which accelerates the activation of H_2 just as in the work of Kyriakou. Hydrogen atoms from dissociated H_2 are then spilled over to the Ag surface where they are only weakly bound and therefore are easily consumed in the hydrogenation reaction.

10(a)

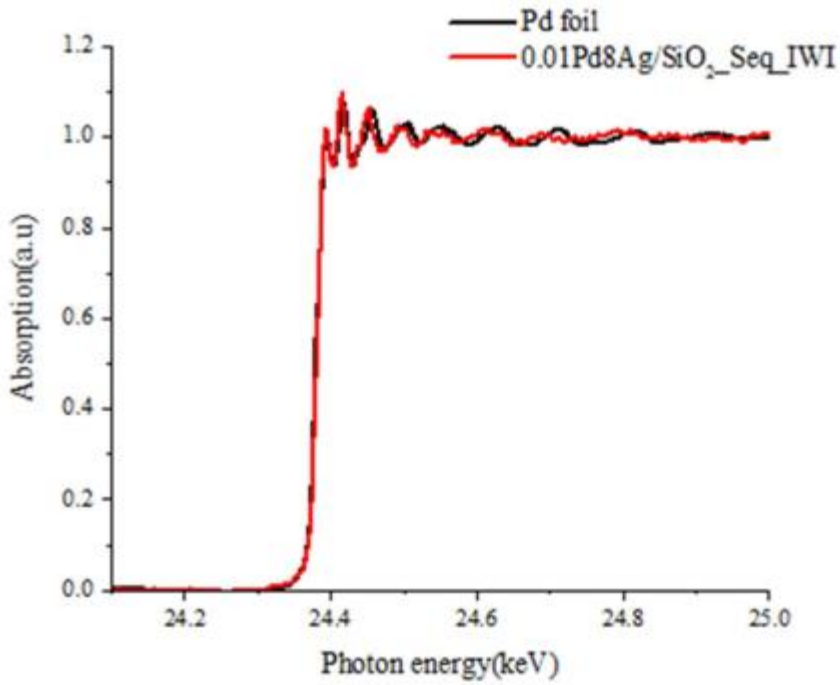

10(b)

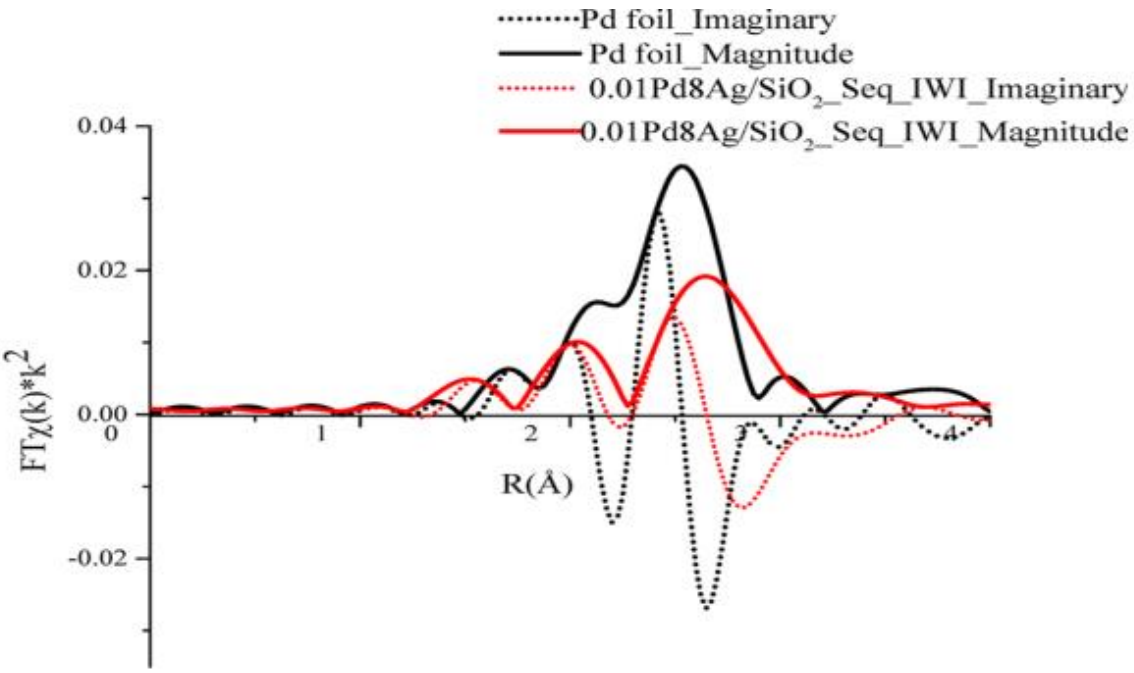

Figure 10 : (a) Pd K edge spectra of Pd foil and 0.01%Pd+8%Ag/SiO2_Seq_IWI alloy (b) Fourier transform of the experimental data in R space25

Table 1 : Bond distances and coordination numbers a Pd-Ag bimetallic catalyst prepared via sequential impregnation compared with bulk Ag and Pd.

	Ag-edge		**Pd-edge**	
	Bond distance/Å	Coordination No.	Bond distance/Å	Coordination No.
0.01%Pd+8%Ag/SiO_2 _SeqIWI	2.87	10.2	2.82	10.5
0.05%Pd+8%Ag/SiO_2 _SeqIWI	2.87	10.0	2.81	11.0
Bulk Ag	2.89	12.0		
Bulk Pd			2.74	12.0

11(a)

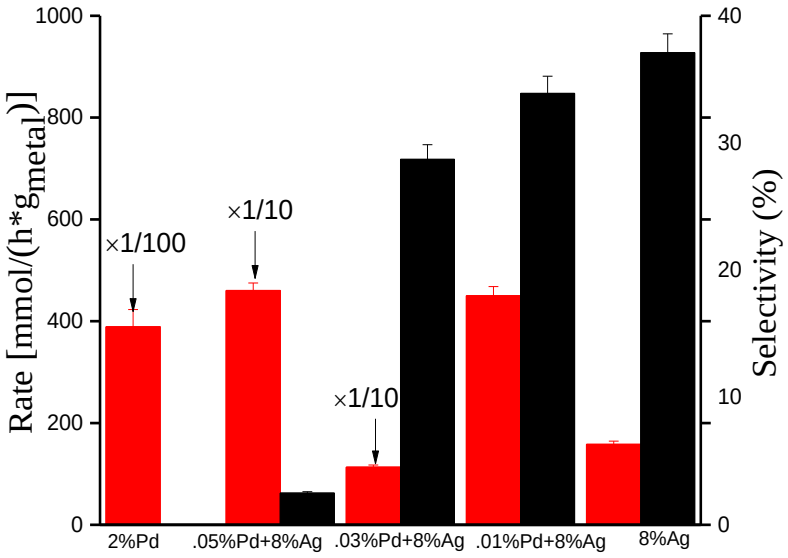

11(b)

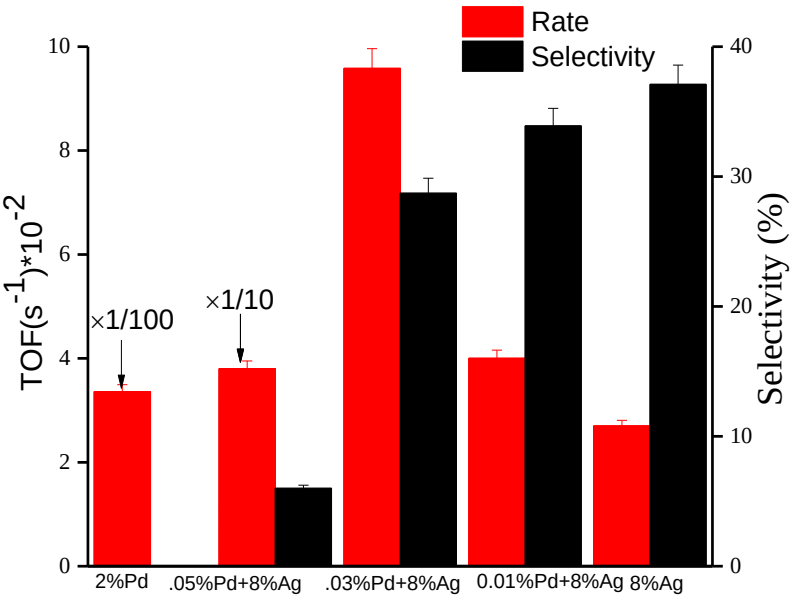

Figure 11: Activities (both per metal atom basis and TOF) and selectivities to allyl alcohol of Pd, Ag, and Pd-Ag catalysts synthesized via Co-IWI. All samples are supported on SiO_2. 2% Pd/SiO_2 and 0.05%Pd+8%Ag/SiO_2 were tested at 100 °C and 5 atm pressure; the reaction temperature of 0.01%Pd+8%Ag, 0.03%Pd+8%Ag/SiO_2 and 8%Ag/SiO_2 was 200 °C and the reaction pressure of them was 5 atm.[25]

Table 2: Bond Distance and Coordination number for Co-Impregnated alloys

	Ag-edge		**Pd-edge**	
	Bond distance/Å	Coordination No.	Bond distance/Å	Coordination No.
0.01%Pd+8%Ag/SiO_2_CoIWI	2.88	9.0	2.81	10.5
0.03%Pd+8%Ag/ SiO_2_CoIWI	2.89	9.4	2.81	10.0
0.05%Pd+8%Ag/ SiO_2_CoIWI	2.89	9.0	2.83	10.0
Bulk Ag	2.89	12.0		
Bulk Pd			2.74	12.0

Since, the presence of Pd clearly improves the activity due to the ability of the alloy to activate H_2, it is desirable to find the optimal Pd loading to maximize activity while maintaining selectivity. However, even a loading of 0.05%Pd resulted in a substantial loss of selectivity. We speculate this is due to the presence of contiguous Pd atoms which results in an unfavorable bonding configuration for acrolein. The alloy catalysts compared in figure 9 (a, b) were synthesized via sequential impregnation. It seems reasonable to suggest that by using a co-impregnation method,

the Pd will be better dispersed in the nanoparticle and higher loadings of Pd could be used with comparable selectivity and higher activity. Therefore, co-IWI was employed in an effort to achieve better isolation of Pd at higher Pd contents and to avoid rapid nucleation of Ag around Pd. Three catalysts were made by changing the ratio of palladium doped in the silver catalyst (.01%, .03% and .05%) by simultaneously mixing the two metal precursors. It is found that the selectivity of .01% Pd + 8%Ag, made by co-impregnation only improves the selectivity by 3-4% (from 31% to 34%) as shown in figure 11(a). However, analysis of the coordination numbers (shown in Table 1 and Table 2) reveals that the silver particle size is decreased to 4 nm as compared to 5.4 nm (from TEM) by making Pd-Ag alloy via co-IWI instead of sequential IWI. The Pd-M bond is found to be 2.81 Å, once again implying that Pd atoms are completely surrounded by Ag. The weak anti-segregation energies [79]combined with the high degree of dilution suggest the creation of single atom sites for catalysis. The results show that the method of preparation is critical to the catalyst performance and that the Ag is still nucleated by the presence of Pd in solution, resulting in smaller particles than the desired target.

Just as in the case for sequential impregnation, the samples made via co-impregnation showed a slightly lower selectivity for allyl alcohol by the 0.01%Pd+8%Ag/SiO_2_CoIWI than the pure silver catalyst.[7] However, if we consider the particle size effect on selectivity (as shown in figure 12), the selectivity is actually not reduced but improved by doping individual Pd atoms. The trend of selectivity vs. particle size over silica supported Ag samples shows that the selectivity of a monometallic silver catalyst (8%Ag/SiO_2) having similar particle size to 0.01%Pd+8%Ag/SiO_2_Seq_IWI_R325 is only around 15%, which is half of the selectivity achieved over 0.01%Pd+8%Ag/SiO_2_Seq_IWI_R325 (figure 9(a)).

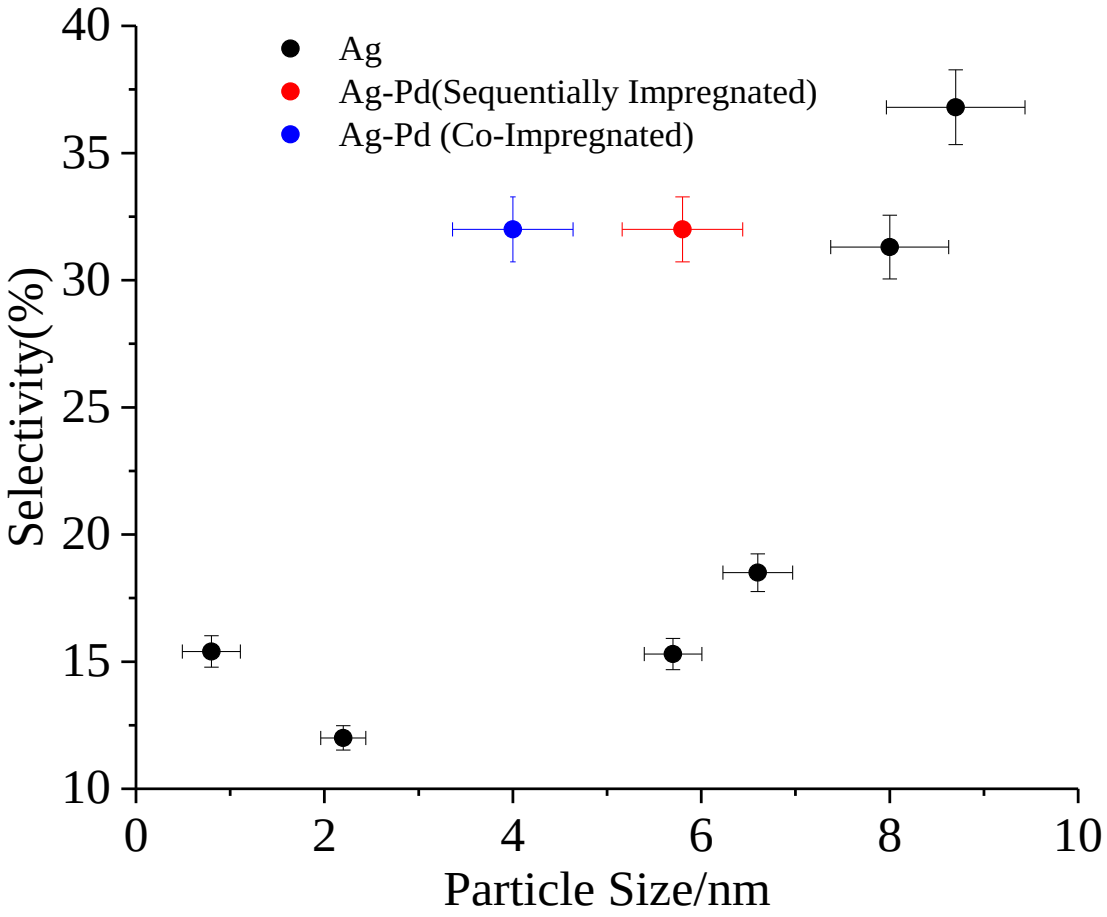

Figure 12: Comparison of selectivities towards allyl alcohol of Pd-Ag alloys and pure Ag catalysts with various particle sizes. All samples are supported on SiO_2. Selectivities compared at 200 °C, 5 atm and 10% conversion[25]

It seems unlikely that the addition of the Pd is changing the reactivity of Ag itself. Since the Ag-M bond distances are largely unchanged, no strain effect appears to be present. Similarly, changes in the local reactivity of Ag atoms neighboring Pd seem unlikely to be significant since most Ag atoms would have zero or one Pd neighbors. Another possible effect of the Pd is that the acrolein molecule adsorbs in a more favorable configuration for selective hydrogenation (i.e. C=O bond down to the surface as opposed to adsorbing through its C=C bond). DFT calculations of acrolein adsorbed on a Ag(111) slab with a single atom of Ag replaced by Pd (figure 13) indicate that in fact while acrolein adsorbs weakly to the pure Ag surface in both orientations, the presence of the Pd atom enhances acrolein adsorption through the C=C bond (1.36 eV) more dramatically than the C=O bond. (0.45 eV O down to the surface and 0.87 eV with both O and C=C bonded to the surface). Extended ensembles of Pd also prefer bonding of acrolein through the C=C bond. For example, in the most extreme case, an extended Pd(111) surface, the acrolein adsorbs most strongly through C=C bond (Eads =-2.15 eV) compared to bonding through the C=O bond (Eads =-0.85 eV, O down and Eads = -1.87 eV with both O and C=C bonded to the surface). It would appear that this is counter to our supposition that C=O orientation toward the surface is critical to selective hydrogenation. However Sautet and co-workers have previously explained this result by noting that preferential attack of the C=O functionality may be possible even if the acrolein molecule is not bound to the surface by the aldehyde functionality. [80]

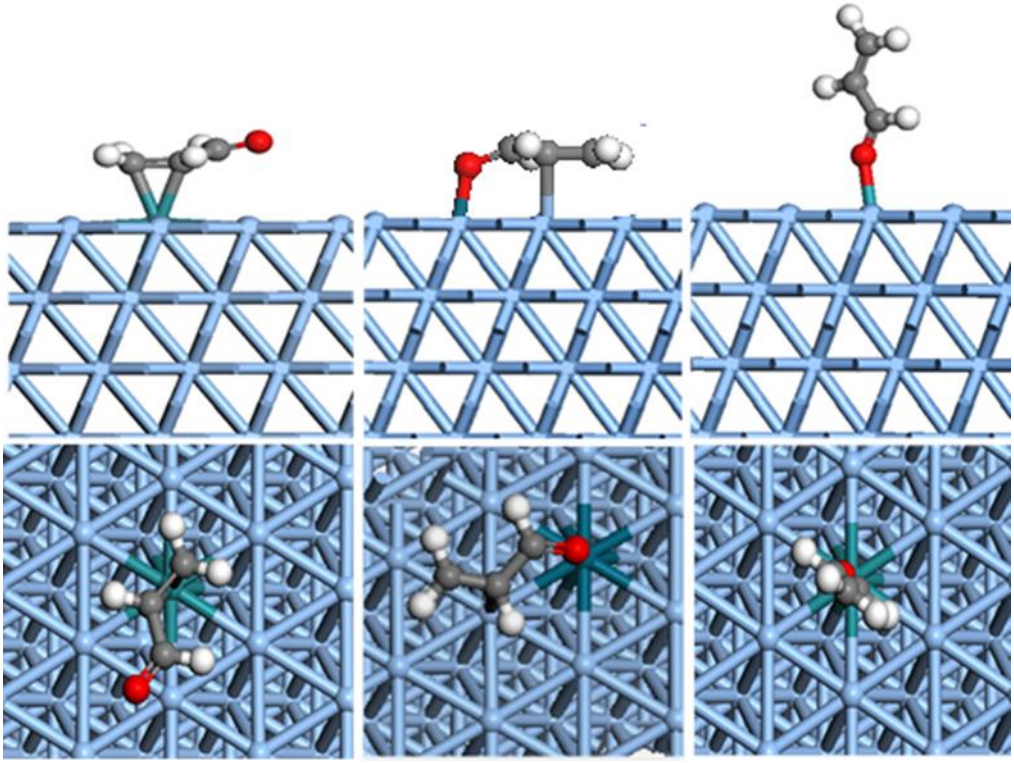

(a) (b) (c)

Figure 13: Presence of Pd atoms preferentially changes the adsorption of acrolein. (a) Acrolein adsorbed on isolated Pd atom through C=C bond and oriented horizontally. (E= -1.36 eV) (b) Acrolein adsorbed on isolated Pd atom through O and C=C bond and oriented horizontally. (E=-0.87eV)(c) Acrolein adsorbed on isolated Pd atom through C=O bond and oriented vertically. (E=-0.45eV)[25]

Atoms by colors; Ag(blue), C(black), O(red),H(white), Pd(green)

The potential energy diagram shown in figure 14 illustrates how introduction of single Pd atoms on Ag(111) surface facilitates dissociation of hydrogen. Although hydrogen dissociation on Pd(111) is not activated ($E_a \approx 0$ eV), the barrier for hydrogen dissociation on Ag(111) is rather high (1.15 eV) . In contrast, the binding energy of H_a on Ag (111) is 0.31 eV (endothermic), which is much weaker than that on Pd (111) (-1.23eV). Interestingly, on Pd/Ag(111) SAA surface, binding energy is reduced from -1.23 to -0.33 eV on Pd(111) while the activation energy is reduced to 0.31 eV from 1.15 eV on Ag(111). So, isolated Pd atoms on Ag(111) surface help to activate the dissociation of H_2 on the surface which results in spillover of H atoms to the Ag(111) surface. The H atoms have a significant barrier to recombination (0.56 eV) which is apparently on par with barriers for hydrogenation of acrolein.[40, 71] Kyriakou et al. [10]has shown how the presence of Pd atoms seems to result a break away from the expected Bronsted Evans Polanyi (BEP) relationship which correlates the reaction barrier with the reaction enthalpy.[81]Similarly, DFT calculations for our case revealed the same trend where the expected BEP relationship is not followed in presence of Pd atoms. In the case of the Pd@Ag (111) alloy surface the barrier for dissociation is low (like Pd (111)) but the adsorption enthalpy for hydrogen is also low (like Ag(111)). This demonstrates a rare case of synergy where the alloy catalyst displays the “best behavior” of both metals.

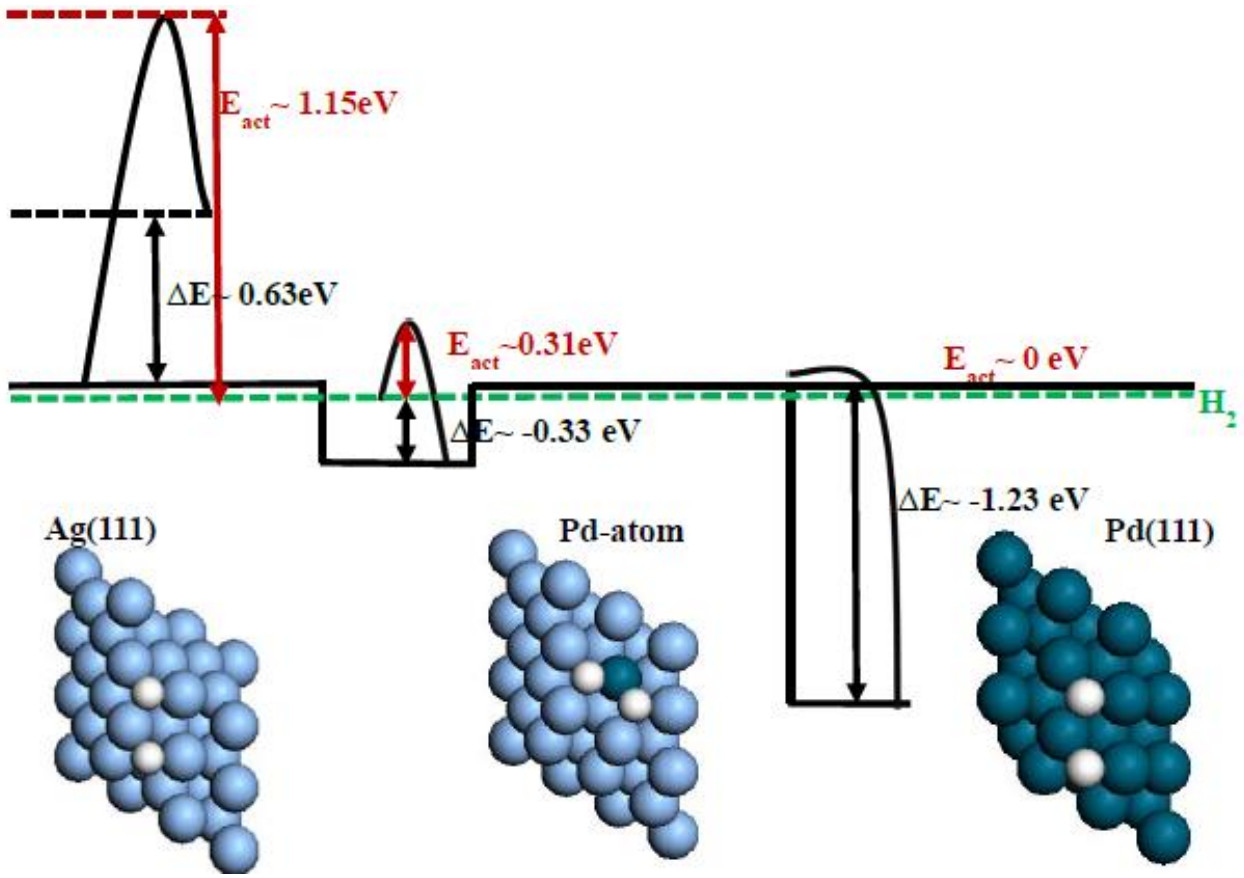

Figure 14: Potential energy diagram showing how Pd SAA surface has an effect on the energies compared to those for Ag (111) and Pd (111) surface. Dissociation of H_2 (white) on Ag (111) (blue) is a significantly activated process. On Pd (111) (green), H_2 dissociation is practically barrierless, however the binding energy of adsorbed atoms is high. For Pd/ Ag (111) SAA surface, the dissociation barrier is reduced as well as binding energy of hydrogen is decreased allowing dissociated hydrogen to get spilled over to Ag surface.(E_{act}=Activation Energy, ΔE=Reaction Enthalpy)[25]

2.4 Conclusion

Pd-Ag alloy catalysts with very dilute levels of Pd were synthesized using traditional impregnation methods in an attempt to create single atom alloys as in the example of Sykes et al.[10, 82] Both the activity and the selectivity for the selective hydrogenation of acrolein were improved as compared to monometallic Ag catalysts of the same size. The EXAFS results indicate that isolated Pd atoms are atomically dispersed in Ag nanoparticles. DFT calculations suggest that the presence of isolated Pd atoms increases the activity by providing active centers for H_2 dissociation and that the selectivity increases due to favorable changes in the configuration of adsorbed acrolein. The results suggest additional improvements may be possible if the larger Ag particles can be synthesized and if larger doping levels could be used while maintaining Pd in an atomically dispersed state.

3.0 Effect of Supports on the Selective Hydrogenation of Acrolein

3.1 Introduction

The choice of catalytic support [28, 29, 83, 84] is not only important for effective dispersion of the active metal, but can also affect the observed reactivity by tuning the electronic structure of the metal or by creation of interface sites. Hydrocarbon hydrogenation reactions typically do not exhibit strong support effects since the reaction occurs exclusively on the metal. .For example, in one of their studies, Boudart et al. [85]investigated effect of mixing η-Al_2O_3 with Pt/SiO_2 on reaction rates for ethylene hydrogenation reaction. They could not find any beneficial effect for ethylene hydrogenation with modification of support. Specifically, there was no evidence of hydrogen spillover from metal to alumina with increased rates of hydrogenation of ethylene adsorbed on alumina support. However, CO hydrogenation has been observed to be among those reactions, most cited for support and promotional effects.

Vannice et al. tested CO hydrogenation [30]over Pt/TiO_2 catalysts in an effort to understand the origin of support effects in this system. Titanium was deposited on ultrahigh-purity 1-μm Pt particles followed by oxidation and reduction. Surface areas determined by BET, H_2 and CO chemisorption measurements did not change considerably for Ti coverages of 1 and 10 monolayers. However, turnover frequencies based on adsorbed hydrogen increased 4-fold and 40-fold, respectively, and approached the values measured on TiO_2 supported Pt. These results suggested presence of special active sites at the Pt-titania interface. Vannice et al. also examined hydrogenation of acetone [83] and crotonaldehyde [30]over Pt catalysts to understand how use of different supports influences the interaction between carbonyl group and metal. It was observed that use of titania as support

improved the selectivity towards isopropyl alcohol or crotyl alcohol, no matter whether carbonyl bond was associated with an olefinic bond or not. The most selective titania supported catalyst provided 37% selectivity to crotyl alcohol in case of crotonaldehyde hydrogenation when tested at 318 K and 1 atm pressure unlike those supported on silica or alumina which showed zero selectivity towards crotyl alcohol. It was believed that new sites, i.e., Ti^{3+} (or Ti^{2+}) or oxygen vacancy were formed at the metal-support interface which helped in activation of C=O bonds. The authors disproved the supposition that hydrogen spill-over was responsible for the selectivity enhancement because no improvement was detected in physical mixtures of Pt and TiO_2 for the hydrogenation of CO and acetone. [30]

Coq and co-workers[86]investigated support effects in liquid phase hydrogenation of cinnamaldehyde over supported Ru based catalysts. Among γ-Al_2O_3, SiO_2, TiO_2 (anatase), graphite and ZrO_2, ZrO_2 showed the best performance in terms of selectivity towards unsaturated alcohol. Ru/ZrO_2 catalyst exhibited around 60% selectivity to cinnamyl alcohol at H/Ru uptake of 0.25 which is much higher than predicted value. In the experiments of Coq et al., the Ru particle sizes varied among the different supports and a plot of selectivity versus hydrogen uptake was developed to distinguish between a support effect and a particle size effect. Ru/Al_2O_3, Ru/SiO_2 and Ru/graphite exhibited similar behavior, showing that the support effect was not prominent on these three supports and the selectivity was only size dependent. However, both Ru/TiO_2 and Ru/ZrO_2 catalysts showed much higher selectivity than what H/Ru values could predict. The unusual behavior of these supports was recognized as a SMSI effect. The authors also suggested that a Ru-Zr phase could have developed during the reduction of ZrO_2 and enhance the selectivity or that partially reduced sites ZrO_2 may have a role in reaction.

Hidalgo-Carrillo et al.[87] also investigated support effects in selective liquid phase hydrogenation of a α, β–unsaturated aldehyde (in this case, crotonaldehyde) over Pt catalysts synthesized on different partially reducible supports including Fe_2O_3, Fe_3O_4, ZrO_2, ZnO, TiO_2 and SnO_2. The catalysts were tested at 30°C in a Parr Instruments 3911 low-pressure reactor with an initial hydrogen pressure of 0.414 kPa for 8 hours and the highest selectivity attained was 75% obtained on Pt/ZnO (which was reduced at 175°C). The extraordinary performance was suggested to result from the formation of ZnO_xCl_y (identified by XPS) around Pt particles (2-3 nm). ZnO_xCl_y was suggested to act as a Lewis acid site and anchor the carbonyl bond in crotonaldehyde during adsorption, resulting in better selectivity to crotyl alcohol.

We have chosen selective hydrogenation of an α, β–unsaturated aldehyde as a probe reaction to understand the changes in kinetics and mechanism of the reaction introduced by interaction of different supports with the active metal which often result in improving catalytic activity and selectivity of the metal catalyst. Selective hydrogenation of α, β–unsaturated aldehydes to unsaturated alcohol is still a challenging task because thermodynamically hydrogenation of the olefinic bond is far more favorable than the carbonyl group (by around 35 KJ/mol).[70] Acrolein hydrogenation was selected as our probe reaction because acrolein, being the smallest of α, β–unsaturated aldehydes is the most difficult one to convert to allyl alcohol (it lacks of substituents on the C=C group) and therefore offers the biggest opportunity for improvement. Surprisingly, substantial selectivity towards allyl alcohol is never achieved on traditional hydrogenation catalysts like Pd, Pt or Ru [28, 83, 84, 86] and instead the best selectivity so far has been achieved on Ag and Ag alloy catalysts. This is unusual because Ag is usually considered inert to H_2 chemisorption and

therefore does not provide large surface concentrations of atomic hydrogen for hydrogenation reactions[5, 88].

Bron et al. [6]and Grünert et al. [89] investigated this reaction and observed both particle size effects and a strong support effect with Ag catalysts. Bron et al. examined acrolein hydrogenation at 250°C and a pressure of 20 bar and attained enhanced selectivity at higher pressure with Ag/SiO_2 catalysts. No allyl alcohol was observed below 75 mbar. Selectivity towards allyl alcohol at 1 bar was around 28% which increased to 36% at 5 bar and then reached a constant value of 42% above 10 bar. Grünert et al. claimed a combined particle size and SMSI effect by examining two Ag/TiO_2 catalysts. While Ag/TiO_2 catalysts reduced at 200°C (LTR) (3nm) exhibited 42% selectivity towards unsaturated alcohol, the catalysts reduced at 500°C (HTR) (1.5nm) exhibited 27% selectivity. According to Grünert et al., Ti suboxide overlayers were formed due to an SMSI (Strong Metal Support Interaction) at a higher reduction temperature (500°C). This resulted in reduced growth of silver particles and truncated particle morphology developed differing from the spherical shape. As a result, both selectivity and activity deteriorated. Wei et al. has performed a systematic study on particle size effects for acrolein hydrogenation examining series of Ag/SiO_2 catalysts of different particle size (1-10nm) and found that higher particle sizes exhibited both higher TOFs (Turn Over Frequency) and selectivity to allyl alcohol.

In another study, Bron et al. investigated support effects for acrolein hydrogenation using Ag catalysts on SiO_2, Al_2O_3 and ZnO, all synthesized by Incipient Wetness Impregnation and tested under same temperature and pressure. SiO_2, Al_2O_3 showed similar selectivities of around 39% and 42%, respectively, while Ag/ZnO exhibited a selectivity of 50%. However, the particle size of the catalysts varied as well (Ag/SiO_2 was only 2.5 nm; that of Ag/Al_2O_3 was 11 nm; Ag/ZnO had very

broad size distribution and the particle size could not be estimated). So, the difference in selectivity could also be a result of a particle size effect rather than a support effect.[4]

Volckmar et al. explored the effect of the support acidity on a series of SiO_2-Al_2O_3 catalysts [90] for acrolein hydrogenation towards allyl alcohol. The SiO_2- Al_2O_3 ratio was altered with the Al_2O_3 content from 0 to 100% Al_2O_3 in 20% steps. The NH_3-TPD and pyridine-IR results showed the highest total acidity at medium Al_2O_3 contents (40% and 60%). These catalysts had a lower TOF (by a factor of 3-4) and only a 30 % selectivity towards allyl alcohol as compared to the >40% selectivity for Ag/Al_2O_3 and Ag/SiO_2 catalysts. It was concluded that lowering the total acidity and the number of strong Lewis acid sites would lead to an enhanced catalytic property. But it is still not obvious if other types of support effects can be exhibited beyond tuning of acid or base properties.

Recently, Hong et al. [91]performed a support effect study on crotonaldehyde hydrogenation to crotyl alcohol using various metal oxide supports (TiO_2, La_2O_3, ZrO_2, CeO_2 and SnO_2) with Iridium as the metal. They showed that the catalytic performance strongly depends on the surface acidity of the catalysts. The highest activity and selectivity are obtained on the Ir/TiO_2 catalyst, with a crotonaldehyde conversion of 43.2% and a selectivity to crotyl alcohol of 80.9% at 80ºC. All the catalysts suffered from deactivation due to polymerization of crotonaldeyde molecules on the surface of the catalyst as observed by FTIR (Fourier Transform Infrared Spectroscopy). They also showed that the deactivation rates can be related to the amount of surface acid sites on the catalysts. The Ir/CeO_2 catalyst with the highest amount of surface acid sites deactivated more rapidly than the Ir/La_2O_3 catalyst with the lowest amount of surface acid sites.

Previous studies on support effect for selective hydrogenation of α, β–unsaturated aldehydes lack a systematic analysis of support effect where they either avoided the particle size effect or did not study the reaction orders and pathways Hence, here we perform a methodical study of support effects on the catalyst performance, choosing some of the most prominent available metal supports: SiO_2, Al_2O_3, TiO_2, La_2O_3, ZrO_2, and CeO_2. Since we have already tested a series of silica supported silver catalysts from our previous study of particle size effects[7], these data are employed to provide comparisons across supports since particle sizes are difficult to alter precisely. The trends can be explained by probing a series of different sizes on each of these supports.

3.2 Experimental

3.2.1 Preparation of catalysts

Al_2O_3 (γ- Al_2O_3, 210 m^2/g), TiO_2 (P25, Degussa, 32 m^2/g), La_2O_3 (Sigma Aldrich, nanopowder, <100 nm particle size (TEM),) ZrO_2 (Gimex, RC-100, ρ= 0.23 gm/ml, monoclinic) and CeO_2 (Rhodia, Actalys HSA; 41 nm-20 μm particle size) were chosen to be the carriers of silver nanoparticles in order to study support effects for this system. These catalysts are compared with SiO_2 (Davisil silica gel, grade 646, Sigma-Aldrich, 250-500 μm, 285 m^2/g) supported catalysts, the synthesis and the catalytic performance of which were described elsewhere [20]. TiO_2, CeO_2 were preheated to 550°C and La_2O_3, ZrO_2 at 500ºC to ensure good thermal stability before use. Supported Ag catalysts were prepared using either incipient wetness impregnation of Ag3NO3 pH neutral aqueous solution or a modified incipient wetness impregnation (mIWI). mIWI is an altered form of normal IWI inspired by strong electrostatic adsorption (SEA) [92] where the pH of the solution is adjusted to enhance interaction of the precursor with the support. For example, instead of using silver

nitrate solution, ammonia hydroxide was added to it adjust pH value. We typically used 1 mL of water to dissolve silver nitrate and added 30% ammonia hydroxide drop by drop until the precipitate was fully dissolved. Water and ammonia hydroxide were added so that the total volume of the solution equaled the amount that was required to fill up the support pores and ensure the final pH was around 11. Under these conditions, the $AgNO_3$ precursor reacts to become $Ag(NH_3)_2NO_3$. The basic solution could deprotonate the hydroxyl groups on the support surfaces and served to help disperse the precursor well. After impregnation, catalysts were first dried at room temperature for an hour then at 125°C overnight. Further a combination of treatments, i.e., calcination, reduction and steaming, were carried out on each sample. The calcination treatments were performed for 2 hours in a furnace open to the atmosphere but without flow. The reduction treatments were performed in a tube furnace with a 50 mL/min flow of 3.5% H_2 for 2 hours. The steaming treatments were performed by flowing 50 ml/min of He over a stainless steel bubbler which was preheated to 55°C, so there was about 15% water vapor in the total flow. The flow was brought to the reactor at the steaming temperature. Steaming treatments were performed for 1-3 hours to vary particle size. The sample name includes the information of metal loading, support, preparation method and treatment. For instance, 8%Ag/Al_2O_3_IWI_R325_S550 represents an alumina supported silver catalyst loaded with 8 wt% of silver by direct incipient wetness impregnation, reduced at 325 °C and steamed at 550 °C. To compare the catalysts having same particle size and thereby control for any particle size effect, samples with a range of different silver particle sizes were created on all three supports. Changes in particle sizes were induced by using different post treatments, e.g. calcination, reduction and steaming. When large particle size was desired, incipient wetness impregnation (IWI) using $AgNO_3$ neutral aqueous solution as the precursor and extreme treatments like steaming at 550

°C were utilized; when small particle size was targeted, mIWI and mild treatments like calcination at 200 °C were preferred.

3.2.2 Characterization

EXAFS (extended X-ray absorption fine structure) is a powerful and efficient tool to estimate particle size. In this work it was used as a method to estimate the particle sizes as well as the coordination number. Ag K edge EXAFS spectra were taken at the beamline of the Materials Research Collaborative Access Team (MRCAT, 10-ID and 10-BM) at the Advanced Photon Source (APS), Argonne National Laboratory. All the samples were grounded before packed into sample holder. They were then reduced in 3.5% H_2/He at 200°C for one hour, cooled in He and scanned at room temperature in He in an environmental cell in transmission mode. Ag foil was scanned at the same time for energy calibration. Data was processed using WINXAS 3.1 and coordination number and bond distance were achieved for particle size estimation. The particle size obtained by EXAFS fitting is a mass averaged number and no distribution is given as by TEM. The least squares fit in k-space of the k^2 weighted Fourier transform is done using data from 2.6 to 12.1 $Å^{-1}$.The Ag-Ag phase and amplitude functions were acquired from the first coordination shell of Ag foil (N_{Ag-Ag} = 12 at 2.889 Å). An empirical relationship between the coordination number and particle size previously obtained from a series of platinum samples was used since both silver and platinum are fcc (face centered cubic) metals.[43] However, since there is no specific rule to choose the Debye–Waller factor (DWF), some error is introduced in our size estimation. This error in the fits was determined by fixing the difference in the DWF between the reference and the samples at 0.001 $Å^2$. The error in the absolute particle diameter we estimate to be ±10% and in R was ±0.02 Å [46], within the normal range of fitting errors of EXAFS. Fits were performed by changing the coordination number (CN),

bond distance (R), σ^2, and energy shift (E0). The σ^2 value was fixed through all sample fits, and CN and R were allowed to change in turn to determine the correct fit.

3.2.3 Catalysis

Acrolein hydrogenation was performed in gas phase in a 1/2 inch OD stainless steel fixed-bed plug flow reactor. Reaction feed gas (hydrogen and argon) flow was controlled by mass flow controllers. Acrolein (Sigma Aldrich CAS 107-02-08) was delivered by a liquid pump (VICI M6), evaporated at 70 °C in a heat tape traced four way cross packed with quartz wool, and carried in to the system by reaction feed gas (argon and hydrogen). The mole ratio of acrolein and H_2 is kept constant at 1:20. 60-400 mg of catalyst was used for each test depending on the activity. The gas phase concentration of acrolein was checked for every run by via a reactor bypass line that connects directly to the gas chromatograph. Catalyst samples were reduced in-situ in 20% H_2/Ar flow at 200 °C for an hour before testing. The reaction temperature was also 200 °C and total pressure was 5 atm. The reactor effluent was analyzed by an on-line gas chromatography (Agilent 6890) equipped with a dual column formed by a RT-Msieve 5A and a RT-QPLOT (Restek) for lighter gaseous species and a EC-Wax (Alltech) column for less volatile species such as alcohols. A TCD (thermal conductive detector) and FID (flame ionization detector) were both used for detecting H_2 and other organic/flammable compounds, respectively. High-pressure-tolerant stainless steel parts were utilized to build the system. The whole system was heat-traced to avoid condensation of any product. Product identification was later confirmed via GC/MS in a separate system. All potential products were calibrated for their retention times by the GC/MS using the same column setup in various trial runs involving calibrated mixtures of acetaldehyde and other products (acrolein, propanal etc.)

3.2.4 Density Functional Theory Calculations

The density functional theory (DFT) calculations are performed using the Vienna Ab Initio Simulation Package (VASP). [73, 74] A plane-wave basis set with a cut off energy of 500 eV and projector-augmented wave (PAW) based pseudopotentials [73, 75]are employed. The Perdew Wang (PW-91) form of the generalized gradient approximation (GGA) exchange and correlation functional is used in all calculations reported herein.[76] A five-layer slab model with 3 × 3 surface unit cell is adopted to model the TiO_2 surface. The Brillouin zone is sampled with a 5 × 5 × 1 k-points grid. [77] The geometries of all structures were located with the conjugate gradient method and were considered to be converged with energy within 0.001 eV and forces of less than 0.025 eV/Å. The top three layers are allowed to relax. A vacuum space of 16 Å was applied to separate the slabs.

3.3 Results and discussion

Different particle sizes on the supports were desired because a trend for each type of support can be derived and a reasonable comparison can be made based on the trends. During synthesis, it is observed that different supports had specific manner in interacting with the loaded metal (Ag). On Al_2O_3, the particles tend to be smaller than those on other supports. For example, by following the same synthesis method, the mean particle size of 8Ag/Al_2O_3_IWI_R325 was 6.4 nm, while 8Ag/SiO_2 _IWI_R325 had a particle size of 8.7 nm. The catalysts on TiO_2, CeO_2, La_2O_3 and ZrO_2 yielded large size compared to other two. The sample sizes, their coordination numbers and Ag-Ag bond distances are listed in Table 4. Acrolein hydrogenation was carried out over all catalysts. Propanal and allyl alcohol were found to be two major products (~95% total). The selectivity is compared at the same conversion (10%).The relationship of selectivity versus particle size is plotted in Figure 15. The particle size effect on selectivity that we observed on silica supported silver

catalysts, i.e., the larger the particle size the higher the selectivity is followed by all the supports studied. The result suggests that larger Ag particles with a higher percentage of terrace sites favor the hydrogenation of C=O bond over the conjugated C=C bond, consistent with our previous results and those of other researchers [6, 86, 93, 94]. Alumina supported samples more or less fell in the same trend line with silica supported samples. The sample with smallest particle size (2%Ag/Al_2O_3_IWI_C200_R200, 2.2 nm) had same selectivity as the silica supported sample with same particle size. The medium size (6.4 nm) sample showed slightly better selectivity to allyl alcohol (22% on Al_2O_3 vs. 18% on SiO_2). However, in contrast to SiO_2 supported catalysts the selectivity only increased by 2% to 24% when the particle size was increased to. 8.2 nm. The titania supported Ag catalysts showed much higher selectivity than either silica supported or alumina supported catalysts. The trend line of selectivity vs. conversion for titania supported samples was obviously above that for either silica or alumina (i.e. beyond typical experimental errors which might be on the order of ± 4% based on repeated runs of the same catalyst). The selectivity of the medium size sample 2%Ag/ TiO_2_mIWI_C250_R100 (4.8nm) was 29 %.(figure 15)

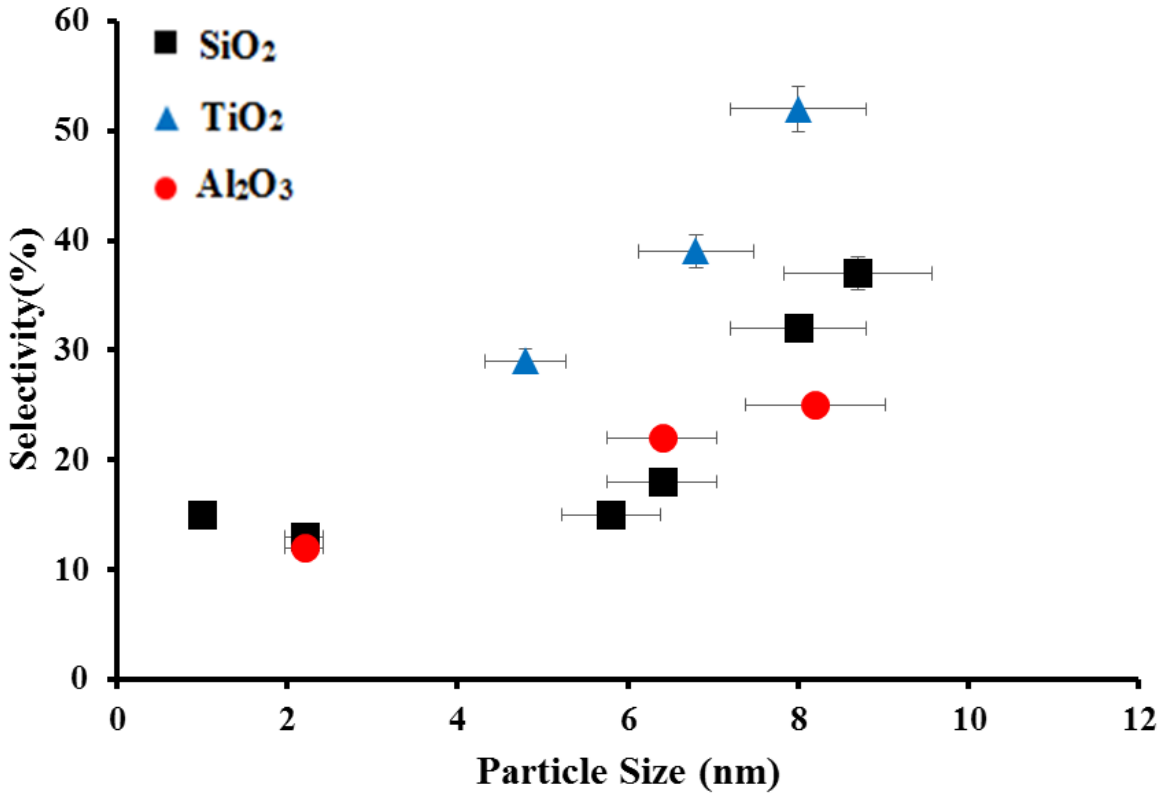

Figure 15: Comparison of selectivities towards allyl alcohol Ag catalysts on SiO_2, TiO_2 and Al_2O_3 with various particle sizes. Selectivities compared at 200 °C, 5 atm and 10% conversion.

This was about twice as large as the selectivity on the same-size silica-supported sample.[7] The sample 8%Ag/TiO_2_IWI_C400_R100, which had a particle size of 8 nm, gave 52% selectivity while silica supported sample having the around same size only exhibited a 32% selectivity toward allyl alcohol according to the trend line of silica samples. In all sizes within the range we studied, catalysts supported on TiO_2 nearly doubled the selectivity compared with SiO_2 at 10% conversion.

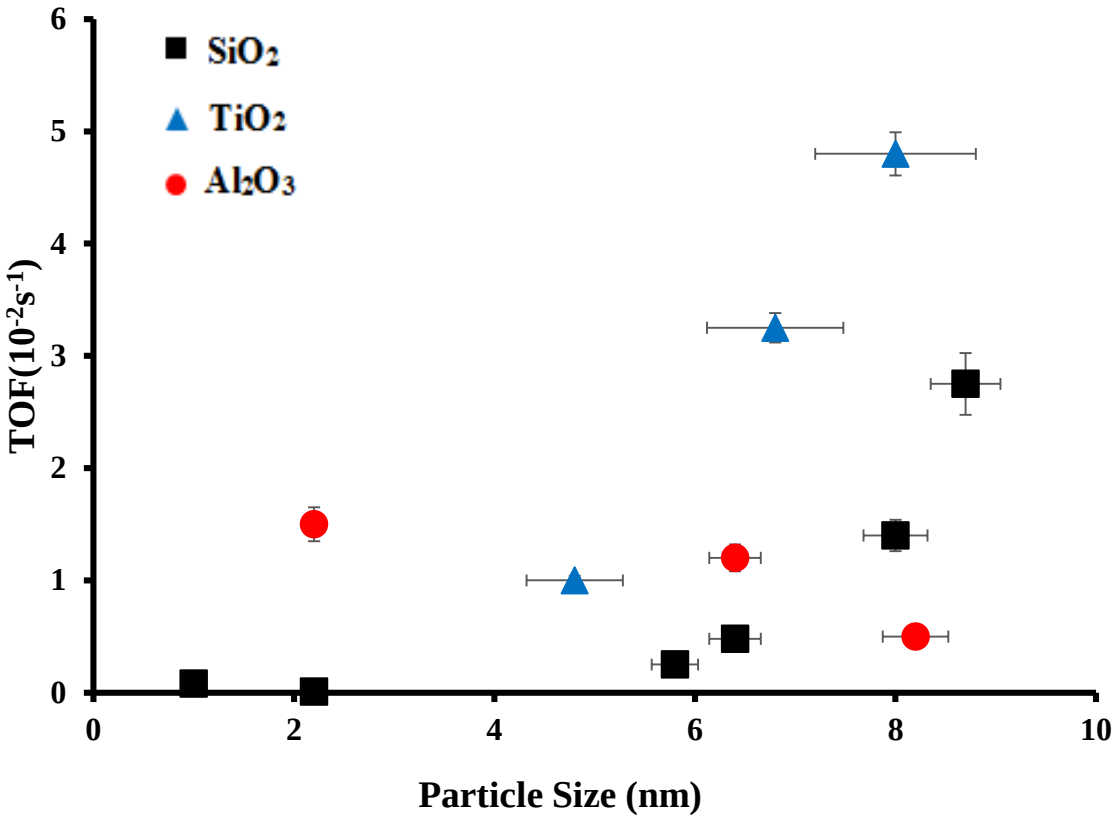

Figure 16: Comparison of Turn Over Frequencies (TOF) of Ag catalysts on SiO_2, TiO_2 and Al_2O_3

As shown in figure 16, not only the selectivity to allyl alcohol but also the TOF (Turnover Frequency) was enhanced by using TiO_2 as support. However, Al_2O_3 supported catalysts do not follow the same trend as the TiO_2 and SiO_2 supported catalysts with respect to their activity.

Over SiO_2 and TiO_2 catalysts turnover frequency for all increased with increasing the particle size, while the trend was inverted over Al_2O_3 supported catalysts. The TOF decreased steadily with

the particle size increasing from 2.2 nm to 8.2 nm. When the particle size was small on Al_2O_3, the TOF of catalyst was 1.6×10^{-2} s^{-1}, about 15 times as large as that over silica supported sample having same particle size. But for a larger size 8%Ag/ Al_2O_3_IWI_R325_S550 (8.2), TOF was 0.5×10^{-2} s^{-1} (figure 16), only 1/5 that of the TOF over the largest silica supported catalyst. This might be because specific surface area of alumina decreased from 210 to 43.9 m^2/g after steaming which may cause a decrease in activity and selectivity with increase of particle size. In contrast, as mentioned before TOF increased with larger particle size on TiO_2 similar to SiO_2. The largest Ag catalyst on TiO_2 (8nm) (figure 17 and Table 4) had a TOF of 4.8×10^{-2} s^{-1} compared to 2.75×10^{-2} s^{-1} on SiO_2 (8.7 nm).

Since, partially reducible support (TiO_2) showed promising results for enhancing the selectivity towards allyl alcohol, we tried other prominent supports of this kind (CeO_2, La_2O_3 and ZrO_2). The oxygen vacancy formation energies (Table 3) are also calculated on each of these oxide surfaces to compare the reducibility of the oxides. Recently, many theoretical studies have been reported to understand effect of O-defects of these metal oxide supports.[95-98] Sauer et al. has investigated O-vacancy energies for reducible oxides like TiO_2, ZrO_2, V_2O_5, and CeO_2.[98] The absolute values of vacancy energies, according to their work follow the order $CeO_2<V_2O_5 < TiO_2 < ZrO_2 <$ MgO trend similar to what we have computed. Also, other observed values, show energies of ZrO_2 and TiO_2 are not so different complying with our computed values. An experimental study on TiO_2 also revealed reduced anatase (101) crystal has isolated as well as ordered intrinsic subsurface defects using scanning tunneling microscopy (STM) unlike a freshly cleaved anatase TiO_2.[99] This result is consistent with density functional theory (DFT) calculations which also confirm that O vacancies at subsurface and bulk sites are considerably more stable than on the surface. However, we found

experimentally that all of these reducible oxides showed better selectivity than SiO_2 but also deactivation was a major problem with all these supports unlike TiO_2.

Table 3 : O-vacancy formation energies of metal oxide supports

Metal Oxide Supports	O-vacancy formation Energy (eV)
CeO_2	-9.49
ZrO_2	-9.78
TiO_2	-9.84
SiO_2	-10.93
La_2O_3	-11.34
Al_2O_3	-11.78

Incipient Wetness Impregnation yielded larger particles for all of these catalysts. So, we compared them in particle size range of 8-10 nm (figure 17 and Table 4) to avoid any particle size effect.

Table 4: Bond Distance and Coordination number for all the catalysts on all the supports (SiO_2, Al_2O_3, and TiO_2, CeO_2, ZrO_2, La_2O_3)

Sample name	**N_{Ag-Ag}**	**R(Å)**	**Estimated Size (nm) by EXAFS**
2Ag/Al_2O_3_IWI_C200_R200	6.9	2.83	2.2
8Ag/Al_2O_3_IWI_R325	10.5	2.87	6.4
8Ag/Al_2O_3_IWI_R325_S550	11.3	2.88	8.2
2Ag/TiO_2_mIWI_C250_R100	9.6	2.87	4.8
3Ag/TiO_2_mIWI_C500_R120	10.7	2.88	6.8
8 Ag/TiO_2_IWI_C400_R100	11.1	2.89	7.7
8Ag/ZrO_2_IWI_C400_R200	11.2	2.88	7.9
8Ag/CeO_2_IWI_ C250_R550	12	2.89	10
8Ag/La_2O_3_IWI_C400_R200	11.5	2.88	8.7

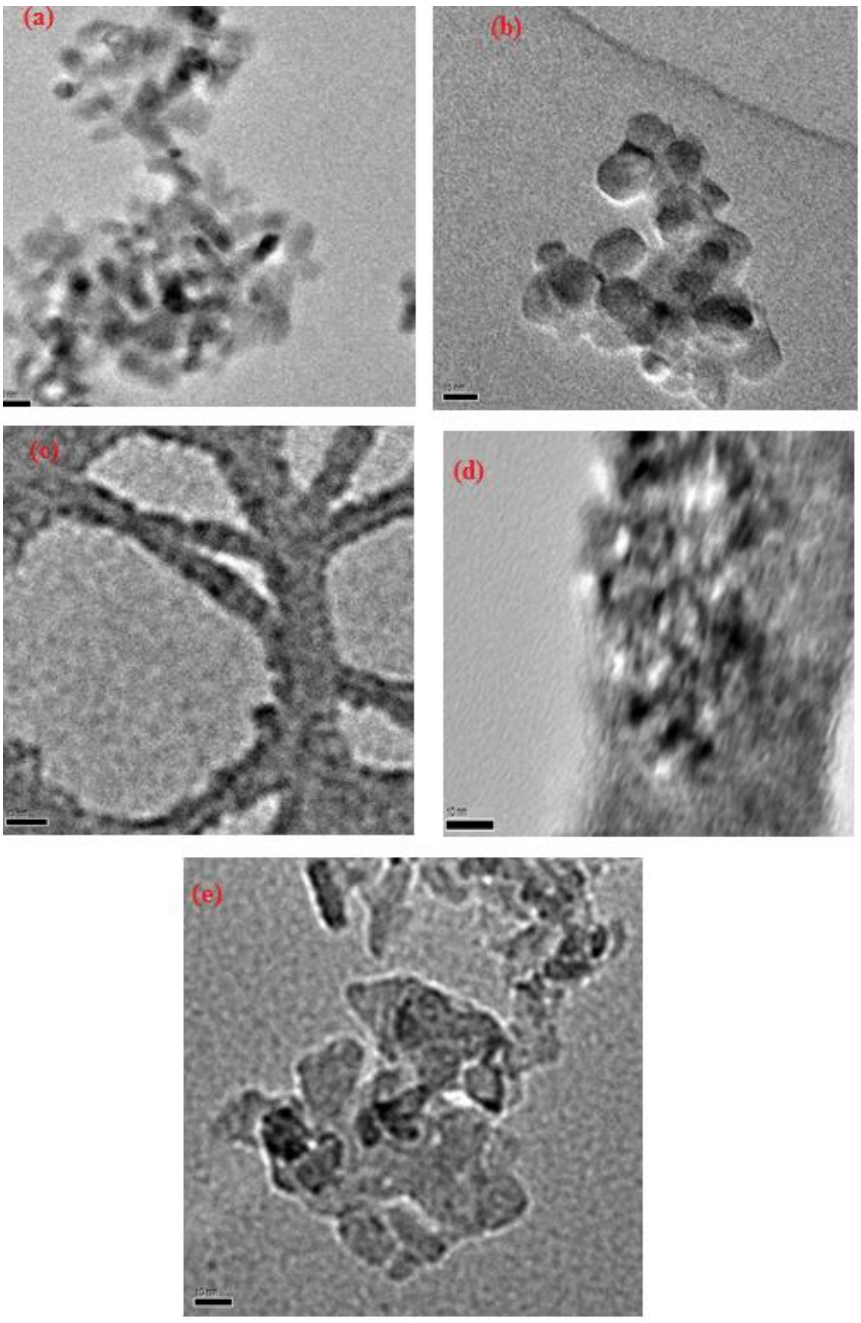

Figure 17: Bright Field TEM images (all scale 10 nm) of (a) 8Ag/ZrO2_IWI_C400_R200; (b) 8Ag/TiO2_IWI_C400_R100; (c) 8Ag/La2O3_IWI_C400_R200; (d) 8Ag/CeO2_IWI_ C250_R550 (e) 8Ag/Al2O3_IWI_ R325

For CeO_2 initial selectivity was very high (68%), for La_2O_3 (46%) at 10% conversion. (figure 18) For ZrO_2, however, it reached a stable selectivity of around 50% and maintained it even with increase of conversion. (figure 18). These are of same particle size to avoid particle size effect.

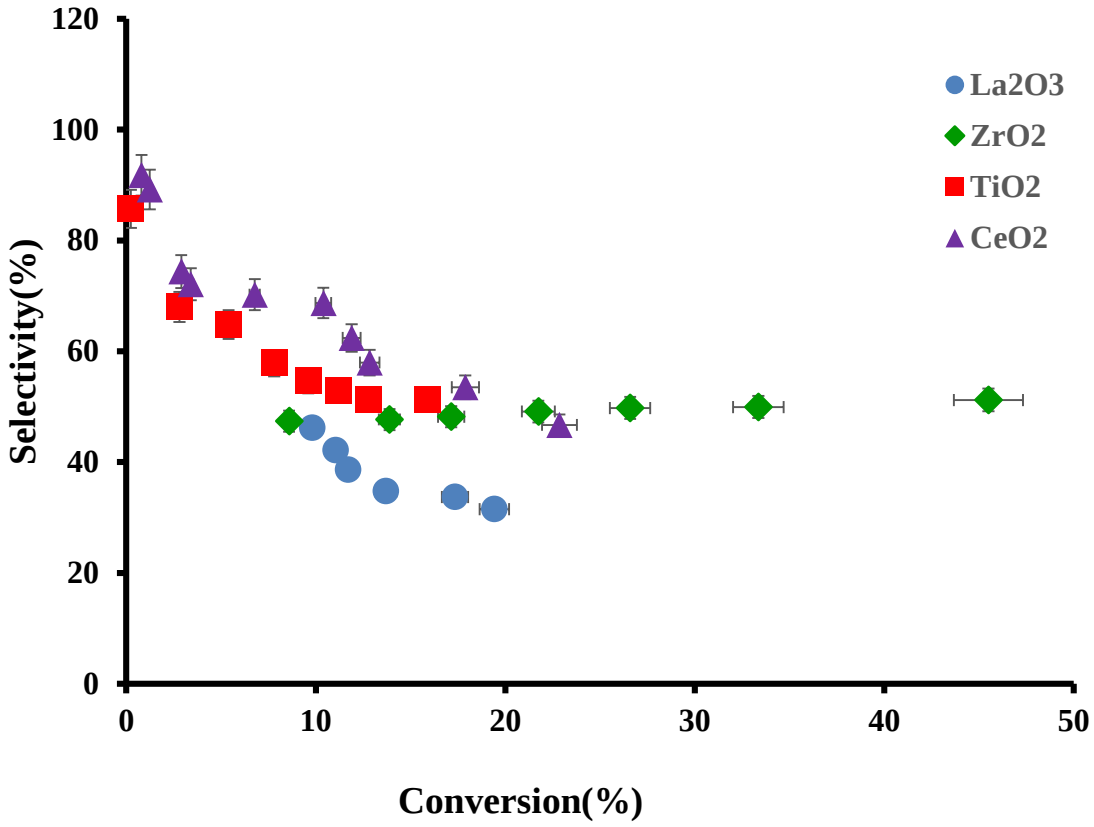

Figure 18: Selectivity (%) vs. Conversion (%) Plot for Ag catalysts on partially reducible supports (TiO_2, La_2O_3, ZrO_2, and CeO2) of same particle size. All catalysts' testing are performed at 200 °C and the reaction pressure was 5 atm.

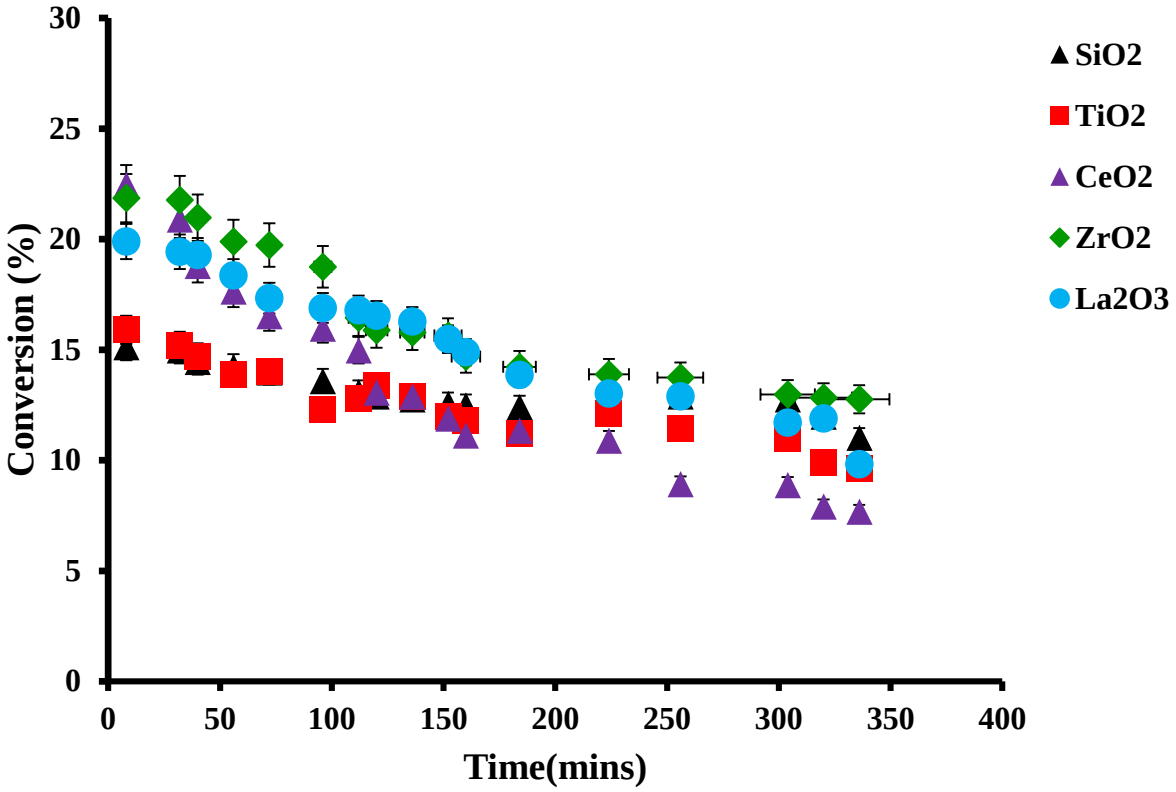

Figure 19 : Deactivation of Ag/SiO_2, Ag/TiO_2, and Ag/CeO_2 catalysts with time on stream.

The deactivation of five catalysts (Ag/SiO_2, Ag/TiO_2, Ag/CeO_2, Ag/ZrO_2, Ag/La_2O_3) with time on-stream are compared in figure 19. Ag/CeO_2 though showed the highest selectivity at lowest conversion, it deactivated faster than Ag/SiO_2, Ag/TiO_2. This might be due to the presence of more surface acid sites on CeO_2 than other two supports that may be detrimental to the stability of the catalyst. [91]

For understanding the detailed kinetics of the reaction on these partially reducible supports, we chose titania as a representative candidate and compared the results with our previous detailed study on silica.[7] The most selective catalyst on titania (8%Ag/TiO_2_IWI_C400_R100) is used to

perform the more in depth analysis. For a complete kinetics study we assumed a simple power rate law:

$r = k[\text{Acrolein}]^m[H_2]^n$

We varied the concentration/partial pressure of acrolein or H_2 to reach the reaction orders of both reactants. Taking the logarithm yields:

$\ln(r) = \ln(k) + m\ln[\text{Acrolein}] + n\ln[H]$

Since k is only a function of temperature here, at fixed T the slope from plotting ln(r) against ln[acrolein] is m when keeping the concentration of H_2 constant (figure 20), n can be determined in an analogous manner. We found order of the reaction with respect to acrolein and hydrogen changed on TiO_2 from 0.77(measured on SiO_2) to 0.18. (Table 5). The lower order of acrolein when the support is changed to TiO_2 may indicate that the surface coverage may be higher possibly due to spillover from the support. . Rate expressions have been derived (presented in the Appendices) to understand the effect of rate determining step of the reaction. From rate expression calculations and thereby determining rate orders from different rate determining steps, it can be inferred for Ag/TiO_2, it seems, second hydrogenation step, ie. Hydrogenation to allyl alcohol is the rate determining step which gives almost the same range of orders for both reactants as experimentally observed. But, for Ag/SiO_2, rate 3 (allyloxy adsorption) or first hydrogenation is found to be the rate determining step which fits the range of orders for both acrolein and hydrogen as observed experimentally (high orders with respect to both hydrogen and acrolein as mentioned in table 5).

Table 5: Comparison of Rate, Activation energy and Reaction Orders between 8Ag//TiO_2_IWI_C400_R100 (8nm) and 8Ag/SiO_2_IWI_R325 (8.7 nm) at 5 atm pressure

Catalyst	**Rate [mol $h^{-1}gAg^{-1}$]**	**Ea [KJ/mol]**	**m(order with respect to acrolein)**	**n(order with respect to H_2)**
8Ag/TiO_2	0.286	30	0.18	0.74
8Ag/SiO_2	0.139	42	0.77	0.65

A pathway analysis following the example of Bhore and Klein [42] was performed to determine if the presence of the reducible support altered the primary pathways of the reaction.

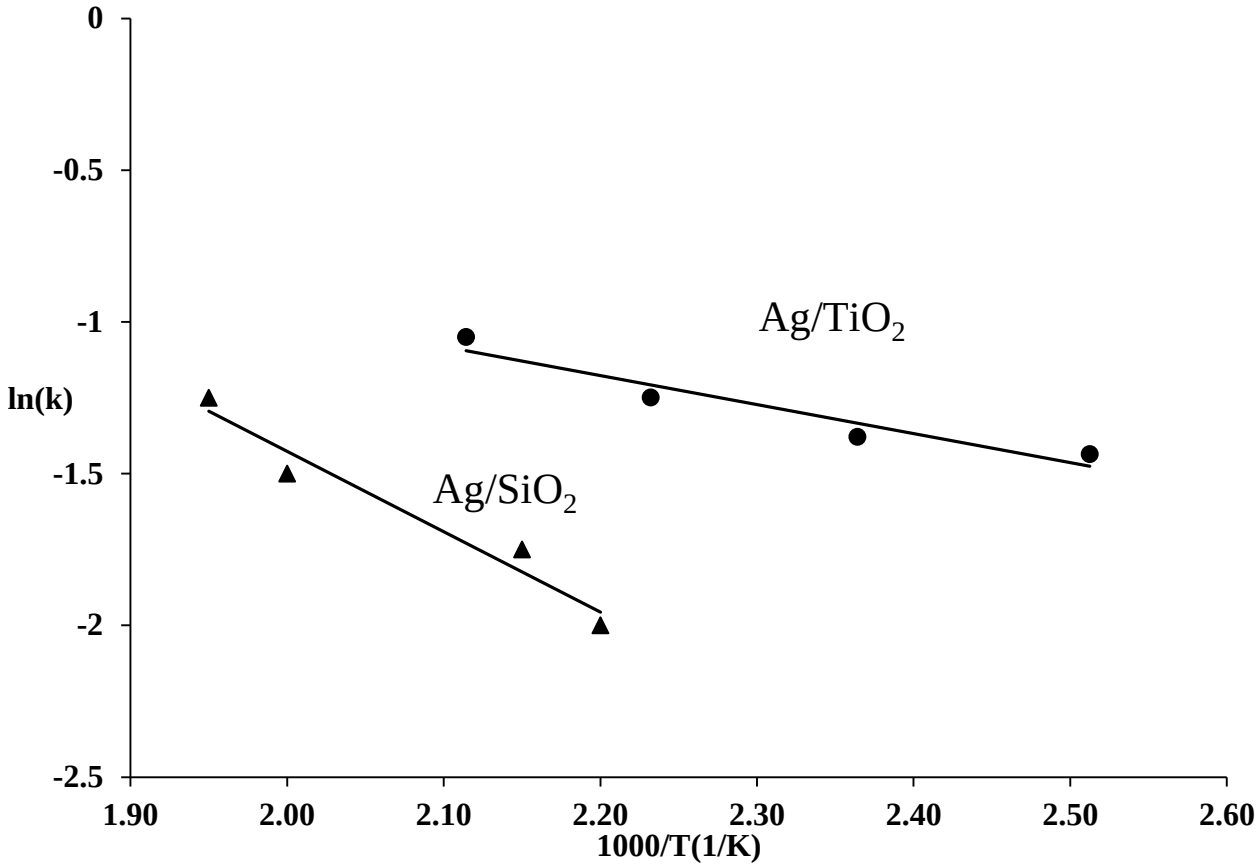

Figure 20: Arrhenius plot of hydrogenation of acrolein over 8Ag/TiO2_IWI_C400_R100 and 8Ag/SiO_2_R325 at 5 atm.

21 (a)

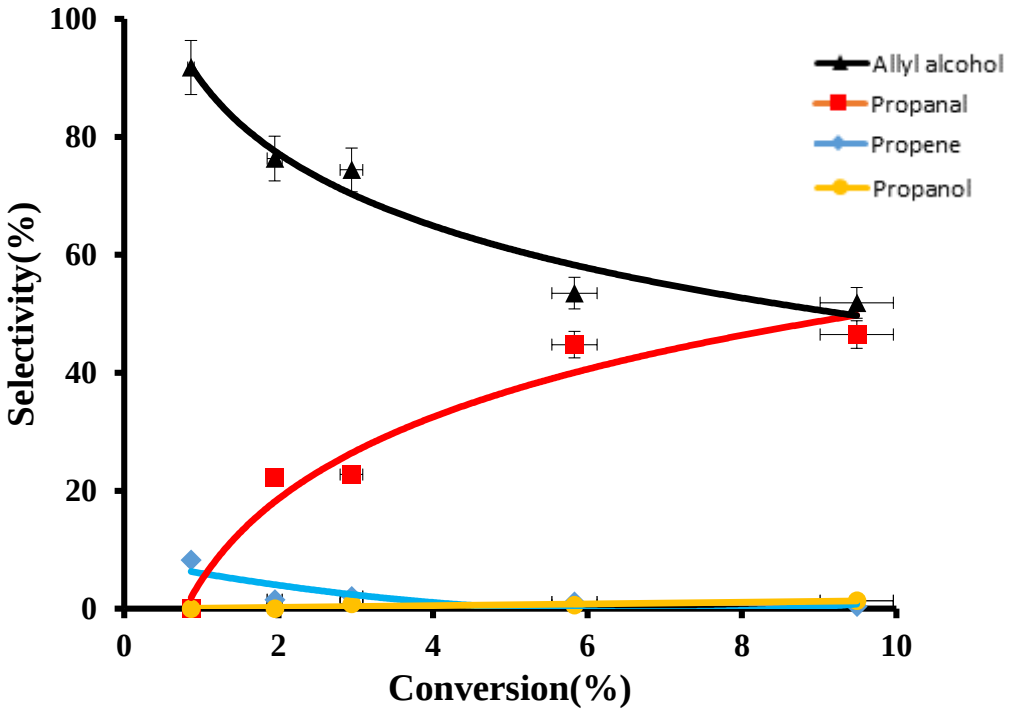

21(b)

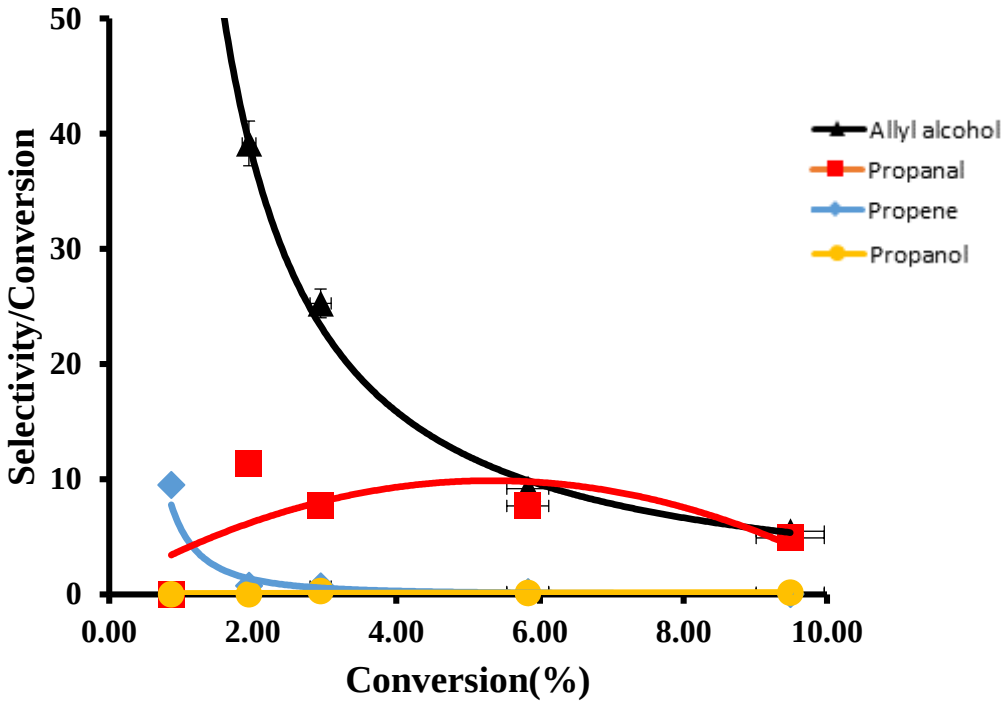

Figure 21: Pathway analysis at 5 atm of 8Ag//TiO2_IWI_C400_R100 : (a) first-rank delplot; (b) second-rank delplot.

From the results in figure 21, it is observed that the intercept of propanal and propene are nonzero, implying they are secondary products, while propanol may be a higher rank product due to its zero intercept. However, the selectivity to propanol may be too low to make an exact assessment. For, Ag/ SiO_2, primary products after pathway analysis revealed to be both propanal and allyl alcohol while for Ag/TiO_2, primary product was only found to be allyl alcohol which supports the experimentally found higher selectivity towards allyl alcohol at a same conversion, temperature and pressure in case of TiO_2 compared to SiO_2.

Also, we have performed DFT calculations to theoretically estimate the absolute O-vacancy formation energies for different metal oxides, used as supports, as mentioned in Table 3. Interestingly, when we compared the selectivities of these different metal supports for Ag catalysts of around same particle size (8-10 nm), we found a linear relationship between the selectivity and reducibility of these supports (figure 22). It was observed that with increase of reducibility (decrease of absolute O-vacancy energies) , there was an increase in selectivity towards allyl alcohol on these supports for Ag catalysts at 10% conversion, 200° C and 5 atm. CeO_2 support showed highest selectivity and also had the highest reducibility (lowest absolute O-vacancy formation energy).

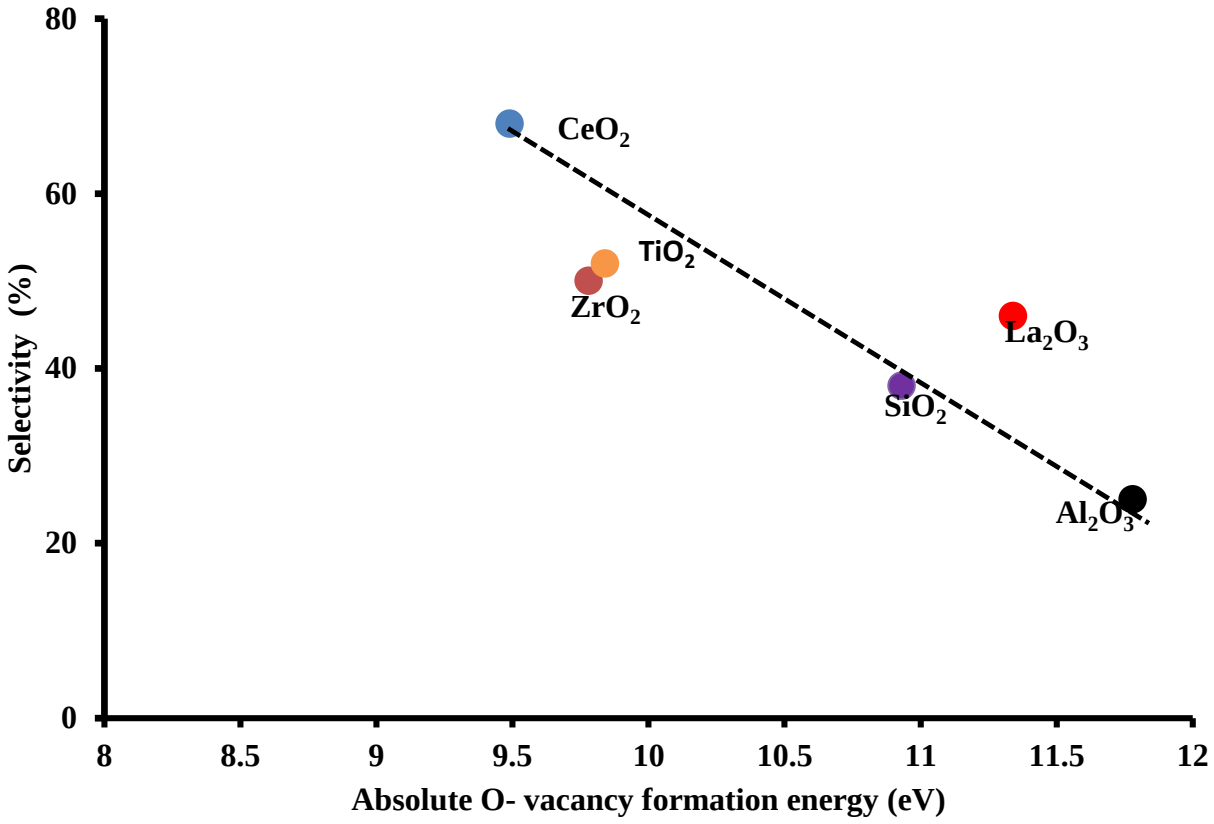

Figure 22: Relationship between reducibility of metal oxide supports and their selectivity for Ag catalysts of same particle size for 10% conversion at 200 °C and 5 atm.

It has been previously reported that partially reducible supports, such as TiO_2, CeO_2 and SnO_2 [87, 91, 100] can improve the catalytic performance. There are a number of explanations but they can be broadly divided into three categories: (i) new sites created at the metal-support interface, including creation of alloy phase by the loaded metal and the reduced support;[84, 88, 100] (ii) formation of support over layer on the metal particles [86] or structural change of the metal particles[32]; (iii) electron transfer between the metal and support [101, 102]. One or more of the effects may be the origin to the apparent support effect in selectivity and/or activity which is discussed later after analyzing the reactivity orders which give us more insight to the support effects for this particular reaction. In our case, since all TiO_2 supported catalysts were reduced at low temperature 100-120 °C, migration of support onto silver particles seems unlikely. Though our catalysts were reduced at 100-120 °C, our reaction temperature is only 200 °C. However, migration of support onto silver particles seems unlikely as restructuring of the support over layer on the metal particles typically occurs at much higher temperature (500 °C) .[89] Thus we propose that TiO_2 changes the properties of Ag through effect (i) or/and (iii). Formation of new sites, for example partially reduced Ti^{3+} species which can serve as a Lewis acid sites, could favor the adsorption of acrolein, especially through C=O bond and result in better selectivity and activity.[103] DFT calculations also suggest that (figure 23), that Ti^{3+} sites more favorably bind acrolein through carbonyl bond (-0.99 eV) than olefinic bond (-0.45eV). This strong

adsorption of acrolein to the TiO_2 substrate could explain the low reaction order for acrolein that we observe.

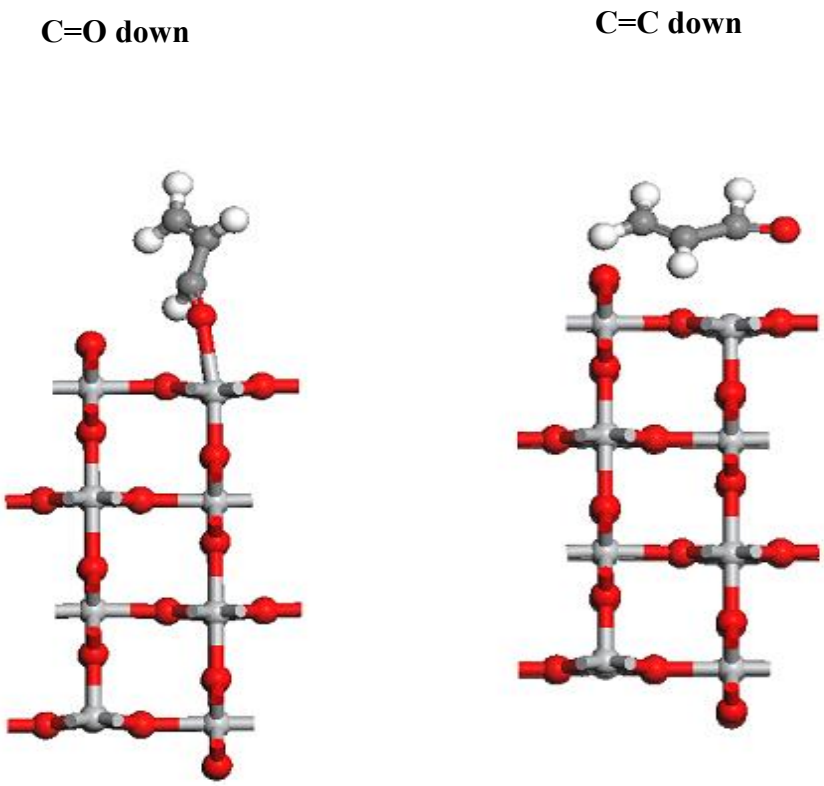

Figure 23: Adsorption of Acrolein favorably through carbonyl bond over Ti^{3+} sites. (Red atoms (Oxygen); White atoms (Hydrogen); Gray (Carbon); Ash (Ti)

It is also mentioned that the selectivity of acrolein hydrogenation to allyl alcohol increases when the interaction with the substrate decreases. If there is a strong interaction between the Ag and the TiO_2 support, then the TiO_2 supported nanoparticle may be less reactive (i.e. the d-band of the Ag nanoparticle moves further away from the Fermi level when supported on TiO_2 vs. Al_2O_3 or SiO_2). Campbell and co-workers have utilized this analysis to the changes in the heats of adsorption of silver on different substrates [104-106]. When the particle size of silver was smaller than 4 nm, the heat of adsorption on slightly reduced CeO_2 (111) and Fe_3O_4 (111) were much higher than that on MgO (110). As a result, it was inferred that reducible supports had stronger interactions with silver than non-reducible supports. Campbell, et al. have further suggested that adsorption of molecules on the metal nanoparticles should be sensitive to the bond strength between the particle and the support. It is also concluded using a simple bond order conservation argument that an adsorbate will bind to a metal nanoparticle on a weak interaction support but the adsorbate would have a weaker interaction with a metal nanoparticle supported on a highly reducible support, where a strong metal support interaction (SMSI) exists [40]. In our study, a decrease in the adsorption strength of acrolein on TiO_2 supported Ag vs. SiO_2 or Al_2O_3 supported Ag (which possess a weaker interaction) may therefore increase the selectivity.

3.4 Conclusion

SiO_2, Al_2O_3 and TiO_2 were selected as primary supports to investigate the support effect of silver catalysts for acrolein hydrogenation. On each support, a similar particle size effect in selectivity (larger particle size, better selectivity) except Al_2O_3, was observed. TiO_2 showed best performance in terms of both selectivity and activity as well as stability. Formation of Ti^{3+} sites may favor the adsorption of acrolein through carbonyl group as also observed by DFT results. Other

representatives of partially reducible supports (CeO_2, ZrO_2, and $La_2O_{3)}$ were also studied but unfortunately they deactivated too rapidly to establish reliable kinetics. Similar to TiO2, these catalysts proved to be better in selectivity towards allyl alcohol than over SiO_2 or Al_2O_3 at same conversion and particle size. All of the partially reducible supports followed the same particle size effect like on SiO_2. [7]Using TiO_2 as a representative candidate, it was shown that the reaction order of acrolein decreases from ~1 to 0.2, indicating a higher acrolein coverage at similar reaction conditions, possibly due to spillover from the support.

4.0 Effect of Structures of Silver on Selective Hydrogenation of Acrolein

4.1 Introduction

The goal of the work will be to predict computationally the structural dependence of Ag surfaces on selective hydrogenation of acrolein. We have found using DFT calculations that acrolein bonds through the carbonyl bond on the Ag(100) surface. This is in stark contrast to other surfaces where acrolein prefers to bond through the C=C bond. It seems logical that strong improvements to the selectivity to allyl alcohol might be realized if nanoparticles with only (100) surfaces could be utilized in this reaction as the C=O will be easier to hydrogenate on this surface.

Theoretically we can investigate the elementary steps by identifying transition steps and their associated activation barriers. However, computing transition states demands intensive quantum chemical computations, and hence the theoretical exploration of complex catalytic reaction networks at solid surfaces remains a remarkable challenge. Faster methods to compute activation energy barriers are therefore needed for a preliminary screening.[107]

One of the simpler approaches is by using Brønsted–Evans–Polanyi (BEP) relations, which classically link kinetics (activation barriers) with thermodynamics (reaction enthalpies).[108] These relationships, observed in current density functional theory (DFT) studies on the dissociation of small molecules over transition-metal surfaces, [109-112] are determined for a given reactant and an elementary step by changing the type of the catalyst. In these studies, the activation energy barrier is plotted against either the reaction energy or the stability of the final dissociated state. But this relation has not been observed for multifunctional reactants, where the chemical nature of the atoms next to the reactive centers changes. This would be really valuable for fine chemistry reactions, mainly in regard to selectivity issues.[107]

In the past, Hirschl *et al.* examined various adsorption modes for acrolein on the (111) surface of Pt [38]and $Pt_{80}Fe_{20}$ [37]with spin-polarized density functional theory. On Pt(111), acrolein showed its main interaction with the surface with the C=C bond, with an eventual additional weak interaction with the oxygen atom, over a large range of coverages. This could evidently result in a predominant hydrogenation of the C=C bond, as was understood experimentally. For the $Pt_{80}Fe_{20}$ (111) surface, a strong segregation of platinum atoms towards the surface layer occurred when the surface was clean. However, the significantly larger aldehyde-surface interaction energy upon the formation of O–Fe bonds can alter the surface composition (the adsorption energy of acrolein on Pt(111) via a di-σ CO configuration was 0.25 eV and its counterpart on $Pt_{80}Fe_{20}$(111) was 0.68 eV)and increase the Fe content in the surface layer. Thus the presence of alloying Pt with Fe allows the potential to influence the hydrogenation selectivity towards unsaturated alcohols.

Silver is especially interesting because of its excellent selectivity for selective hydrogenation of acrolein. Rösch and co-workers investigated the adsorption of acrolein on flat Ag(110) and stepped Ag(221) surfaces [39]. The C=O bond was predicted to be activated according to experimental results. However, the calculations showed acrolein to interacting only weakly with all adsorption sites studied, (by at most 35 $kJ \cdot mol^{-1}$, obtained on Ag(221) step through a η4(C,C,C,O) configuration), resulting very limited C=O bond activation. They also revealed that weaker adsorption was found on denser Ag(111) surface (~ 10 $kJ \cdot mol^{-1}$) with the molecular plane parallel to the surface. Rösch and co-workers also examined hydrogenation of acrolein over Ag(110) and Ag(111) with O in the subsurface [40]. The authors found that while hydrogenation of the C=O bond

was less favorable over the bare silver (and thus propanal is the favored product) but when O was present in the subsurface, the energetics switched such that the selectivity favors allyl alcohol.

While Rosch and co-workers only considered a coverage of 1/8 ML, Ferullo et al [13]showed that there was a coverage dependence of the structure of adsorbed acrolein on Ag(111) surface. They calculated the adsorption modes of acrolein at various coverages by changing the sizes of Ag(111) supercells. *p*(4×4) and *p*(2×2) configurations were used in the case of "head to tail" adsorption, representing low and high coverages. In this situation, all acrolein molecules were oriented in the same way. Yet another possibility of acrolein arrangement exists. Acrolein can adsorb in a "head to head" adsorption configuration, meaning the C=O bond of one acrolein molecule is adjacent to C=O of another molecule. Thus supercells *p* (5×3) and *p* (4×2) were employed to examine the "head-to - head" adsorption mode. When acrolein molecules were directed in head-to-tail manner, changing coverage did not vary the adsorption mode. Acrolein remained parallel to the Ag(111) surface at both low and high coverages. For the *p* (5×3) supercell, the adsorbates form almost isolated dimers and adsorbed parallel to the surface. However, for the *p* (4×2) structure, a molecular network involving chains of adsorbed acrolein in a zigzag pattern was found, where each molecule intermingled with two nearest neighbors through O···H contacts (figure 5).

It is obvious that in one row of the zigzag structure the molecules are almost perpendicular to the surface. Thus oxygen atoms from the carboxyl group should react more easily with adsorbed atomic hydrogen due to their proximity to the surface. This result gives an explanation of the phenomena [4, 6] mentioned in Wei et al.[7] that increasing reaction pressure could increase the selectivity to allyl alcohol.

In a previously mentioned study of Rosch *et al.*, they examined adsorption of acrolein with coadsorbed hydrogen atoms on Ag(110) and observed that hydrogenation can occur through hydrogenation at four particular points: the terminal oxygen of acrolein or at any of the three other carbon atoms. Hydrogenation of the terminal oxygen results in the formation of hydroxyallyl (H_2C=CH-CHOH) while hydrogenation of the carbon of the aldehyde functionality leads to the formation of allyloxy (H_2C=$CHCH_2O$). Further hydrogenation of hydroxyallyl or allyloxy leads to the formation of the desired product, the unsaturated alcohol, allyl alcohol. However, hydrogenation of the olefinic bond can lead to the formation of either 1-formylethyl ($H_3CCHCOH$) or 2-formylethyl (H_2CCH_2COH). Further hydrogenation of 1-formylethyl or 2-formylethyl leads to the formation of the saturated aldehyde, propanal. By modeling a Ag(110) surface with a sublayer of oxygen, Rosch demonstrated that the outcome of oxygen treatment affects both the activity and selectivity by lowering the barrier to hydrogen dissociation and shifting the stability of key intermediates on the surface. [40, 113] However, it was not clear if subsurface O could be stabilized in Ag catalysts following reductive treatments or in the reducing environment of the hydrogenation reactor.

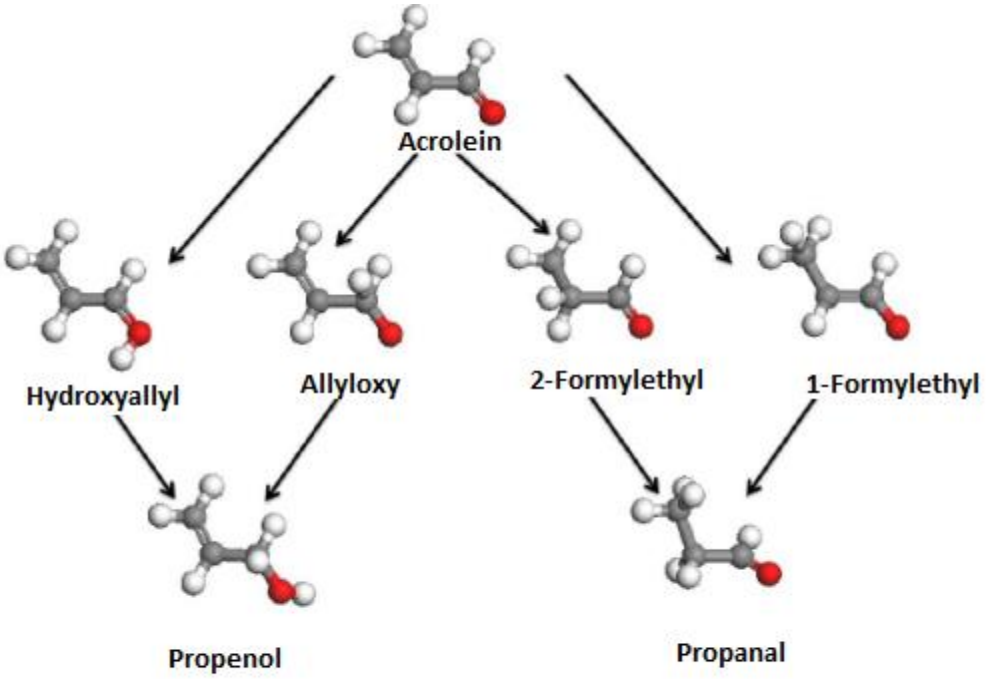

Figure 24: Reaction pathway of acrolein hydrogenation including intermediates. [40]

In a their DFT study of acrolein hydrogenation over Au [211], Yang et al. found that the acrolein's C=C bond has a weak interaction with atoms located at steps (E_{ads} = 21 kJ/mol).[114] On the contrary, the C=O functionality does not react with the step atoms at all suggesting that the edge sites contribute to lower selectivity to allyl alcohol formation. On Pt[211] the step site is also preferred, as the acrolein molecule adsorbs via the C=C double bond (Eads = 157 kJ/mol) about 60 kJ/mol more strongly than on a terrace site. On Pt[211] the desorption of allyl alcohol was found to be important to the overall rate due to the strong adsorption energy of the final products onto the surface (76 kJ/mol for propanal and 140 kJ/mol for allyl alcohol) . In addition, on Pt[211] the barrier for hydrogenation of hydroxyallyl was observed to favor the formation of the enol over allyl alcohol

by approximately 19 kJ/mol [114], although the enol is not a stable species in the gas phase but it has been shown to be stabilized by bonding to metals [113, 115].

In their recent studies, Sautet and co-workers studied all the first and second hydrogenation routes of acrolein on Pt(111) by DFT calculations. Linear relations are extracted when the energies of the transition states are plotted against those of the precursor states for the hydrogenation of unsaturated aldehydes on platinum. This relationship allows a quick and exact analysis of the energy barriers of the reaction when altering the chemical environment of the reactive center. A preliminary micro kinetic model based on the energy barriers calculated by DFT [80] displayed a better selectivity for SAL(saturated aldehyde) on platinum, in agreement with experimental observations.[66]

This selectivity results from a competition between the energy barriers of the surface hydrogenation steps and adsorption energies of the partially hydrogenated products. However, the picture remains unfinished in regard to the third and fourth hydrogenations that lead to SOL (saturated alcohol). [12] No explanation is offered to interpret the differences observed in the selectivity between acrolein and other unsaturated aldehydes, such as crotonaldehyde or prenal, aside from their adsorption energies.[66] In their study, Sautet et al. described by employing an original definition of the Brønsted–Evans–Polanyi relation how the activation barriers of this prototype reaction can be predicted in a fast and accurate way. First, the linear scaling relations are proved for the hydrogenation pathways at the various sp^2 centers of acrolein and its hydrogenated derivatives. They are then confirmed with the hydrogenation of prenal and a few other derivatives. It was thus described how the reactivity of these centers can be computed from the calculation of only a few of them, thereby permitting the selectivity of a complete family of reactants to be explained. [107]

4.2 Computational methods

The density functional theory (DFT) calculations are performed using the Vienna Ab Initio Simulation Package (VASP).[73, 74] A plane-wave basis set with a cut off energy of 500 eV and projector-augmented wave (PAW) based pseudopotentials [73, 75] are employed. The Perdew Wang (PW-91) form of the generalized gradient approximation (GGA) exchange and correlation functional is used in all calculations reported herein.[76] A five-layer slab model with 3 × 3 surface unit cell is adopted to model the Ag(111) surface. The Brillouin zone is sampled with a 3× 3 × 1 k-points grid.[77] The geometries of all structures were located with the conjugate gradient method and were considered to be converged with energy within 0.001 eV and forces of less than 0.025 eV/Å. The top three layers are allowed to relax. A vacuum space of 16 Å was applied to separate the slabs. The transition states (TS) are determined by the climbing nudged elastic band (NEB) method of Henkelman and Jónsson.[78]

4.3 Results and Discussions

In our study we looked at three different structures of silver; Ag(221), Ag(111), Ag(100). We had studied acrolein adsorption for low (1/16 ML) and high(1/4 ML) coverage in two different modes, carbonyl bond down and olefinic bond down on the surface. The higher coverage is 4 times larger than the lower coverage as also considered by Ferullo et al. [13] For both coverages, the Ag(100) surface showed higher affinity towards hydrogenation through C=O bond. For lower coverage (with only one acrolein adsorbed on the surface or 1/16 ML), the acrolein adsorption energy through C=O down was 0.35 eV compared to 0.29 eV through C=C down on the Ag(100) surface. However, for other surfaces, it was not similar. For Ag(111) and Ag(221), acrolein was more favorably adsorbed C=C down compared to C=O down. For Ag(111), the acrolein adsorption energy was 0.55 eV when

bonded through C=C compared to 0.34 eV through C=O down while for Ag(221) , it was 0.69 eV through C=C down compared to 0.27 eV through C=O down. This suggests that structure sensitivity, is playing a role for this particular reaction, controlling the way acrolein, getting adsorbed on the surface. This motivated us to probe three of these surfaces in detail to understand if Ag (100) was certainly playing a role to adsorb the acrolein favorably through C=O bond, facilitating hydrogenation to the desired product allyl alcohol.

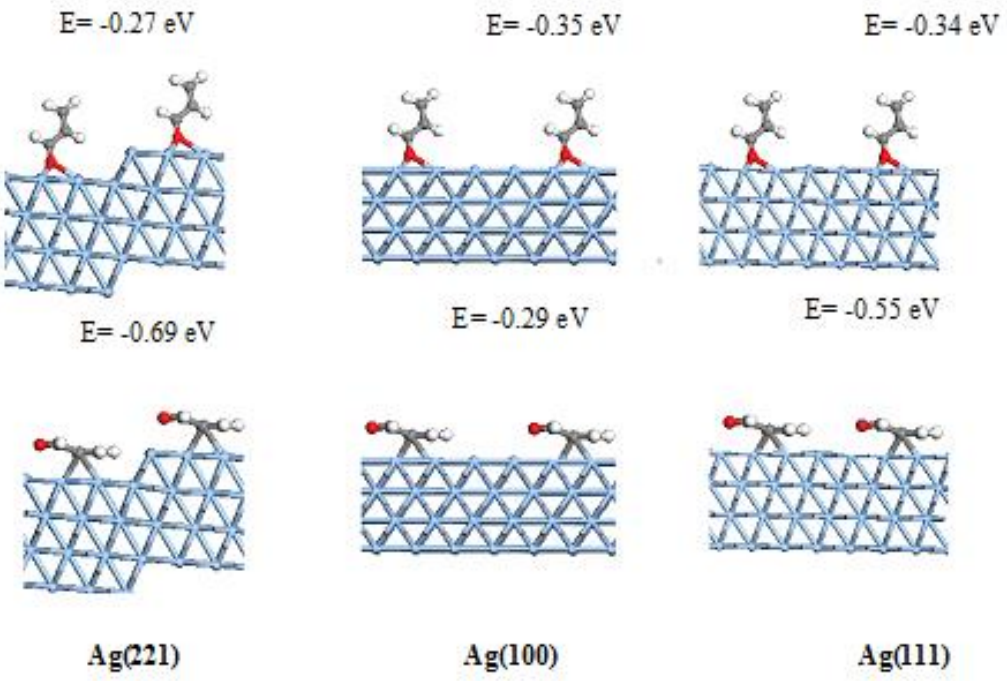

Figure 25: Adsorption Energies of Acrolein through C=C and C=O bond on Ag(100), Ag(221), Ag(111).

We studied two different cases of adsorption of acrolein on each surface. In the first case, we compared the adsorption energies of acrolein for different bonding modes on the surfaces and in the second case, we did the same but with four acrolein molecules on the surface .We found that for both of these cases (figure 25, 26), Ag(100) was the only structure of silver which showed affinity towards adsorption for acrolein through carbonyl bond. This was markedly different from other two surfaces, Ag(221) which is a stepped surface and Ag(111) which is a flat surface.

This suggests silver nanocubes will be a structure favorable for hydrogenation of acrolein to unsaturated alcohol. Christopher et al.[116] for example, showed how catalytic selectivity in the epoxidation of ethylene to form ethylene oxide on alumina-supported silver catalysts is dependent on the geometric structure of the catalytically active Ag particles and reaction conditions.

To understand the surface specificity for adsorption of acrolein in more detail, we looked at adsorption energies of four different intermediates, allyloxy,hydroxyallyl, 2-formylethyl, and 1-formylethyl. This choice was inspired from Rosch and coworkers' work mentioned previously .[40] The adsorption of all these intermediates on each surface are computed at 1/4 ML coverage of acrolein. For each intermediate, the favorable adsorption mode for that particular intermediate was used. In case of allyloxy and hydroxyallyl, the adsorption was through C=O down since the ultimate hydrogenation product will be allylalcohol while for the other two intermediates(1-formylethyl and 2-formylethyl), the adsorption energy on the surface was computed through C=C down in which case ultimate hydrogenation product was propanal.

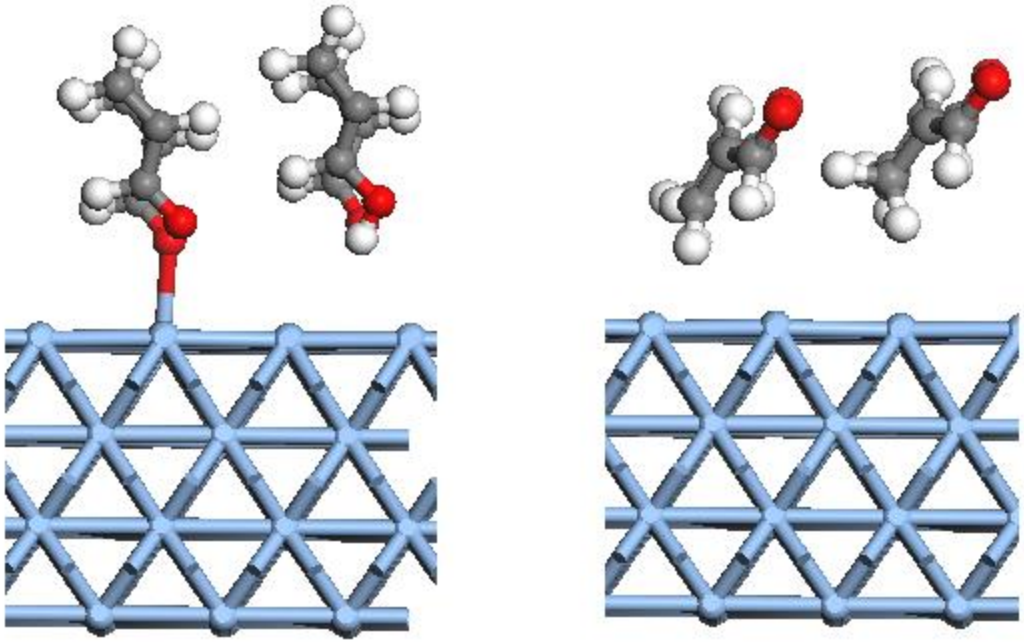

Figure 26: Adsorption of Hydroxyallyl and 1-formylethyl on Ag (100) surface.

Table 6 : Adsorption Energy of Intermediates on Ag (100), Ag (221), Ag (111) with respect to corresponding bare surfaces with gas phase acrolein and hydrogen

Ag111 Intermediates	**Energy (eV)**
Ag111_3Acrol_Allyloxy	0.16
Ag111_3Acrol_Hydoxyallyl	-0.22
Ag111_3Acrol_2Formylethyl	-0.17
Ag111_3Acrol_1Formylethyl	-0.19

Ag100 Intermediates	**Energy (eV)**
Ag100_3Acrol_Allyloxy	-0.29
Ag100_3Acrol_Hydoxyallyl	-0.27
Ag100_3Acrol_2Formylethyl	-0.031
Ag100_3Acrol_1Formylethyl	0.30

Ag221 Intermediates	**Energy (eV)**
Ag221_3Acrol_Allyloxy	-0.39
Ag221_3Acrol_Hydoxyallyl	-0.48
Ag221_3Acrol_2Formylethyl	-0.51
Ag221_3Acrol_1Formylethyl	-0.50

Adsorption energies of all the intermediates on three surfaces of silver for higher coverage of acrolein are reported in Table 6 above. It was observed for Ag(100), adsorption energy of both hydroxyallyl and allylalcohol are favored over 1-formylethyl, 2-formylethyl adsorption unlike other two surfaces , suggesting on Ag(100), hydrogenation of acrolein is favored towards the unsaturated alcohol rather than the saturated alcohol. On Ag(221), the preferred adsorption of the formylethyl intermediates over allyloxy and hydroxyallyl confirming it prefers the hydrogenation of acrolein to

the saturated alcohol. For the Ag(111) surface, the two pathways are competitive as one of the preferred adsorption intermediates was allyloxy which leads to formation of allyl-alcohol eventually, while the other preferred adsorption intermediate was 1-formylethyl which eventually gets converted to propanal.

However, this analysis is purely based on thermodynamics and does not give us an insight on the kinetics of the reaction. The computation of energies only suggested the preference of pathways for intermediate formation on three different surfaces of the silver. To investigate further on the kinetics of the reaction, we must perform transition state analysis for this intermediate formation on each of these surfaces. This led us to resort to the classical BEP relationship [81], which helps us to compare the energetics on different surfaces for adsorption of intermediates.

In figure 27. , the BEP relationship is shown for hydroxyallyl formation on Ag(100), Ag(111), and Ag(100) . It is seen for both Ag(100) and Ag(111), the hydroxyallyl formation energy barrier are low. For Ag(100), the activation energy was 0.383 eV and for Ag (111) was 0.41 eV. This suggests both faces favored hydroxyallyl formation compared to Ag(221) which showed high barriers for formation of hydroxyallyl, around 1.08 eV.

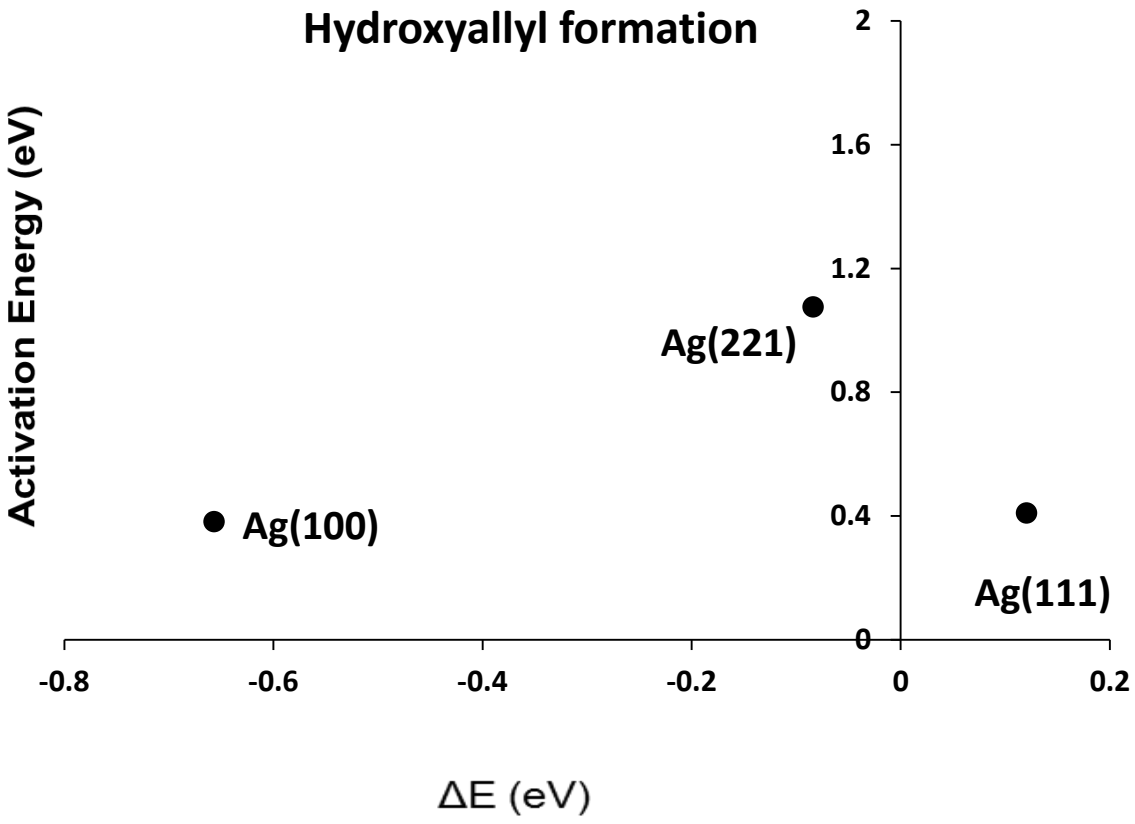

Figure 27: BEP relationship for hydroxyallyl formation on Ag (111), Ag (221), Ag (100).

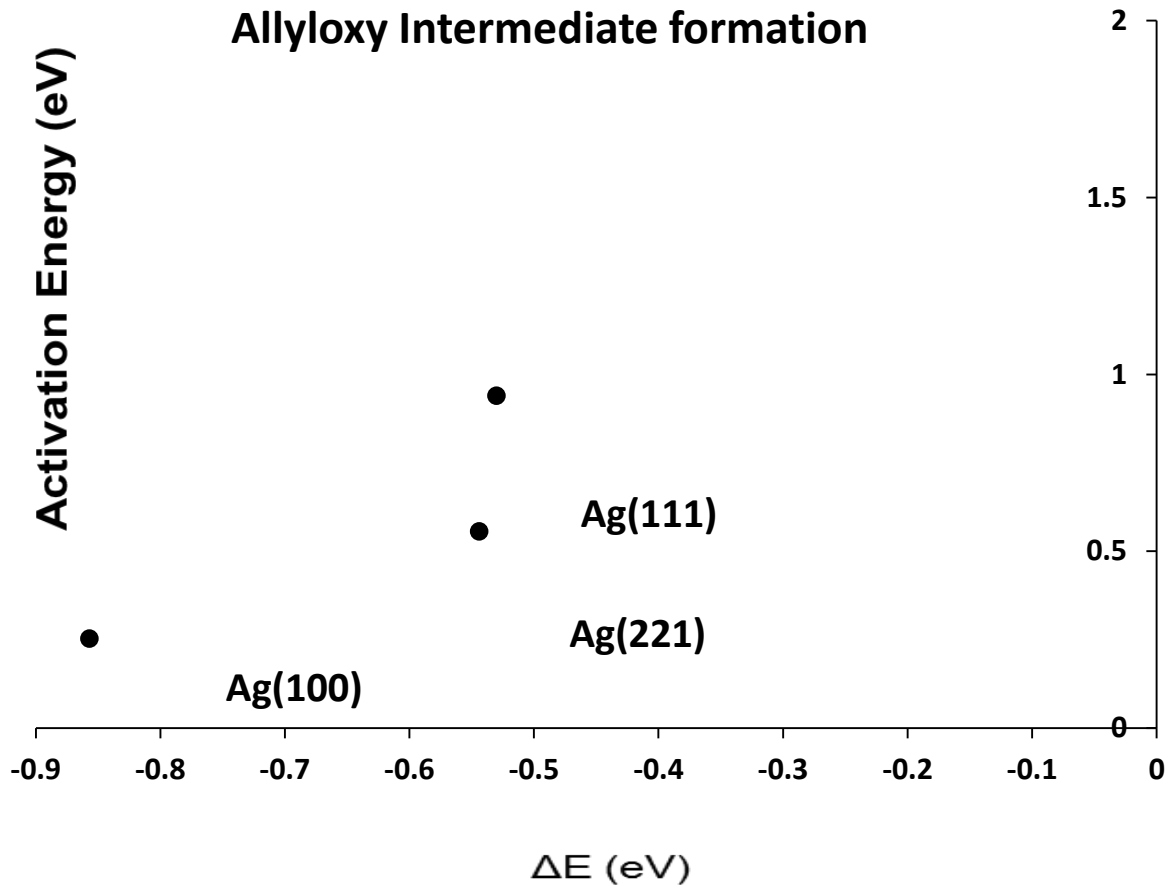

Figure 28: BEP relationship for allyloxy formation on Ag (111), Ag (221), Ag (100).

However, for allyloxy formation, clearly Ag(100) was a favored surface as it showed the lowest energy compared to Ag(111) and Ag(221) . So for Ag(100) surface, energy for Allyloxy formation was around 0.25 eV while for Ag(221) and Ag(111) , energy was around 0.56 and 0.94 eV respectively. Since, Ag(100) exhibited a lower activation energy for both allyloxy and hydroxyallyl formation (which are the intermediates of allyl alcohol) , it clearly suggests the most favorable facet is Ag(100) surface for hydrogenation to allyl alcohol.(figure 28)

On the contrary, the activation energy for formation of formylethyls, which are the intermediates towards formation of the saturated aldehyde (propanal), are quite high for Ag(100)

surface compared to Ag(111) and Ag(221) . For Ag(100) surface, the activation energy for the formation of 1-formylethyl and 2-formylethyl were 0.63 eV and 0.74 eV respectively , which where were pretty higher than the other two surfaces. Probing the transition states on three different surfaces, it was fairly clear that Ag(100) surface was the most favorable one to adsorb acrolein through carbonyl bond and thus hydrogenating it towards unsaturated alcohol, allyl alcohol.

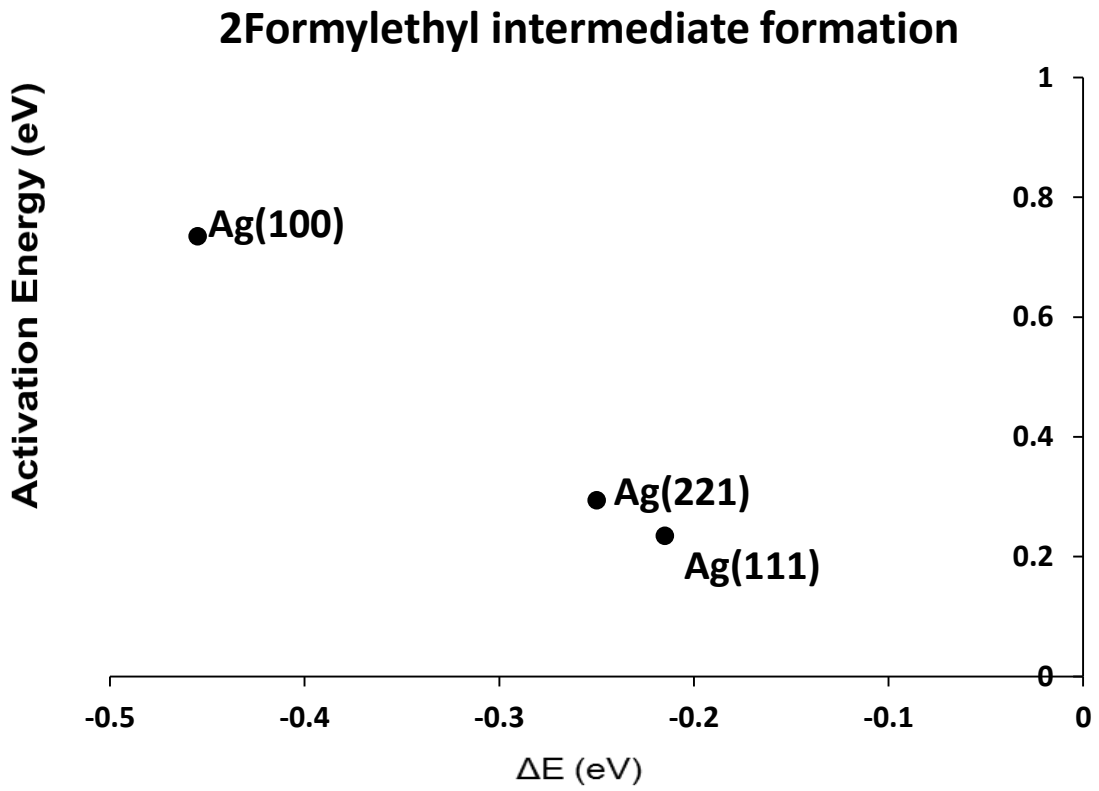

Figure 29: BEP relationship for 2-formylethyl formation on Ag (111), Ag (221), Ag (100)

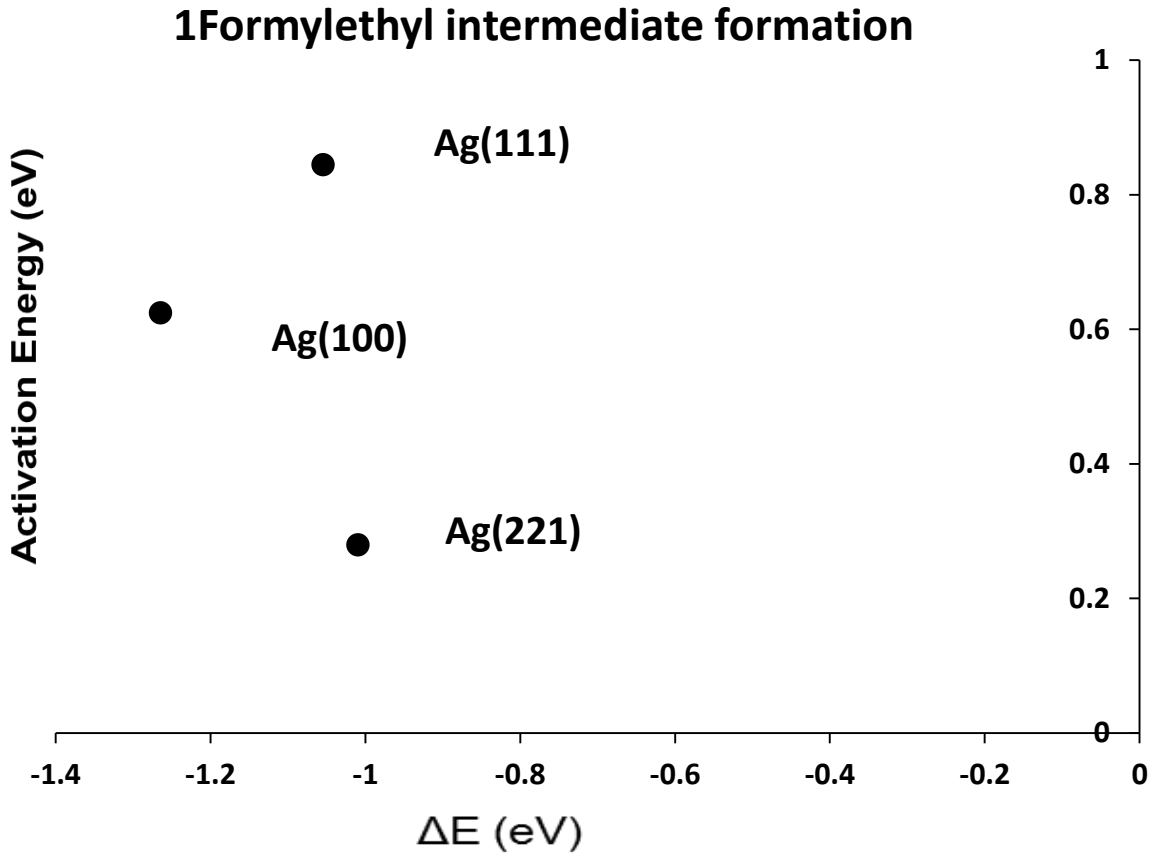

Figure 30: BEP relationship for 1-formylethyl formation on Ag (111), Ag (221), Ag (100)

4.4 Conclusion

We have observed Ag(100) surface is the most favorable surface to selectively hydrogenate to allyl alcohol as it favorably adsorbs the acrolein through carbonyl bond over the olefinic bond unlike other two surfaces, flat Ag(111) and stepped Ag(221) surface. We have also done transition state analysis to probe the kinetics and energetics of acrolein hydrogenation on these three different surfaces of silver which suggested that Ag(100) is the most conducive surface for selective hydrogenation of acrolein towards allyl alcohol.

5. Summary and Future Work

In this particular study, we have examined some important factors affecting the selectivity in the selective hydrogenation of α, β-aldehydes to α, β-unsaturated alcohols using acrolein as a probe molecule over supported silver and alloyed silver catalysts. We made several key observations through our study.

1**) Alloying effect:** Selectivity and activity towards allyl alcohol are both enhanced by adding small amounts of an active metal Pd in Ag. To this point, the maximum selectivity is observed only at .01%Pd in 8%Ag. Sequence of impregnation of the alloying metal with the host metal also is observed to affect the selectivity towards the product.

2) **Support Effect:** TiO_2 is observed to be the best support among SiO_2, Al_2O_3 and TiO_2. Ag/TiO_2 showed higher activity and selectivity to allyl alcohol. An important difference between TiO_2 and the other two supports is that TiO_2 is partially reducible. Ti^{3+} species is considered to play a crucial role in the reaction. We speculate that Ti^{3+} sites (especially the ones locating at the interface with silver particles) are apt to adsorb acrolein via the C=O bond permitting better selectivity towards the hydrogenation of C=O is obtained. . We also studied the kinetics and pathways on Ag/TiO_2 and found change of support changed reaction order for acrolein substantially and there was also a change in primary and secondary products classification for Ag/TiO_2 as compared to Ag/SiO_2. For Ag/SiO_2, the primary product was both propanal and allyl alcohol while for Ag/TiO_2, only allyl alcohol is found to be the primary product.

3) **Structure Sensitivity:** Ag(100) surface is found out to be the most favorable surface to selectively hydrogenate acrolein to allyl alcohol as it preferentially adsorbs the acrolein through carbonyl bond

over the C=C bond unlike other two surfaces, flat Ag(111) and stepped Ag(221) surface. Transition state analysis of intermediates also suggested that Ag(100) is the most conducive surface for selective hydrogenation of acrolein towards allyl alcohol.

Following are the future goals of this project to probe more into the critical factors which control the kinetics and energetics of this particular reaction.

1. **Role of the Pd for Single Atom Alloy Pd/Ag Catalyst for Selective Hydrogenation of Acrolein**

   The objective of this future project is a more detailed study into the promotion mechanism of SAA Pd alloyed Ag catalyst.

   A significant change in selectivity even when controlling the diluent concentration (Pd) at very low levels has already been observed as mentioned in Chapter 2, where upon the increase of Pd loading from 0.01% to 0.05% with 8% Ag on SiO_2 support, selectivity decreased from 34% to 1%.[25] It was hypothesized that the drop in selectivity could be due to the presence of contiguous Pd atoms which results in an unfavorable bonding configuration for acrolein. Typical hydrogenation catalysts using Pt, Pd or Rh are very active but not selective to allyl alcohol (the desired product) [Table 7] shows how Pt, Pd, Rh show higher affinity towards acrolein adsorption through C=C bond and not C=O and thus not selective towards unsaturated alcohol]. Instead the primary metal of choice is Ag, which has been shown to exhibit higher selectivity, but low activity. This low activity is not surprising since silver is known to exhibit poor hydrogen activation. Therefore one factor for increasing the reaction is to facilitate the dissociation of H_2.

[Table 8] But, there is a trade-off between high selectivity and high activity in that high selectivity to allyl alcohol is a result of the weak binding of acrolein (which is favored over Ag) whereas the efficient dissociation of H_2 takes place over metals such as Pd and Pt which are too reactive for molecular adsorption of acrolein and selectivity shifts towards undesired products.[25] However, a systematic kinetics study is still missing to understand the role of Pd, for Pd/Ag SAA. Hence, our future goal is to extract activation energies, study kinetics of these dilute alloys to elucidate the effect of addition of Pd to Ag which also in turn will control the selectivity.

Table 7 : Adsorption energies of different acrolein binding modes on different Single Atom Alloy Surfaces

Single Atom Alloy	**Adsorption Energy C=C bound [eV]**	**Adsorption Energy C=O bound [eV]**
Ag(111)	**-0.05**	**-0.03**
Ru@Ag(111)	**-1.44**	**-0.91**
Co@Ag(111)	**-1.05**	**-0.87**
Rh@Ag(111)	**-1.20**	**-0.53**
Ir@Ag(111)	**-1.39**	**-0.60**
Ni@ Ag(111)	**-0.68**	**-0.51**
Pd@ Ag(111)	**-0.46**	**-0.11**
Pt@ Ag(111)	**-0.59**	**-0.02**
Cu@ Ag(111)	**-0.05**	**-0.11**
Au@ Ag(111)	**-0.05**	**-0.04**

Table 8: Energy Barriers for H_2 dissociation on different Sing Atom Alloy surfaces.

Single atom alloy surface	**ΔE (eV)**	**Barrier (eV)**
Ag Ag(111)	0.87	1.38
Ru@ Ag(111)	-1.26	Barrierless
Co@Ag Ag(111)	-0.88	Barrierless
Rh@Ag Ag(111)	-0.49	Barrierless
Ir@Ag Ag(111)	-1.03	Barrierless
Ni@Ag Ag(111)	-1.51	Barrierless
Pd@Ag Ag(111)	-0.33	0.389
Pt@Ag Ag(111)	-0.54	Barrierless
Cu@Ag Ag(111)	0.24	1.17
Au@Ag Ag(111)	0.56	0.46

To prove the presence of isolated Pd atoms, we did more advanced characterization study to investigate the Ag-Pd SAA surface employing energy dispersive spectroscopy and high resolution TEM.

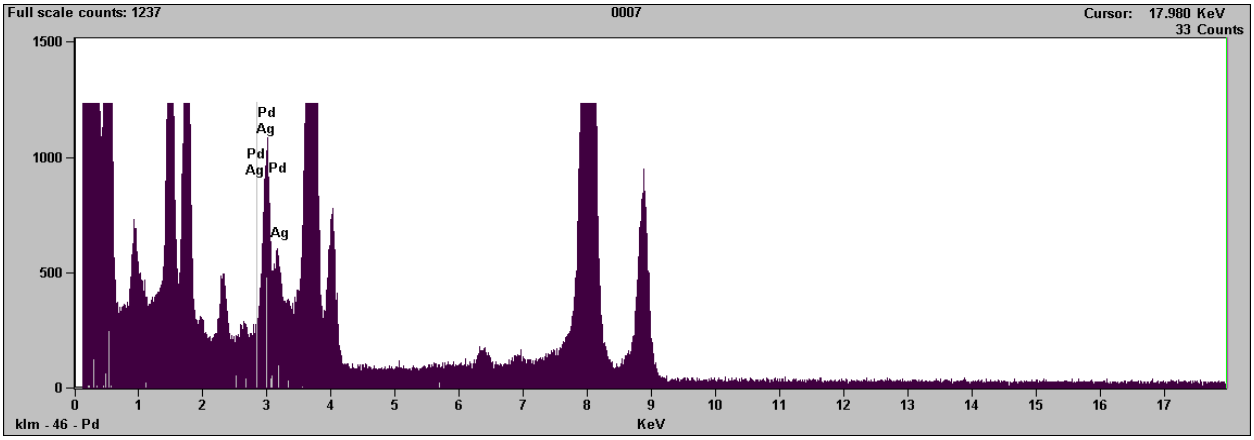

Figure 31: EDX spectra (X-ray intensity vs. photon energy) on 0.01%Pd+8%Ag/SiO2_ co_IWI

The EDX data obtained for 0.01%Pd_8%Ag/SiO_2 catalyst is shown in figure 31. Both Ag, and Pd peaks are present near 3 keV. Ag has a much stronger signal than Pd, but the amounts cannot be quantified in a precise manner. Furthermore the large spot size (60-70 nm) prevents any statement with regard to the presence of isolated Pd atoms. However, when Pd peaks are present, they are always accompanied by Ag peaks, indicating that Pd is not aggregating or segregating in an obvious manner. In addition to Pd and Ag, other observable features are related to the presence of the silica support and the holey carbon grid.

We also did Transmission Electron microscopy to confirm particle size effect due to alloying. TEM results (figure 32) are in agreement to what we obtained from EXAFS. However, larger distributions are indicated than were observed previously with monometallic Ag particles as indicated in Table 9.

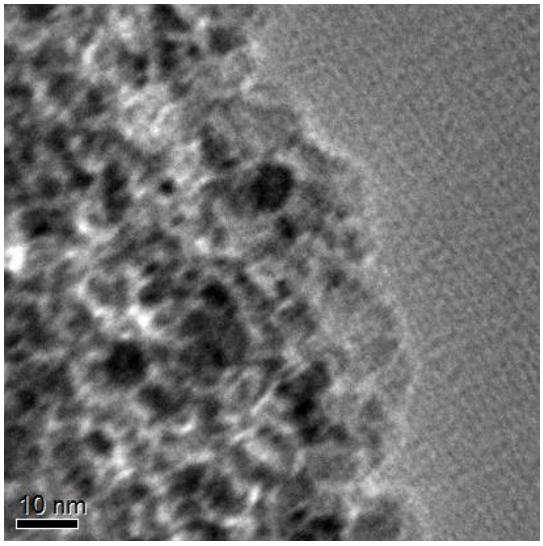

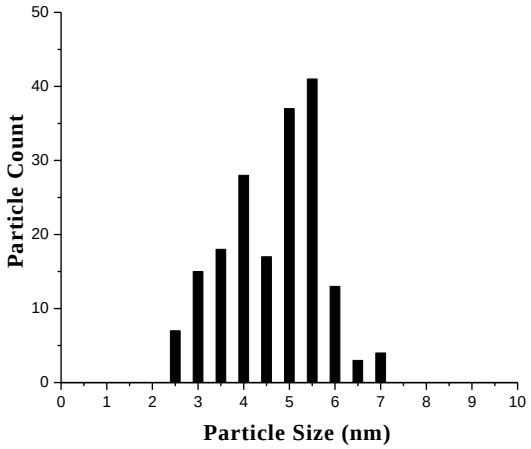

0.01%Pd+8%Ag SeqIWI

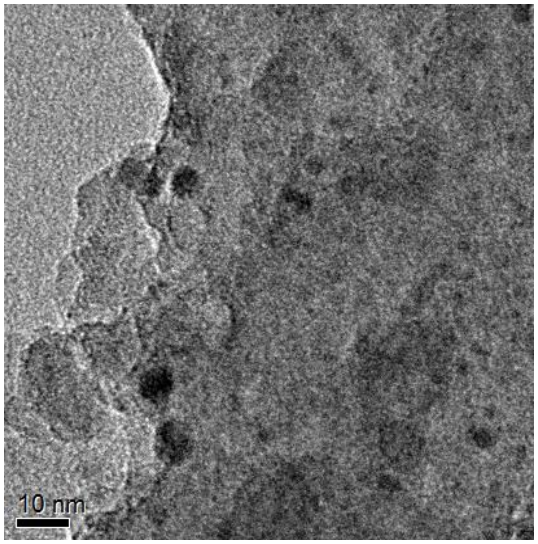

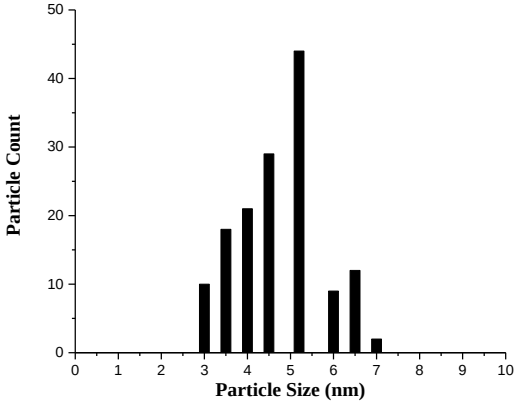

0.05%Pd+8%Ag_SeqIWI

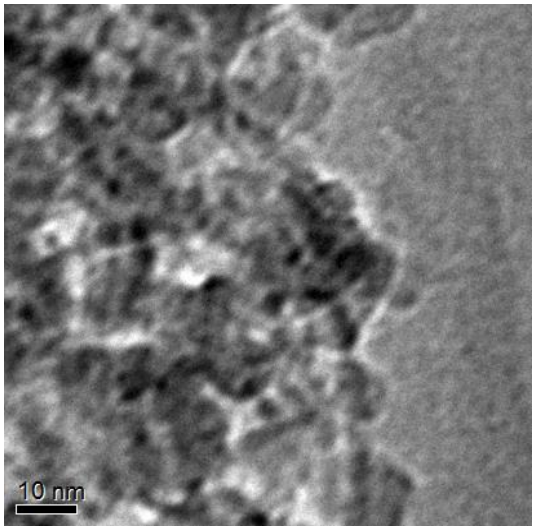

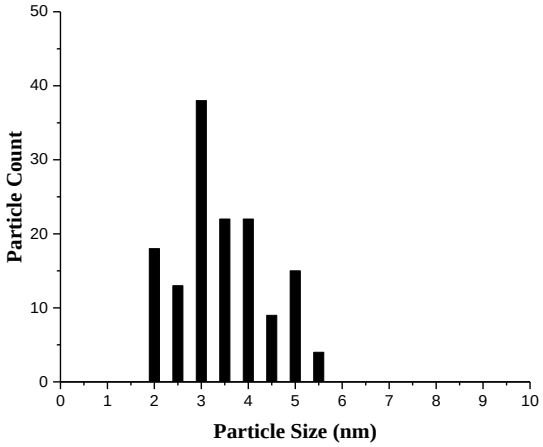

0.01%Pd+8Ag% CoIWI

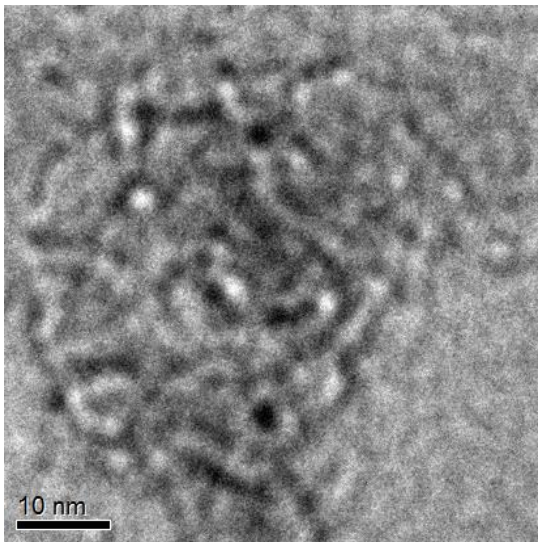

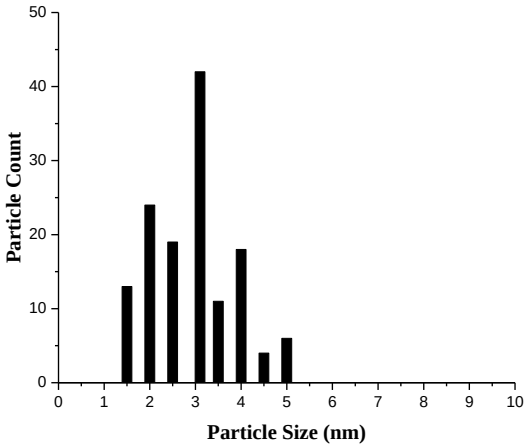

0.03Pd%+8%Ag CoIWI

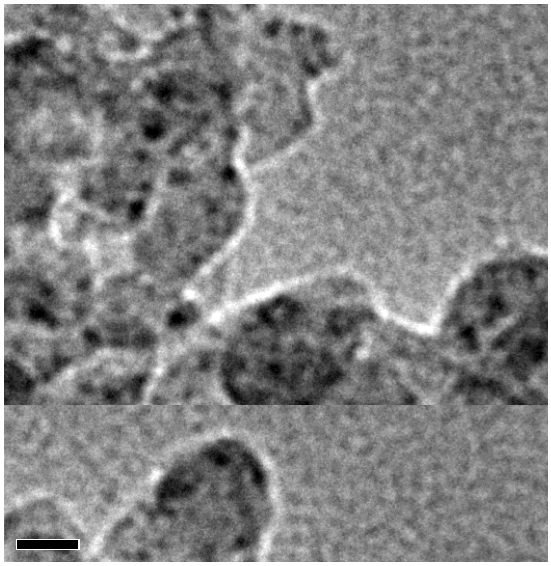

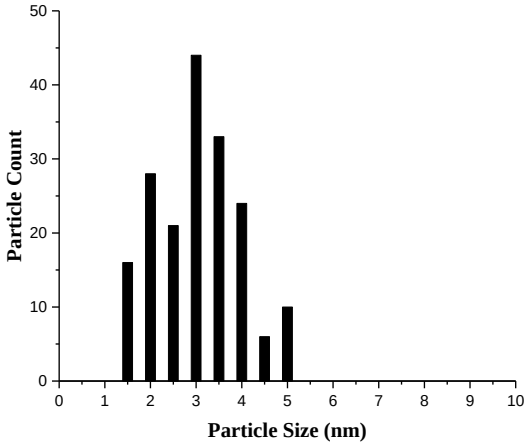

0.05%Pd+8%Ag CoIWI

Figure 32: Bright Field TEM images of Pd-Ag alloys

Table 9: Particle Size by EXAFS and TEM

Sample Name	TEM Size	EXAFS Size
0.01%Pd+8%Ag/SiO_2 _CoIWI	3.0±1.4 nm	4.0±0.4 nm
0.03%Pd+8%Ag/ SiO_2 _CoIWI	3.1±1.5 nm	4.0±0.4 nm
0.05%Pd+8%Ag/ SiO_2 _CoIWI	3.0±1.75 nm	4.0±0.4 nm
0.01%Pd+8%Ag/SiO_2 _SeqIWI	5.5±2.25nm	5.8±0.6 nm
0.05%Pd+8%Ag/ SiO_2 _SeqIWI	5.2±1.8nm	5.4±0.5 nm

Recently, a study published in Angewandte Chemie[117] showed the preparation and hydrogenation performance of a single-site palladium catalyst that was obtained by the anchoring of Pd atoms into the cavities of mesoporous polymeric graphitic carbon nitride. Perez-Ramirez et al. have done a detailed characterization using aberration corrected STEM to confirm the atomic dispersion of the palladium phase throughout the sample. The catalyst was applied for three-phase hydrogenations of alkynes and nitroarenes in a continuous-flow reactor, showing its high activity and product selectivity in comparison with benchmark catalysts based on nanoparticles. This suggests that the SAA catalyst should have essentially higher amount of Pd but at the same time selectivity should not decrease due to more amount of active metal in the catalyst.

2. Experimental study of structural dependence of Ag for selective hydrogenation of acrolein

Initial computational and transitional state studies have indicated Ag(100) may be favorable for adsorption of acrolein through carbonyl bond. This can be proved by experimental study of reaction kinetics using silver nanocubes as the catalysts for the reaction. This may give us an insight of the theoretical prediction we had from our study of energetics and transition on different surfaces of silver.

Christopher et al.[116] for example, showed how catalytic selectivity in the epoxidation of ethylene to form ethylene oxide on alumina-supported silver catalysts is controlled by geometric structure of catalytically active Ag particles and reaction conditions. It was observed that silver nanocubes exhibit higher selectivity than nanowires and nanospheres. The improved selectivity towards ethylene oxide was attributed to the nature of the exposed Ag surface facets; Ag nanocubes and nanowires are controlled by (100) surface facet while Ag nanospheres are dominated by (111)

facets. The authors also suggested that the number of under coordinated surface sites will reduce selectivity to ethylene oxide.[116] In a similar way, we predict the Ag(100) surface is conducive to acrolein hydrogenation to allyl alcohol by studying adsorption energies on the surface and analyzing transition states of intermediates.

Thus, using Ag nanowires, nanospheres and nanocubes as catalysts for this particular reaction may give a new insight in understanding structural dependence of selectivity towards unsaturated alcohol for acrolein hydrogenation reaction.

In all, there are many issues left to explore in this system. Although acrolein hydrogenation is a simple reaction, it can act as a probe reaction to understand many concepts related to heterogeneous catalysis. Future goals will be to understand in detail, change of mechanism or pathways, kinetics due to various effects. These effects may lead from introduction of a dopant, synthesis effects to effect of reducibility of supports by doing more advanced kinetics and characterization study on various catalysts.[117, 118]

Appendices

Study of rate mechanism by breaking down the overall reaction into elementary steps also helps us to understand the pathway and effect on order of the reaction by predicting the rate determining step. We have started doing so, by assuming either of the five elementary reactions as the rate limiting steps. Future goal will be to predict the appropriate rate determining step to elucidate the mechanism, including Pd sites too.

1. $C_3H_4O + X \longrightarrow C_3H_4O_{ads}$
2. $H_2 + 2X \longrightarrow 2H_{ads}$
3. $C_3H_4O_{ads} + H_{ads} \longrightarrow C_3H_5O_{ads} + X$
4. $C_3H_5O_{ads} + H_{ads} \longrightarrow C_3H_5OH_{ads} + X$
5. $C_3H_5OH_{ads} \longrightarrow C_3H_5OH + X$

For Rate 1 as rate determining step,

$r = K_1 P_{C3H4O} \hat{C}_x$

Rate 2 $\longrightarrow$

$\hat{C}_H = \sqrt{K_{H2} P_{H2}}\ \hat{C}_x$

Rate 3 ⟶

$$\hat{C}_{C3H4O} = \frac{\hat{C}_{C3H5O}\,\hat{C}x}{K_3\hat{C}_H}$$

Rate 4 ⟶

$$\hat{C}_{C3H5O} = \frac{\hat{C}_{C3H5OH}\,\hat{C}x}{K_4\hat{C}_H}$$

Rate 5 ⟶

$$\hat{C}_{C3H5OH} = K_{C3H5OH}P_{C3H5OH}\,\hat{C}x$$

By substitutions,

Rate 3 ⟶

$$\hat{C}_{C3H4O} = \frac{K_{C3H5OH}P_{C3H5OH}\hat{C}x}{K_3K_4\ K_{H2}P_{H2}}$$

Rate 4 ⟶

$$\hat{C}_{C3H5O} = \frac{K_{C3H5OH}P_{C3H5OH}\,\hat{C}x}{K_4\sqrt{K_{H2}P_{H2}}}$$

$$\hat{C}_{Total} = \hat{C}_H + \hat{C}_{C3H4O} + \hat{C}_{C3H5O} + \hat{C}_{C3H5OH}$$

$$\hat{C}x = \frac{\hat{C}_{Total}}{1+\sqrt{K_{H2}P_{H2}}+\frac{K_{C3H5OH}P_{C3H5OH}}{K_3K_4\ K_{H2}P_{H2}}+\frac{K_{C3H5OH}P_{C3H5OH}}{K_4\sqrt{K_{H2}P_{H2}}}+K_{C3H5OH}P_{C3H5OH}}$$

So, the rate becomes,

$$r = K_1 P_{C3H4O} \frac{\hat{C}_{Total}}{1 + \sqrt{K_{H2} P_{H2}} + \frac{K_{C3H5OH} P_{C3H5OH}}{K_3 K_4 \ K_{H2} P_{H2}} + \frac{K_{C3H5OH} P_{C3H5OH}}{K_4 \sqrt{K_{H2} P_{H2}}} + K_{C3H5OH} P_{C3H5OH}}$$

Order with respect to H_2 = 0, 0.5, -0.5, 1

Order with respect to C_3H_4O = 1

For Rate 2 as the rate determining step,

$r^* = K_{H2} P_{H2} \hat{C}_x^2$

Rate 1 ⟶

$\hat{C}_{C3H4O} = K_{C3H4O} P_{C3H4O} \hat{C}x$

Rate 3 ⟶

$\hat{C}_H = \sqrt{\frac{K_{C3H5OH} P_{C3H5OH}}{K_3 K_{C3H4O} P_{C3H4O}}} \hat{C}_x$

Rate 4 ⟶

$\hat{C}_{C3H5O} = \sqrt{K_3 K_{C3H4O} P_{C3H4O} K_{C3H5OH} P_{C3H5OH}} \ \hat{C}_x$

Rate 5 ⟶

$\hat{C}_{C3H5OH} = K_{C3H5OH} P_{C3H5OH} \hat{C}x$

$$\hat{C}x = \frac{\hat{C}_{Total}}{1 + K_{C3H4O}P_{C3H4O} + \sqrt{\frac{K_{C3H5OH}P_{C3H5OH}}{K_3 K_{C3H4O}P_{C3H4O}}} + \sqrt{K_3 K_{C3H4O} P_{C3H4O} K_{C3H5OH} P_{C3H5OH}} + K_{C3H5OH}P_{C3H5OH}}$$

So the rate becomes;

$$r = K_{H2}P_{H2}\left[\frac{\hat{C}_{Total}}{1 + K_{C3H4O}P_{C3H4O} + \sqrt{\frac{K_{C3H5OH}P_{C3H5OH}}{K_3 K_{C3H4O}P_{C3H4O}}} + \sqrt{K_3 K_{C3H4O} P_{C3H4O} K_{C3H5OH} P_{C3H5OH}} + K_{C3H5OH}P_{C3H5OH}}\right]^2$$

Order with respect to H_2 = 1

Order with respect to C_3H_4O = -2,-1, 0, 1

For Rate 3, as the rate determining step,

$$r = K_3 K_{C3H4O} P_{C3H4O} \sqrt{K_{H2}P_{H2}}\left[\frac{\hat{C}_{Total}}{1 + K_{C3H4O}P_{C3H4O} + \frac{K_{C3H5OH}P_{C3H5OH}}{K_4\sqrt{K_{H2}P_{H2}}} + \sqrt{K_{H2}P_{H2}} + K_{C3H5OH}P_{C3H5OH}}\right]^2$$

Order with respect to H_2 = 0.5, 1.5, -0.5

Order with respect to C_3H_4O = 1,-1

For Rate 4, as the rate determining step

r=

$$K_3K_4K_{C3H4O}P_{C3H4O}\,K_{H2}P_{H2}\left[\frac{\hat{C}_{Total}}{1+K_{C3H4O}P_{C3H4O}+K_3K_{C3H4O}P_{C3H4O}\sqrt{K_{H2}P_{H2}}+\sqrt{K_{H2}P_{H2}}+K_{C3H5OH}P_{C3H5OH}}\right]^2$$

Order with respect to H_2 = 1, 0

Order with respect to C_3H_4O = 1,-1

For Rate 5, as the rate determining step

r

$$= K_{C3H5OH}P_{C3H5OH}\frac{\hat{C}_{\mathrm{Total}}}{1+\sqrt{\mathrm{K_{H2}P_{H2}}}+K_3K_{C3H4O}P_{C3H4O}\sqrt{K_{H2}P_{H2}}+K_3K_4K_{C3H4O}P_{C3H4O}K_{H2}P_{H2}+K_{C3H4O}P_{C3H4O}}$$

Order with respect to H_2 = 0, -0.5, -1 Order with respect to C_3H_4O = 0, -1

Licenses and Copyrights

License for using figure from Surface Science journal publication, figure number; 1

This is a License Agreement between Payoli Aich and Elsevier provided by Copyright Clearance Center ("CCC"). License number **3783191364919**; Type of Use reuse in a thesis/dissertation Portion figures/tables/illustrations Number of figures/tables/illustrations; 1.

Licensed content title; Clusters and islands on oxides: from catalysis via electronics and magnetism to optics

License for using figure from Journal of Chemical Physics journal publication, figure number; 2

This is a License Agreement between Payoli Aich and AIP Publishing LLC provided by Copyright Clearance Center ("CCC"). License number **378320075522**; Type of Use reuse in a thesis/dissertation Portion figures/tables/illustrations Number of figures/tables/illustrations; 1

Licensed content title; Calorimetric heats for CO and oxygen adsorption and for the catalytic CO oxidation reaction on Pt{111}

Licensed content Science journal publication for figure number; 4

License Number **3782061452039**

Licensed content publisher The American Association for the Advancement of Science

Licensed content title; Isolated Metal Atom Geometries as a Strategy for Selective Heterogeneous Hydrogenations

Type of Use Thesis / Dissertation

Licensed content for American Chemical Society journal publication for figure number; 5

Title: Coverage Dependence of the Structure of Acrolein Adsorbed on Ag(111) Author: Ricardo Ferullo, Maria Marta Branda, Francesc Illas Publication: Journal of Physical Chemistry Letters Publisher: American Chemical Society Date: Sep 1, 2010 Copyright © 2010, American Chemical Society

Payoli Aich Account #: 3000987083 PERMISSION/LICENSE IS GRANTED FOR YOUR ORDER AT NO CHARGE This type of permission/license, instead of the standard Terms & Conditions, is sent to you because no fee is being charged for your order. Please note the following: Permission is granted for your request in both print and electronic formats, and translations. If figures and/or tables were requested, they may be adapted or used in part. Please print this page for your records and send a copy of it to your publisher/graduate school.

Screenshot of the permission to reuse the work from *Aich et al.* publication

Title:	Single-Atom Alloy Pd–Ag Catalyst for Selective Hydrogenation of Acrolein
Author:	Payoli Aich, Haojuan Wei, Bridget Basan, et al
Publication:	The Journal of Physical Chemistry C
Publisher:	American Chemical Society
Date:	Aug 1, 2015

PERMISSION/LICENSE IS GRANTED FOR YOUR ORDER AT NO CHARGE

This type of permission/license, instead of the standard Terms & Conditions, is sent to you because no fee is being charged for your order. Please note the following:

- Permission is granted for your request in both print and electronic formats, and translations.
- If figures and/or tables were requested, they may be adapted or used in part.
- Please print this page for your records and send a copy of it to your publisher/graduate school.
- Appropriate credit for the requested material should be given as follows: "Reprinted (adapted) with permission from (COMPLETE REFERENCE CITATION). Copyright (YEAR) American Chemical Society." Insert appropriate information in place of the capitalized words.
- One-time permission is granted only for the use specified in your request. No additional uses are granted (such as derivative works or other editions). For any other uses, please submit a new request.

Cited Literature

1. Freund, H. J. (2002) Clusters and islands on oxides: from catalysis via electronics and magnetism to optics, *Surface Science 500*, 271-299.

2. Beeck, O. (1950) Hydrogenation catalysts, *Discussions of the Faraday Society 8*, 118-128.

3. Yeo, Y., Vattuone, L., and King, D. (1997) Calorimetric heats for CO and oxygen adsorption and for the catalytic CO oxidation reaction on Pt {111}, *The Journal of chemical physics 106*, 392-401.

4. Bron, M., Teschner, D., Knop-Gericke, A., Jentoft, F. C., Kröhnert, J., Hohmeyer, J., Volckmar, C., Steinhauer, B., Schlögl, R., and Claus, P. (2007) Silver as acrolein hydrogenation catalyst: intricate effects of catalyst nature and reactant partial pressures, *Physical Chemistry Chemical Physics 9*, 3559-3569.

5. Masel, R. I. (1996) Principles of adsorption and reaction on solid surfaces, John Wiley & Sons Inc., New York,.

6. Bron, M., Teschner, D., Knopgericke, A., Steinhauer, B., Scheybal, A., Havecker, M., Wang, D., Fodisch, R., Honicke, D., and Wootsch, A. (2005) Bridging the pressure and materials gap: in-depth characterisation and reaction studies of silver-catalysed acrolein hydrogenation, *Journal of Catalysis 234*, 37-47.

7. Wei, H., Gomez, C., Liu, J., Guo, N., Wu, T., Lobo-Lapidus, R., Marshall, C. L., Miller, J. T., and Meyer, R. J. (2013) Selective hydrogenation of acrolein on supported silver catalysts: A kinetics study of particle size effects, *Journal of Catalysis 298*, 18-26.

8. Brandt, K., Chiu, M. E., Watson, D. J., Tikhov, M. S., and Lambert, R. M. (2009) Chemoselective catalytic hydrogenation of acrolein on Ag (111): Effect of molecular orientation on reaction selectivity, *Journal of the American Chemical Society 131*, 17286-17290.

9. Tierney, H. L., Baber, A. E., and Sykes, E. C. H. (2009) Atomic-Scale Imaging and Electronic Structure Determination of Catalytic Sites on Pd/Cu Near Surface Alloys, *The Journal of Physical Chemistry C 113*, 7246-7250.

10. Kyriakou, G., Boucher, M. B., Jewell, A. D., Lewis, E. A., Lawton, T. J., Baber, A. E., Tierney, H. L., Flytzani-Stephanopoulos, M., and Sykes, E. C. (2012) Isolated metal atom geometries as a strategy for selective heterogeneous hydrogenations, *Science 335*, 1209-1212.

11. Boucher, M. B., Zugic, B., Cladaras, G., Kammert, J., Marcinkowski, M. D., Lawton, T. J., Sykes, E. C. H., and Flytzani-Stephanopoulos, M. (2013) Single atom alloy surface analogs in Pd 0.18 Cu 15 nanoparticles for selective hydrogenation reactions, *Physical Chemistry Chemical Physics 15*, 12187-12196.

12. Claus, P. (1998) Selective hydrogenation of ά, β-unsaturated aldehydes and other C= O and C= C bonds containing compounds, *Topics in Catalysis 5*, 51-62.

13. Ferullo, R., Branda, M. M., and Illas, F. (2010) Coverage dependence of the structure of acrolein adsorbed on Ag (111), *The Journal of Physical Chemistry Letters 1*, 2546-2549.

14. Galvagno, S., Staiti, P., Antonucci, P., Donato, A., and Pietropaolo, R. (1983) Kinetics of propene hydrogenation over platinum and platinum–tin catalysts supported on polyamide, *Journal of the Chemical Society, Faraday Transactions 1: Physical Chemistry in Condensed Phases 79*, 2605-2612.

15. Ponec, V. (1997) *Appl. Catal. 149*, 27.

16. Raab, C., Englisch, M., Marinelli, T., and Lercher, J. (1993) Selective hydrogenation of crotonaldehyde over Pt derived catalysts, *Studies in Surface Science and Catalysis 78*, 211-218.

17. Margitfalvi, J., Tompos, A., Kolosova, I., and Valyon, J. (1998) Reaction Induced Selectivity Improvement in the Hydrogenation of Crotonaldehyde over Sn–Pt/SiO_2 Catalysts, *Journal of Catalysis 174*, 246-249.

18. Sokolskii, D., Anisimova, N., Zharmagambetova, A., Mukhamedzhanova, S., and Edygenova, L. (1987) Pt− Fe2O3 catalytic system for hydrogenation reactions, *Reaction Kinetics and Catalysis Letters 33*, 399-403.

19. Galvagno, S., Poltarzewski, Z., Donato, A., Neri, G., and Pietropaolo, R. (1986) Selective hydrogenation of α, β-unsaturated aldehydes to give unsaturated alcohols over platinum–germanium catalysts, *Journal of the Chemical Society, Chemical Communications*, 1729-1731.

20. Galvagno, S., Poltarzewski, Z., Donato, A., Neri, G., and Pietropaolo, R. (1986) Liquid phase hydrogenations over platinum-tin catalysts, *Journal of molecular catalysis 35*, 365-375.

21. Delbecq, F. (2003) Influence of Sn additives on the selectivity of hydrogenation of α-β-unsaturated aldehydes with Pt catalysts: a density functional study of molecular adsorption, *Journal of Catalysis 220*, 115-126.

22. Waghray, A., Oukaci, R., and Blackmond, D. (1993) Selective Hydrogenation of α, β-Unsaturated Aldehydes Over Supported Ru, *Studies in Surface Science and Catalysis 75*, 2479-2482.

23. Waghray, A., and Blackmond, D. G. (1993) Infrared spectroscopic studies of the adsorption and reaction of 3-methyl-2-butenal over alkali-promoted ruthenium/silica catalysts, *The Journal of Physical Chemistry 97*, 6002-6006.

24. Waghray, A., Wang, J., Oukaci, R., and Blackmond, D. G. (1992) Influence of alkali promoters in the selective hydrogenation of 3-methyl-2-butenal over ruthenium/silica catalysts, *The Journal of Physical Chemistry 96*, 5954-5959.

25. Aich, P., Wei, H., Basan, B., Kropf, A. J., Schweitzer, N. M., Marshall, C. L., Miller, J. T., and Meyer, R. (2015) Single-Atom Alloy Pd–Ag Catalyst for Selective Hydrogenation of Acrolein, *The Journal of Physical Chemistry C 119*, 18140-18148.

26. Lucas, M., and Claus, P. (2005) Hydrogenations over Silver: A Highly Active and Chemoselective Ag-In/SiO2 Catalyst for the One-Step Synthesis of Allyl Alcohol from Acrolein, *Chemical Engineering & Technology 28*, 867-870.

27. Haass, F., Bron, M., Fuess, H., and Claus, P. (2007) In situ X-ray investigations on $AgIn/SiO_2$ hydrogenation catalysts, *Applied Catalysis A: General 318*, 9-16.

28. Vannice, M. A., and Sudhakar, C. (1984) A model for the metal-support effect enhancing carbon monoxide hydrogenation rates over platinum-titania catalysts, *The Journal of Physical Chemistry 88*, 2429-2432.

29. Tauster, S. J., Fung, S. C., and Garten, R. L. (1978) Strong metal-support interactions. Group 8 noble metals supported on titanium dioxide, *Journal of the American Chemical Society 100*, 170-175.

30. Vannice, M. A., and Vasco-Jara, J. (1982) The Nature of Active Sites in SMSI Catalysts: Mixtures Of Ni/TiO_2 and Pt/TiO_2, *Studies in Surface Science and Catalysis 11*, 185-192.

31. Vannice, M. (1992) Hydrogenation of CO and carbonyl functional groups, *Catalysis today 12*, 255-267.

32. Claus, P., Hofmeister, H., and Mohr, C. (2004) Identification of active sites and influence of real structure of gold catalysts in the selective hydrogenation of acrolein to allyl alcohol, *Gold Bulletin 37*, 181-186.

33. Van Santen, R., and Sachtler, W. (1974) A theory of surface enrichment in ordered alloys, *Journal of Catalysis 33*, 202-209.

34. Williams, F. L., and Boudart, M. (1973) Surface composition of nickel-gold alloys, *Journal of Catalysis 30*, 438-443.

35. Bouwman, R., and Biloen, P. (1974) Surface composition and depth concentration profile of platinum/tin alloys from combined X-ray photoelectron and Auger spectroscopic data, *Surface Science 41*, 348-358.

36. Verbeek, H., and Sachtler, W. (1976) The study of the alloys of platinum and tin by chemisorption, *Journal of Catalysis 42*, 257-267.

37. Hirschl, R., Delbecq, F., Sautet, P., and Hafner, J. (2003) Adsorption of unsaturated aldehydes on the (111) surface of a Pt–Fe alloy catalyst from first principles, *Journal of Catalysis 217*, 354-366.

38. Delbecq, F., and Sautet, P. (2002) A density functional study of adsorption structures of unsaturated aldehydes on Pt (111): A key factor for hydrogenation selectivity, *Journal of Catalysis 211*, 398-406.

39. Lim, K. H., Chen, Z.-X., Neyman, K. M., and Rösch, N. (2006) Adsorption of acrolein on single-crystal surfaces of silver: Density functional studies, *Chemical physics letters 420*, 60-64.

40. Lim, K. H., Mohammad, A. B., Yudanov, I. V., Neyman, K. M., Bron, M., Claus, P., and Rösch, N. (2009) Mechanism of Selective Hydrogenation of α, β-Unsaturated Aldehydes on Silver Catalysts: A Density Functional Study, *The Journal of Physical Chemistry C 113*, 13231-13240.

41. Bron, M., Teschner, D., Knop-Gericke, A., Steinhauer, B., Scheybal, A., Hävecker, M., Wang, D., Födisch, R., Hönicke, D., and Wootsch, A. (2005) Bridging the pressure and materials gap: in-depth characterisation and reaction studies of silver-catalysed acrolein hydrogenation, *Journal of Catalysis 234*, 37-47.

42. Bhore, N. A., Klein, M. T., and Bischoff, K. B. (1990) The delplot technique: a new method for reaction pathway analysis, *Industrial & Engineering Chemistry Research 29*, 313-316.

43. Lei, Y., Jelic, J., Nitsche, L. C., Meyer, R., and Miller, J. (2011) Effect of Particle Size and Adsorbates on the L3, L2 and L1 X-ray Absorption Near Edge Structure of Supported Pt Nanoparticles, *Topics in Catalysis 54*, 334-348.

44. Jaklevic, J., Kirby, J. A., Klein, M. P., Robertson, A. S., Brown, G. S., and Eisenberger, P. (1993) Fluorescence detection of EXAFS: Sensitivity enhancement for dilute species and thin films, *Solid State Communications 88*, 1105-1108.

45. Kropf, A. J., Finch, R. J., Fortner, J. A., Aase, S., Karanfil, C., Segre, C. U., Terry, J., Bunker, G., and Chapman, L. D. (2003) Bent silicon crystal in the Laue geometry to resolve x-ray fluorescence for x-ray absorption spectroscopy, *Rev. Sci. Instrum. 74*, 4696.

46. Miller, J. T., Kropf, A. J., Zha, Y., Regalbuto, J. R., Delannoy, L., Louis, C., Bus, E., and van Bokhoven, J. A. (2006) The effect of gold particle size on AuAu bond length and reactivity toward oxygen in supported catalysts, *Journal of Catalysis 240*, 222-234.

47. McMorn, P., and Hutchings, G. J. (2004) Heterogeneous enantioselective catalysts: strategies for the immobilisation of homogeneous catalysts, *Chem Soc Rev 33*, 108-122.

48. Likhar, P. R., Roy, M., Roy, S., Subhas, M., Kantam, M. L., and Sreedhar, a. B. (2008) Highly Efficient and Reusable Polyaniline-Supported Palladium Catalysts for Open-Air Oxidative Heck Reactions under Base-and Ligand-Free Conditions, *Advanced Synthesis & Catalysis 350*, 1968-1974.

49. Van Berlo, B., Houthoofd, K., Sels, B. F., and Jacobs, P. A. (2008) Silica Immobilized Second Generation Hoveyda-Grubbs: A Convenient, Recyclable and Storageable Heterogeneous Solid Catalyst, *Advanced Synthesis & Catalysis 350*, 1949-1953.

50. Karamé, I., Boualleg, M., Camus, J. M., Maishal, T. K., Alauzun, J., Basset, J. M., Copéret, C., Corriu, R. J., Jeanneau, E., Mehdi, A., Reyé, C., Veyre, L., and Thieuleux, C. (2009) Tailored Ru-NHC heterogeneous catalysts for alkene metathesis, *Chemistry 15*, 11820-11823.

51. Yang, H., Gao, H., and Angelici, R. J. (2000) Hydrogenation of arenes under mild conditions using rhodium pyridylphosphine and bipyridyl complexes tethered to a silica-supported palladium heterogeneous catalyst, *Organometallics 19*, 622-629.

52. Thomas, J. M., Raja, R., and Lewis, D. W. (2005) Single-Site Heterogeneous Catalysts, *Angewandte Chemie International Edition 44*, 6456-6482.

53. Thomas, J. M., Saghi, Z., and Gai, P. L. (2011) Can a single atom serve as the active site in some heterogeneous catalysts?, *Topics in Catalysis 54*, 588-594.

54. Le Roux, E., Taoufik, M., Copéret, C., de Mallmann, A., Thivolle-Cazat, J., Basset, J. M., Maunders, B. M., and Sunley, G. J. (2005) Development of Tungsten-Based Heterogeneous Alkane Metathesis Catalysts Through a Structure–Activity Relationship, *Angewandte Chemie International Edition 44*, 6755-6758.

55. McKittrick, M. W., and Jones, C. W. (2004) Toward single-site, immobilized molecular catalysts: site-isolated Ti ethylene polymerization catalysts supported on porous silica, *Journal of the American Chemical Society 126*, 3052-3053.

56. Dzwigaj, S., and Che, M. (2011) Toward redox framework single site zeolite catalysts, *Catalysis Today 169*, 232-241.

57. Corma, A., and Garcia, H. (2006) Silica-bound homogenous catalysts as recoverable and reusable catalysts in organic synthesis, *Advanced Synthesis and Catalysis 348*, 1391-1412.

58. Nicholas, C. P., Ahn, H., and Marks, T. J. (2003) Synthesis, spectroscopy, and catalytic properties of cationic organozirconium adsorbates on “super acidic” sulfated alumina.“Single-site” heterogeneous catalysts with virtually 100 active sites, *Journal of the American Chemical Society 125*, 4325-4331.

59. Gajan, D., and Copéret, C. (2011) Silica-supported single-site catalysts: to be or not to be? A conjecture on silica surfaces, *New Journal of Chemistry 35*, 2403-2408.

60. Barteau, M. A., Lyons, J. E., and Song, I. K. (2003) Surface chemistry and catalysis on well-defined oxide surfaces: nanoscale design bases for single-site heterogeneous catalysts, *Journal of Catalysis 216*, 236-245.

61. Sinfelt, J. H. (1985) Bimetallic Catalysts, *Sci Am 253*, 90-98.

62. Gross, A. (2006) Reactivity of Bimetallic Systems Studied from First Principles, *ChemInform 37*.

63. Schweitzer, N., Xin, H., Nikolla, E., Miller, J. T., and Linic, S. (2010) Establishing Relationships Between the Geometric Structure and Chemical Reactivity of Alloy Catalysts Based on Their Measured Electronic Structure, *Topics in Catalysis 53*, 348-356.

64. Győrffy, N., and Paál, Z. (2008) Acrolein hydrogenation on PdPt powder catalysts prepared by colloid synthesis, *Journal of Molecular Catalysis A: Chemical 295*, 24-28.

65. Reyes, P., Pecchi, G., and Fierro, J. L. G. (2001) Surface Structures of Rh−Cu Sol−Gel Catalysts and Performance for Crotonaldehyde Hydrogenation, *Langmuir 17*, 522-527.

66. Marinelli, T. (1995) A Study on the Selectivity in Acrolein Hydrogenation on Platinum Catalysts: A Model for Hydrogenation of α,β-Unsaturated Aldehydes, *Journal of Catalysis 156*, 51-59.

67. Haubrich, J., Loffreda, D., Delbecq, F., Sautet, P., Krupski, A., Becker, C., and Wandelt, K. (2009) Adsorption of α,β-Unsaturated Aldehydes on Pt(111) and Pt−Sn Alloys: II. Crotonaldehyde, *The Journal of Physical Chemistry C 113*, 13947-13967.

68. Murillo, L. E., Goda, A. M., and Chen, J. G. (2007) Selective Hydrogenation of the CO Bond in Acrolein through the Architecture of Bimetallic Surface Structures, *Journal of the American Chemical Society 129*, 7101-7105.

69. Murillo, L. E., Menning, C. A., and Chen, J. G. (2009) Trend in the CC and CO bond hydrogenation of acrolein on Pt–M (M=Ni, Co, Cu) bimetallic surfaces, *Journal of Catalysis 268*, 335-342.

70. Mohr, C., Hofmeister, H., Radnik, J., and Claus, P. (2003) Identification of Active Sites in Gold-Catalyzed Hydrogenation of Acrolein, *Journal of the American Chemical Society 125*, 1905-1911.

71. Mohammad, A. B., Hwa Lim, K., Yudanov, I. V., Neyman, K. M., and R?sch, N. (2007) A computational study of H2 dissociation on silver surfaces: The effect of oxygen in the added row structure of Ag(110), *Physical Chemistry Chemical Physics 9*, 1247.

72. Zanella, R. (2004) Crotonaldehyde hydrogenation by gold supported on TiO2: structure sensitivity and mechanism, *Journal of Catalysis 223*, 328-339.

73. Kresse, G., and Furthmüller, J. (1996) Efficiency of ab-initio total energy calculations for metals and semiconductors using a plane-wave basis set, *Computational Materials Science 6*, 15-50.

74. Kresse, G., and Furthmüller, J. (1996) Efficient iterative schemes for ab initio total-energy calculations using a plane-wave basis set, *Physical review B 54*, 11169-11186.

75. Perdew, J. P., and Wang, Y *Physical review*. (1992) Accurate and simple analytic representation of the electron-gas correlation energy, *Physical review B 45*, 13244-13249.

76. Blöchl, P. E. (1994) Projector augmented-wave method, *Physical review B 50*, 17953-17979.
77. Monkhorst, H. J., and Pack, J. D. (1976) Special points for Brillouin-zone integrations, *Physical review B 13*, 5188-5192.

78. Henkelman, G., Uberuaga, B. P., and Jónsson, H. (2000) A climbing image nudged elastic band method for finding saddle points and minimum energy paths, *The Journal of Chemical Physics 113*, 9901.

79. Ruban, A. V., Skriver, H. L., and Nørskov, J. K. (1999) Surface segregation energies in transition-metal alloys, *Physical review B 59*, 15990-16000.

80. Loffreda, D., Delbecq, F., Vigné, F., and Sautet, P. (2006) Chemo−Regioselectivity in Heterogeneous Catalysis: Competitive Routes for CO and CC Hydrogenations from a Theoretical Approach, *Journal of the American Chemical Society 128*, 1316-1323.

81. Bligaard, T., Nørskov, J. K., Dahl, S., Matthiesen, J., Christensen, C. H., and Sehested, J. (2004) The Brønsted–Evans–Polanyi relation and the volcano curve in heterogeneous catalysis, *Journal of Catalysis 224*, 206-217.

82. Baber, A. E., Tierney, H. L., Lawton, T. J., and Sykes, E. C. H. (2011) An Atomic-Scale View of Palladium Alloys and their Ability to Dissociate Molecular Hydrogen, *ChemCatChem 3*, 607-614.

83. Sen, B. (1988) Metal-support effects on acetone hydrogenation over platinum catalysts, *Journal of Catalysis 113*, 52-71.

84. Vannice, M. A., and Sen, B. (1989) Metal-support effects on the intramolecular selectivity of crotonaldehyde hydrogenation over platinum, *Journal of Catalysis 115*, 65-78.

85. Schlatter, J., and Boudart, M. (1972) Hydrogenation of ethylene on supported platinum, *Journal of Catalysis 24*, 482-492.

86. Coq, B., Kumbhar, P. S., Moreau, C., Moreau, P., and Warawdekar, M. G. (1993) Liquid phase hydrogenation of cinnamaldehyde over supported ruthenium catalysts: Influence of particle size, bimetallics and nature of support, *Journal of Molecular Catalysis 85*, 215-228.

87. Hidalgo-Carrillo, J., Aramendía, M. A., Marinas, A., Marinas, J. M., and Urbano, F. J. (2010) Support and solvent effects on the liquid-phase chemoselective hydrogenation of crotonaldehyde over Pt catalysts, *Applied Catalysis A: General 385*, 190-200.

88. Hohmeyer, J., Kondratenko, E., Bron, M., Kröhnert, J., Jentoft, F. C., Schlögl, R., and Claus, P. (2010) Activation of dihydrogen on supported and unsupported silver catalysts, *Journal of Catalysis 269*, 5-14.

89. Grünert, W., Brückner, A., Hofmeister, H., and Claus, P. (2004) Structural Properties of Ag/TiO_2 Catalysts for Acrolein Hydrogenation, *The Journal of Physical Chemistry B 108*, 5709-5717.

90. Volckmar, C., Bron, M., Bentrup, U., Martin, A., and Claus, P. (2009) Influence of the support composition on the hydrogenation of acrolein over $Ag/SiO_2–Al_2O_3$ catalysts, *Journal of Catalysis 261*, 1-8.

91. Hong, X., Lu, J., Li, B., Jin, L., Hu, G., Wang, Y., and Luo, M. (2013) Selective hydrogenation of crotonaldehyde over supported Ir catalysts: Effect of surface acidity on catalyst deactivation, *Indian Journal Of Chemistry Section A 52*, 28-33.

92. Regalbuto, J. (2006) *Catalyst preparation: science and engineering*, CRC Press.

93. Englisch, M., Jentys, A., and Lercher, J. A. (1997) Structure Sensitivity of the Hydrogenation of Crotonaldehyde over Pt/SiO_2 and Pt/TiO_2, *Journal of Catalysis 166*, 25-35.

94. Chambers, A., David Jackson, S., Stirling, D., and Webb, G. (1997) Selective Hydrogenation of Cinnamaldehyde over Supported Copper Catalysts, *Journal of Catalysis 168*, 301-314.

95. Liu, Z. P., Jenkins, S. J., and King, D. A. (2004) Role of Nanostructured Dual-Oxide Supports in Enhanced Catalytic Activity: Theory of CO Oxidation Over $Au/IrO_2/TiO_2$, *Physical review letters 93*, 156102.

96. Ganduglia-Pirovano, M. V., Popa, C., Sauer, J., Abbott, H., Uhl, A., Baron, M., Stacchiola, D., Bondarchuk, O., Shaikhutdinov, S., and Freund, H.-J. (2010) Role of ceria in oxidative dehydrogenation on supported vanadia catalysts, *Journal of the American Chemical Society 132*, 2345-2349.

97. Vayssilov, G. N., Lykhach, Y., Migani, A., Staudt, T., Petrova, G. P., Tsud, N., Skála, T., Bruix, A., Illas, F., and Prince, K. C. (2011) Support nanostructure boosts oxygen transfer to catalytically active platinum nanoparticles, *Nature materials 10*, 310-315.

98. Ganduglia-Pirovano, M. V., Hofmann, A., and Sauer, J. (2007) Oxygen vacancies in transition metal and rare earth oxides: Current state of understanding and remaining challenges, *Surface Science Reports 62*, 219-270.

99. Wendt, S., Schaub, R., Matthiesen, J., Vestergaard, E., Wahlström, E., Rasmussen, M., Thostrup, P., Molina, L., Lægsgaard, E., and Stensgaard, I. (2005) Oxygen vacancies on TiO_2(110) and their interaction with H_2O and O_2: A combined high-resolution STM and DFT study, *Surface Science 598*, 226-245.

100. Consonni, M., Jokic, D., Yu Murzin, D., and Touroude, R. (1999) High Performances of Pt/ZnO Catalysts in Selective Hydrogenation of Crotonaldehyde, *Journal of Catalysis 188*, 165-175.

101. Milone, C., Ingoglia, R., Schipilliti, L., Crisafulli, C., Neri, G., and Galvagno, S. (2005) Selective hydrogenation of α,βα,β-unsaturated ketone to α,βα,β-unsaturated alcohol on gold-supported iron oxide catalysts: Role of the support, *Journal of Catalysis 236*, 80-90.

102. Milone, C., Crisafulli, C., Ingoglia, R., Schipilliti, L., and Galvagno, S. (2007) A comparative study on the selective hydrogenation of α, β unsaturated aldehyde and ketone to unsaturated alcohols on Au supported catalysts, *Catalysis today 122*, 341-351.

103. Moberg, D. R., Thibodeau, T. J., Amar, F. G., and Frederick, B. G. (2010) Mechanism of Hydrodeoxygenation of Acrolein on a Cluster Model of MoO_3, *The Journal of Physical Chemistry. C 114*, 13782-13795.

104. Larsen, J. H., Ranney, J. T., Starr, D. E., Musgrove, J. E., and Campbell, C. T. (2001) Adsorption energetics of Ag on MgO(100), *Physical review B 63*.

105. Farmer, J. A., Baricuatro, J. H., and Campbell, C. T. (2010) Ag Adsorption on Reduced CeO_2 (111) Thin Films †, *The Journal of Physical Chemistry C 114*, 17166-17172.

106. Campbell, C. T., Sharp, J. C., Yao, Y. X., Karp, E. M., and Silbaugh, T. L. (2011) Insights into catalysis by gold nanoparticles and their support effects through surface science studies of model catalysts, *Faraday Discuss. 152*, 227.

107. Loffreda, D., Delbecq, F., Vigné, F., and Sautet, P. (2009) Fast prediction of selectivity in heterogeneous catalysis from extended Brønsted–Evans–Polanyi relations: a theoretical insight, *Angewandte Chemie International Edition 48*, 8978-8980.

108. Nørskov, J. K., Bligaard, T., Logadottir, A., Bahn, S., Hansen, L. B., Bollinger, M., Bengaard, H., Hammer, B., Sljivancanin, Z., and Mavrikakis, M. (2002) Universality in heterogeneous catalysis, *Journal of Catalysis 209*, 275-278.

109. Pallassana, V., and Neurock, M. (2000) Electronic factors governing ethylene hydrogenation and dehydrogenation activity of pseudomorphic Pd ML/Re (0001), Pd ML/Ru (0001), Pd (111), and Pd ML/Au (111) Surfaces, *Journal of Catalysis 191*, 301-317.

110. Loffreda, D., Delbecq, F., Simon, D., and Sautet, P. (2001) Breaking the NO bond on Rh, Pd, and Pd3Mn alloy (100) surfaces: A quantum chemical comparison of reaction paths, *The Journal of Chemical Physics 115*, 8101-8111.

111.Van Santen, R. A. (2008) Complementary structure sensitive and insensitive catalytic relationships, *Accounts of chemical research 42*, 57-66.

112. Michaelides, A., Liu, Z.-P., Zhang, C., Alavi, A., King, D. A., and Hu, P. (2003) Identification of general linear relationships between activation energies and enthalpy changes for dissociation reactions at surfaces, *Journal of the American Chemical Society 125*, 3704-3705.

113. Gomez, C. (2013) Fundamental Studies of d-Band Transition Metal Alloys.

114. Yang, B., Wang, D., Gong, X.-Q., and Hu, P. (2011) Acrolein hydrogenation on Pt (211) and Au (211) surfaces: a density functional theory study, *Physical Chemistry Chemical Physics 13*, 21146-21152.

115. Turecek, F., Brabec, L., and Korvola, J. (1988) Unstable enols in the gas phase. Preparation ionization, energies, and heats of formation of (E)-and (Z)-2-buten-2-ol, 2-methyl-1-propen-1-ol, and 3-methyl-2-buten-2-ol, *Journal of the American Chemical Society 110*, 7984-7990.

116. Christopher, P., and Linic, S. (2010) Shape-and Size-Specific Chemistry of Ag Nanostructures in Catalytic Ethylene Epoxidation, *ChemCatChem 2*, 78-83.

117. Vilé, G., Albani, D., Nachtegaal, M., Chen, Z., Dontsova, D., Antonietti, M., López, N., and Pérez-Ramírez, J. (2015) A Stable Single-Site Palladium Catalyst for Hydrogenations, *Angewandte Chemie International Edition 54*, 11265-11269.

118. Thomas, J. M. (2015) Catalysis: Tens of thousands of atoms replaced by one, *Nature 525*, 325-326.

VITA
PAYOLI AICH

EDUCATION

August, 2011-January, 2016(Expected)	Ph.D in Chemical Engineering Supervisor: Dr. Randall J. Meyer	University of Illinois at Chicago	3.68/4

INDUSTRY EXPERIENCE

ExxonMobil Research and Development, Annandale, NJ June 2013-August 2013

Supervisor: Dr. Javier Guzman
Topic: Systematic study of bimetallics using selective hydrogenation reactions

- Screened several bimetallic catalysts using selective hydrogenation reactions
- Characterized catalysts using *In situ IR spectroscopy*

- Analyzed several *TG/DTA* data and TEM images to understand the effect of synthesis on catalyst activity
- Analyzed kinetics using Selective hydrogenation of Crotonaldehyde as reaction

University of Illinois at Chicago
Graduate Research Assistant, Department of Chemical Engineering

Advisor: Professor Randall Meyer, Dr. Jeff Miller & Dr. Chris Marshall

Topic: Selective Hydrogenation of Acrolein; Experimental and Theoretical Insight

- Synthesized Ag, Ru, Rh, Pd and bimetallic catalysts using Incipient Wetness Impregnation.
- Characterized catalysts using **Transmission Electron Microscopy (TEM), Extended X-ray Absorption Spectroscopy (EXAFS), BET, Energy Dispersive Spectroscopy (EDS**).
- Analyzed kinetics using Acrolein Hydrogenation as reaction.

- Determined a relationship between the sequence of impregnation of Silver and Pd with the selectivity towards allyl alcohol for acrolein hydrogenation reaction.

- Investigated Support effect on selectivity using acrolein hydrogenation as the reaction.
- Collaborated with several research groups to provide STEM images, EXAFS spectra.
- Determined Structural Effect of Silver on Selectivity using DFT calculations.

TEACHING EXPERIENCE

University of Illinois at Chicago August, 2011 – May, 2012
Teaching Assistant

- CHE 321(Chemical Reaction Engineering), CHE 301 (Thermodynamics),

CHE 205(Introduction to Computational Methods in Cheimical Engineering),

- General Chemistry 112 (August 2015-December 2015
- Held office hours, graded homeworks, Exams, Quizzes and taught classes as a substitute to instructors.

SKILLS

Strong Communication Skills	EXAFS	Fluent (CFD)
Experienced Working in a Team	EDX	Gambit
Incipient Wetness Impregnation	Origin	Matlab
Python	TEM	AutoCad
VASP 5.2	Aspen	Material Studio

ACADEMIC ACHIEVEMENTS

Conference Proceeding (Talks)

1. **Selective Hydrogenation of Acrolein over Single Atom Alloy Catalyst**

Payoli Aich, Haojuan Wei, A. Jeremy Kropf, Christopher L. Marshall, Jeffrey T. Miller and Randall J. Meyer. AIChE 2014, Atlanta, Georgia

2. **The Role of Surface Oxides in NOx Storage Reduction Catalysts: A DFT and kMC Study**

Zhenjuan Ni, Max Hoffmann, **Payoli Aich**, Karsten Reuter and Randall J. Meyer. NAM 2013, Louisville, Kentucky

3. **Systematic Study of support Effects on Acrolein Hydrogenation**

Payoli Aich, Haojuan Wei, Ruzica Todorvic, Christopher L. Marshall, Jeffrey T. Miller and Randall Meyer. NAM 2015, Pittsburgh, Pennsylvania.

Posters

1. **Selective Hydrogenation of Acrolein over Single Atom Alloy Catalysts**

Payoli Aich, Haojuan Wei, Christopher L. Marshall, Jeffery T. Miller, Randall J. Meyer.BP Napervile, Chicago, Spring symposium of Catalysis Club of Chicago, May 13, 2014

2. **Alloying effect on selective hydrogenation of acrolein: Single Atom alloy**

Payoli Aich, Haojuan Wei, Christopher L. Marshall, Jeffery T. Miller, Randall J. Meyer.BP Napervile, Chicago, Spring symposium of Catalysis Club of Chicago, May 7, 2013

3. **kMC simulations of NO oxidation on PdO(101)**

Payoli Aich, Zhenjuan Ni, Randall J. Meyer. BP Napervile, Chicago, Spring symposium of Catalysis Club of Chicago, May 15, 2012

Publications

1. **Single Atom Alloy Pd-Ag Catalyst for Selective Hydrogenation of Acrolein**

Payoli Aich, Haojuan Wei, Bridget Basan, A. Jeremy Kropf, Neil M. Schweitzer, Christopher L. Marshall, Jeffrey T. Miller and Randall Meyer. *Journal of Physical Chemistry C. Accepted*

2. **Single-Site Zinc on Silica Catalysts for Propylene Hydrogenation and Propane Dehydrogenation.Synthesis and Reactivity Evaluation Via High-Throughput Atomic Layer Deposition-Catalysis Experimentation**

Jeffrey Camacho-Bunquin, **Payoli Aich**, Magali Ferrandon, Andrew "Bean" Getsoian,Ujjal Das,Larry A. Curtiss,Jeffrey T. Miller,Christopher L. Marshall,Adam S. Hock and Peter C. Stair. *To be Submitted*

3. **Atomic Layer Deposition Over coating: Tuning Catalyst Selectivity for Biomass Conversion**

Hongbo Zhang, Xiang-Kui Gu, Christian Canla, A. Jeremy Kropf, **Payoli Aich**, Jeffrey P. Greeley, Jeffrey W. Elam, Randall J. Meyer, James A. Dumesic ,Peter C. Stair and Christopher L. Marshall. *Angewandte Chemie; 126 (2014), 12328–12332.*

4. **Effect of Support Reducibility on the Selective Hydrogenation of Acrolein**

Payoli Aich, Haojuan Wei, Ruzica Todorvic, Christopher L. Marshall, Jeffrey T. Miller and Randall Meyer. *In Preparation*

5. **Studies of Adsorption of Reactive Red 120 on Bentonite**

Sangita Bhattacharjee, Siddhartha Moulik, **Payoli Aich**, Chiranjib Bhattacharya. *International Journal of Environmental and Pollution; 32(2012), 194-200.*

6. **Catalyst synthesis and evaluation using an integrated atomic layer deposition synthesis–catalysis testing tool**

Jeffrey Camacho-Bunquin, Heng Shou, Payoli Aich, David R. Beaulieu, Helmut Klotzsch, Stephen Bachman, Christopher L. Marshall, Adam Hock, and Peter Stair, *Review of Scientific Instruments*; 86(2015), 084103

Leadership Activity

Graduate Student representative, Chemical Engineering Graduate Student Council; May 2012-May 2013

Awards and Honors

Kokes Award 2015, North American Catalysis Society

CRE Division Travel Award 2014, AIChE